Volume 11, Number 1, 2025

Some Characteristics of Air Distribution at Application of Linear Crevice Diffuser

Yaroslav Chemerynskyi*, Orest Voznyak

Lviv Polytechnic National University, 12 Stepana Bandery St., Lviv, 79013, Ukraine

Received: April 22, 2025. Revised: May 23, 2025. Accepted: May 30, 2025.

Abstract

The organization of air distribution is one of the key aspects of creating a comfortable and healthy indoor climate. The effectiveness of this process affects not only temperature and humidity, but also overall air quality, which directly impacts people's well-being. To ensure optimal air distribution, a variety of ventilation devices are used, including grilles and diffusers, which differ in design and technical characteristics. Recently, louvered linear diffusers have gained considerable popularity, combining high functionality with modern design. These devices are in line with current architectural and design trends, where special attention is paid to aesthetics, integration into the interior and small details. With an innovative design with multiple parallel air outlets, louvered linear diffusers create unique airflows that actively interact with each other, contributing to turbulence and ensuring even air distribution in the room. This approach not only increases the efficiency of ventilation systems, but also creates comfortable conditions for staying, minimizing drafts and temperature fluctuations.

Keywords: linear diffuser; air distribution; flat jet; microclimate; air flow turbulence; thermal comfort.

1. Introduction

To ensure a comfortable stay of people in the room, create safe working and rest conditions, it is necessary to provide optimal microclimate parameters. These parameters of the microclimate, thermal comfort, depend on temperature, humidity, air velocity [1] and are mainly ensured by ventilation systems. In order for ventilation systems to correctly fulfill the task of ensuring thermal comfort, they must be designed properly. Proper design of the ventilation system requires accurate data on the operation of the diffusers.

2. Analysis of the recent publications and research works on the problem

The parameters of diffusers are the object of many studies [2], [3], [4], [5] which were carried out experimentally and using numerical simulations. However, such studies mainly concern vortex diffusers. Linear diffusers are a separate type of ceiling diffusers [6]. There are several studies of linear slotted diffusers [7], [8] with different aspect ratios, in which the parameters of the operation of ceiling diffusers and isothermal conditions were studied. Based on the results of these studies, a calculation technique was described that makes it possible to calculate the attenuation of the air jet velocity of a linear diffuser in two dimensions. When conducting research [9], the effect of the aspect ratio of a linear slotted diffuser on the appearance of drafts in a small office room and a large office space was studied.

* Corresponding author. Email address: Yaroslav.R.Chemerynskyi@lpnu.ua

This paper should be cited as: Y. Chemerynskyi, O. Voznyak. (2025) Some characteristics of air distribution at application of linear crevice diffuser. *Energy Engineering and Control Systems*, Vol. 11, No. 1, pp. 21 – 26. https://doi.org/10.23939/jeecs2025.01.021

Also, studies [10] were carried out on the flow characteristics of a linear slotted diffuser and the possibility of their effective operation even in operating rooms [11] by the CFD simulation method.

The various air diffusers available on the market and offered by different manufacturers often have significant differences in design, despite the external similarities. Due to different ways of representing performance characteristics and differences in measurement methods, the selection and comparison of diffusers is not an easy task. Due to the insufficient level of knowledge about the operation of linear diffusers, there is a need for further study of this type of diffuser. In this article, we present some characteristics of the operation of diffusers.

3. Formulation of the goal of the paper

The article aims to analyze the effectiveness of using linear slotted diffusers in ventilation systems, to determine their optimal operating parameters, to assess the impact on the uniformity of air distribution in rooms, as well as to investigate their aerodynamic characteristics.

4. Presentation of research results

Like compact jets, flat jets have a similar structure. It is possible to delineate the core of the jet clearly, the pole of the jet and the boundaries of the jet, formed by the lines that pass through the pole of the jet and the boundaries of the linear louver diffuser.

During the experimental study of individual plane jets and their interaction, it can be noted that in the main area, the development of the jet is characterized by a gradual uniform drop in axial velocity v_x, and excess temperature, which is the difference in air temperature in the jet and in the room t_{in}: $\Delta t_x = t_x - t_{in}$. The question arises: how does their combination in a linear slotted diffuser affect the characteristics of flat jets?

It can be assumed that in the presence of parallel air outlets in the louvered linear diffuser, the interaction of flat jets occurs at the outlet of the diffuser, which causes significant turbulence of the total air flow and a sharper attenuation of the jet velocity as a result.

The axial velocity in isothermal jets v_x, m/s, is determined by the formula [12]:

$$v_x = DC/x, \tag{1}$$

where x is the current longitudinal coordinate, m; DC is dynamic characteristic, m^2/s.

The dynamic characteristic, in turn, is defined as [12]:

$$DC = \frac{0.66}{\mathrm{tg}\alpha}\sqrt{\frac{T_{in}}{T_n}}\cdot\sqrt[4]{\xi}\cdot V_n\cdot\sqrt{F_n}, \tag{2}$$

where α is the angle of opening of the jet ($\alpha = 12°25'$; $\mathrm{tg}\alpha = 0.22$); ξ is local resistance coefficient of the diffuser slit under study (ξ =1); T_{in}, T_n are room temperature and diffuser slot outlet temperature, respectively, K; V_n is initial velocity at the diffuser slot outlet in a linear slotted diffuser, m/s; F_n is area of the air outlet nozzle in the linear diffuser, m^2.

For simplification and convenience of calculations, the velocity attenuation coefficient *VD* is used [12]:

$$VD = \frac{0.66}{\mathrm{tg}\alpha}\sqrt{\frac{T_{in}}{T_n}}\cdot\sqrt[4]{\xi}. \tag{3}$$

Axial velocity is now calculated by the following formula [12]:

$$v_x = VD\cdot V_n\cdot\frac{\sqrt{F_n}}{x}. \tag{4}$$

In horizontally released weakly non-isothermal jets, the excess temperature is determined by the formula [12]:

$$\Delta t_x = \frac{TC}{x}, \tag{5}$$

where TC is thermal characteristic, °C·m, determined by the following formula [12]:

$$TC = \frac{0.54}{\mathrm{tg}\alpha}\sqrt{\frac{T_{in}}{T_n}}\cdot\frac{1}{\sqrt[4]{\xi}}\cdot\Delta t_n\cdot\sqrt{F_n}, \tag{6}$$

where Δt_n is initial excess temperature ($\Delta t_n = t_n - t_{in}$), °C.

For the convenience of calculations, a temperature attenuation coefficient *TD* is introduced [12]:

$$TD = \frac{0.54}{\mathrm{tg}\alpha}\sqrt{\frac{T_{in}}{T_n}}\cdot\frac{1}{\sqrt[4]{\xi}}. \tag{7}$$

Then the formula for determining the axial excess temperature Δt_x will be as follows [12]:

$$\Delta t_x = TD\ \cdot\Delta t_n\cdot\frac{\sqrt{F_n}}{x}. \tag{8}$$

Accordingly, in any section "x" at a distance "y" from the axis, the excess temperature $\Delta t_y = t_y - t_{in}$ is determined by the Taylor's formula [12]:

$$\Delta t_y = \Delta t_x\cdot\exp\left(-0.7\sigma_T\overline{y}^2\right) \tag{9}$$

where σ_T is Prandtl's turbulent number (σ_T = 0.65 ÷ 0.7 for compact jets); $\overline{y} = y/(cx)$; y is current transverse coordinate, m; c is an experimental constant ($c = 0.28$).

However, for simplification, it is advisable to use the relative values of excess temperatures, axial $\Delta\bar{t}_x = \Delta t_x/\Delta t_{in}$ and in any section $\Delta\bar{t}_y = \Delta t_y/\Delta t_{in}$.

The study of the parameters of the jet formed during the operation of a linear louver diffuser took place at a laboratory experimental facility. The installation diagram is shown in Fig.1.

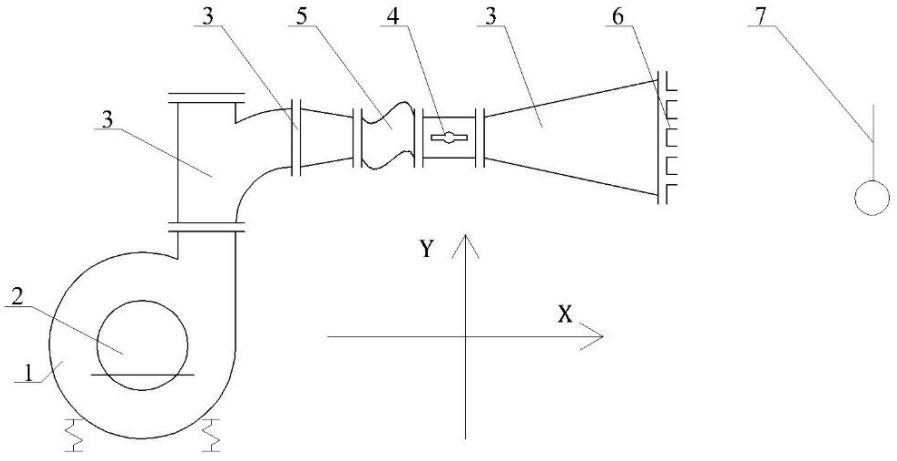

Fig.1. Scheme of the experimental setup: 1 – centrifugal fan; 2 – electric motor; 3 – air duct; 4 – control valve; 5 – flexible insert; 6 – linear slot diffuser; 7 – testo-405 thermal electrical anemometer.

The study was carried out for a linear slotted diffuser with four outlet slots. The diffuser under study, the experimental setup, and the research process, including the location of the sensors, are shown in Fig.2. The installation consists of a centrifugal fan on a vibration-insulated base for a stable air supply, a control choke to set the required flow, an air duct system that ensures even air distribution in front of the built-in linear diffuser, and an air velocity and temperature measurement system.

a)

b)

c)

d)

Fig.2. Experimental setup photographs: *a)* linear diffuser; *b)* general view of installation; *c)* visualization of jet; *d)* jet boundary.

As a result of processing the array of received data, the following dependence was confirmed and obtained:

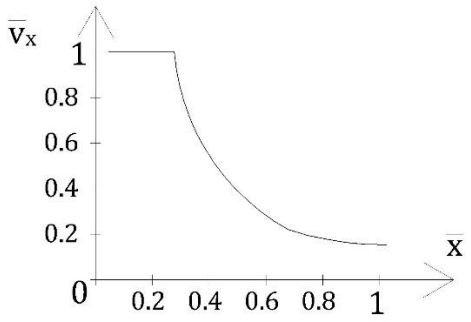

Fig.3. Dependence of relative axial velocity on longitudinal coordinate $\overline{v}_x = f(\bar{x})$ for linear slot diffuser.

From the dependence shown in Fig.3, it can be concluded that the air flow is intensely turbulent, the velocity attenuation in the jet occurs actively. The value of the velocity attenuation coefficient for a linear slot diffuser is equal to *VD* = 1.0, which is smaller compared to the same coefficient for a rectangular flat slot, for which *VD* = 2.5.

5. Conclusion

1) The conducted studies and obtained dependences of the velocity drop in an isothermal flat jet make it possible to supplement the existing methods of calculating linear slot diffusers and using them in premises for various purposes.

2) The hypothesis put forward on the interaction of several jets in a linear slot diffuser has been confirmed. The interaction of several jets at the outlet of the linear diffuser results in a sharper decrease in the axial velocity of the supply jet by 10 - 20% depending on the current coordinate in comparison with conventional air distributors.

3) The velocity attenuation coefficient for a linear slot diffuser *VD* = 1.0 gives us a possibility to use them in ventilation systems for premises with special requirements. Such characteristics allow organizing ventilation in premises without the occurrence of drafts.

4) A specific velocity profile is observed in the cross section of the jet due to the design features.

References

[1] ASHRAE. 2010. ASHRAE/ANSI Standard 55-2010 Thermal environmental conditions for human occupancy. Atlanta: *ASHRAE*.

[2] Li, A., Yang, C., Ren, T., Bao, X., Qin, E., and R. Gao. 2017. PIV experiment and evaluation of air flow performance of swirldiffuser mounted on the floor. *Energy and Buildings* 156:58–69.

[3] Borowski, M., Karch, M., Łuczak, R., Życzkowski, P., and M. Jaszczur. 2019. Numerical and experimental analysis of the velocity field of air flowing through swirl diffusers. E3S *Web Conf.* 128:1-6.

[4] Borowski, M., Zwolińska, K., & Halibart, J. (2023). Air Distribution Assessment-Ventilation Systems with Different Types of Linear Diffusers. https://www.aivc.org/sites/default/files/1_C28.pdf.

[5] Yau, Y.H., Poh, K.S., and A. Badarudin. 2018. A numerical airflow pattern study of a floor swirl diffuser for UFAD system. *Energy and Buildings* 158:525-535.

[6] Voznyak O., Spodyniuk N., Yurkevych Yu., Sukholova I., Dovbush O. (2020) Enhancing efficiency of air distribution by swirled-compact air jets in the mine using the heat utilizators. *Naukovyi Visnyk Natsionalnoho Hirnychoho Universytetu*, No.5(179), p. 89 – 94 doi:10.33271/nvngu/2020-5/089.

[7] Cao, G., Ruponen, M., Hagström, K and J. Kurnitski. 2011. Experimental Studies on Air Distribution Using Ceiling Slot Diffusers in a Room. *International Journal of Ventilation.* 9:4, 385-392.

[8] Vozniak O. T. et al. “Research of Device for Air Distribution With Swirl and Spread Air Jets at Variable Mode.” *Eastern-European Journal of Enterprise Technologies,* vol. 6, no. 7(78), 2015, p. 15. DOI:10.15587/1729-4061.2015.56235

[9] Both, B., Szánthó, Z., and R. Goda. 2017. Evaluation of air diffuser flow modelling methods experiments and computational fluid dynamics simulations*. Energy Procedia* 112:352-359.

[10] Yu, H., Liao, C-M., and H-M. Liang. 2003. Scale model study of airflow performance in a ceiling slot-ventilated enclosure: isothermal condition. *Building and Environment* 38:1271-1279.

[11] Keshtkar, M. M. and M. Nafteh. 2016. Investigation of influence of linear diffuser in the ventilation of operating rooms. *Advances in Energy Research*, Vol. 4, No. 3 239-253.

[12] Voznyak O. (2020) Experiment Planning and Optimization of Solutions in Ventilation Technology. Monograph – Lviv: Lviv Polytechnic National University, 220 p. (in Ukrainian)

Деякі характеристики повітророзподілу при застосуванні лінійного щілинного дифузора

Ярослав Чемеринський, Орест Возняк

Національний університет «Львівська політехніка», вул. С. Бандери, 12 , Львів, 79013, Україна

Анотація

Організація повітророзподілу є одним із ключових аспектів створення комфортного та здорового мікроклімату в приміщеннях. Від ефективності цього процесу залежить не лише температура й вологість, а й загальна якість повітря, що безпосередньо впливає на самопочуття людей. Для забезпечення оптимального розподілу повітря використовуються різноманітні вентиляційні пристрої, зокрема решітки та дифузори, які відрізняються конструкцією й технічними характеристиками. Останнім часом значної популярності набули жалюзійні лінійні дифузори, що поєднують високу функціональність із сучасним дизайном. Ці пристрої відповідають актуальним архітектурним і дизайнерським тенденціям, де особлива увага приділяється естетиці, інтеграції в інтер'єр та дрібним деталям. Завдяки інноваційній конструкції з кількома паралельними повітровипускними щілинами, жалюзійні лінійні дифузори створюють унікальні повітряні потоки, які активно взаємодіють між собою, сприяючи турбулізації та забезпечуючи рівномірний розподіл повітря в приміщенні. Такий підхід не лише підвищує ефективність вентиляційних систем, а й створює комфортні умови для перебування, мінімізуючи протяги та температурні перепади.

Ключові слова: лінійний дифузор; подача повітря; плоский струмінь; мікроклімат; турбулізація повітряного потоку; тепловий комфорт.

Volume 11, Number 1, 2025

Experimental Studies of Power Quality Indicators of Autonomous Low-Power Generators

Ivan Hlad, Vitalii Tsykh*, Yaroslav Batsala

Ivano-Frankivsk National Technical University of Oil and Gas, 15 Karpatska St., Ivano-Frankivsk, 76019, Ukraine

Received: April 16, 2025. Revised: May 21, 2025. Accepted: June 17, 2025.

Abstract

Experimental studies of the main indicators of power quality at the terminals of autonomous low-power generators were carried out. The content of higher voltage harmonics, as well as voltage and frequency deviations from the nominal value were determined. In the course of the research, the technical means of data collection and analysis by National Instruments were used. The main indicators of the power quality of autonomous inverter generators are shown to fully comply with the EN 50160-2022 standard. It is established that the voltages of even harmonics of the studied autonomous generators are absent in all operating modes. As a result of the experimental studies, it was found that with an increase in the connected load, the content of higher harmonics in inverter generators slightly increases, but the amount of distortion does not exceed the permissible values. It has also been found that with an increase in the electrical load of synchronous generators, the magnitude of voltage curve distortions is significantly reduced compared to the no-load voltage. Based on the studies, to reduce the content of higher voltage harmonics, it is advisable to connect electrical consumers with an active load character, which will allow powering parallel devices sensitive to higher harmonics.

Keywords: power quality; measurements; synchronous generator; inverter; harmonics.

1. Definition of the problem to be solved

As a result of the military aggression by the Russian Federation, Ukraine's power system suffered many critical damages that significantly affected its overall operation. Emergency power outages were observed in almost all settlements, and later scheduled hourly power outages were introduced. To ensure the operation of critical consumers, the use of mobile autonomous power sources became an urgent issue. The main emphasis was placed on the most widespread segment, namely stand-alone generators of low power. Among these power sources, generators driven by internal combustion engines have the longest battery life: synchronous and inverter generators. However, during their operation, there were frequent cases of incorrect operation of household and office equipment. The likely reason for this is the deviation of certain indicators of the quality of electricity produced by such generators. Therefore, an urgent task is to conduct experimental studies of the power quality parameters of low-power generators and formulate basic recommendations for their improvement. Identification of key parameters of power quality control and electromagnetic compatibility of local generation sources will reduce problems with switching on low-power generators and avoiding failures during operation.

2. Analysis of the recent publications and research works on the problem

Currently, there is a significant amount of research on the operation of high-power synchronous generators installed at power plants (transients, accuracy of maintaining the voltage at the terminals, rotor speed, etc.) [1], [2], [3]. These studies are important due to the assessment of the electromagnetic compatibility of power system components and

* Corresponding author. Email address: vitalii.tsykh@nung.edu.ua

This paper should be cited as: I. Hlad, V. Tsykh, Y. Batsala. (2025) Experimental studies of power quality indicators of autonomous low-power generators. *Energy Engineering and Control Systems*, Vol. 11, No. 1, pp. 27 – 32. https://doi.org/10.23939/jeecs2025.01.027

the proposed intelligent methods of power system coordination, which improves the stability and controllability of such systems. However, the results obtained for large generators cannot always be directly applied to low-power generators, especially those operating in stand-alone or hybrid mode. A feature of high-power synchronous generators is that they provide an almost sinusoidal voltage waveform at the terminals in the range from no-load to rated load. This is due to the fact that the large size of the magnetic system and windings of high-power synchronous generators allows us to take into account most of the factors that affect the content of higher voltage harmonics. In such systems, power quality issues, such as voltage stability, frequency accuracy, and the impact of higher harmonics, become critically important, requiring separate studies taking into account the specifics of operating modes and control schemes. Among these factors are the uneven distribution of magnetic induction in the air gap between the poles and the generator armature, the value of the maximum magnetic induction in the teeth and the stator back, and the generator winding dissipation inductance [4]. The author used the idea of invariants of the sums of squares of winding coefficients to analyze the harmonic composition of currents in the windings of electric machines. Their existence determines the limitation on the value of the fundamental harmonic and the possibility of compensating for harmful harmonics arising in multiphase winding circuits, which was introduced by Willem Klima in 1979. The paper considers the case of symmetrical three-phase currents in single- or double-layer winding schemes consisting of four sections in 24 slots. The peculiarity of the presentation is that the authors of the publication not only repeat Klima's conclusions, but also generalize the approach by applying mathematical and structural transformations to modern winding configurations. The ideas for harmonic spectrum analysis can be applied to low-power generators, and the invariance of winding coefficients can explain the limitations in reducing harmonic distortion in systems with a fixed winding structure. This is the basis for optimizing the winding layout of inverter-synchronous generators to improve the quality of electricity.

As for low-power electric machines, they are designed to strike a balance between the price of the product and operational parameters, including the quality of electricity. This is due to the fact that it is difficult to ensure a uniform magnetic field in the magnetic system because this requires increasing the number of winding grooves and, accordingly, stator teeth. Since stators are made of electrical steel plates by stamping, it is technologically impossible to produce narrow teeth. Thus, there is a limitation on the maximum number of stator winding slots and teeth for low-power synchronous generators [5].

The maximum magnetic induction in the magnetic system of a low-power synchronous generator is often located at the limit of the linear section of the magnetization curve of electrical steel. Therefore, the transition to the nonlinear part of the magnetization curve usually causes nonlinear distortions of the magnetic flux and, consequently, the voltage at the generator terminals. If a low-power synchronous generator is designed and manufactured to ensure that there is no distortion in the voltage curve, its cost increases significantly, or, otherwise, at the optimal cost, we will have a reduction in its rated power.

Today, a variety of models of stand-alone low-power synchronous generators are available on the market, both single-phase and three-phase. Most of them belong to the budget price range. At the same time, such generators have become the most widespread in our country over the past few years and are used to power important consumers, including public buildings, residential buildings, and medical facilities. Given that low-cost generators can deviate from certain power quality indicators in different operating modes, this can lead to the failure of expensive equipment that is sensitive to deviations in power quality indicators. Such equipment includes transformerless power supplies for gas boilers, individual power supplies for LED lamps, and medical equipment with sensitive sensors.

Leading manufacturers of stand-alone power supplies have invented a way to significantly improve the quality of electricity by incorporating a built-in voltage inverter into the design of an autonomous generator [5]. In inverter generators, the alternating voltage is first generated by a synchronous generator, then rectified, filtered from ripples, and inverted by a built-in inverter into a nearly sinusoidal alternating voltage. At the same time, the frequency, rms value and content of higher harmonics of the alternating voltage in the circuit between the synchronous generator and the built-in voltage inverter are not normalized. The main disadvantage of inverter generators is their low resistance to overloads caused, for example, by the starting currents of electric motors.

The issue of voltage control in distribution power grids is addressed in [7]. However, these studies concern only the analysis of voltage control methods in distribution networks, and do not contain studies on the voltage quality of autonomous low-power generators.

Work [8] contains a study of methods for improving the quality of electricity from diesel generators with millisecond pulse load, which were carried out by mathematical modeling of diesel generator transients and do not contain experimental voltage measurements.

Paper [9] contains the results of measuring the higher harmonics of currents and voltages at the points of joint connection of distribution power grids, which show a significant increase in the content of higher current harmonics in distribution power grids.

Article [10] discusses the impact of the transition to low-inertia systems on frequency stability in power systems. The authors analyze the interaction between synchronous machines and grid-forming inverters, which can ensure system stability in the absence of traditional sources of inertia.

Article [11] emphasizes the relevance of electromagnetic compatibility of power devices in local power grids, especially in conditions of high-frequency and fast electromagnetic processes. The authors analyze the mechanisms of overvoltage occurrence during switching and propose effective ways to limit them with the help of properly selected protective equipment, as well as the problem of protecting power electronic converters based on thyristors with forced shutdown (GTO) from switching overvoltage. The presence of autonomous inverter and synchronous low-power generators in local networks necessitates experimental studies, and their inconsistency can lead to malfunctions, overheating, or even equipment failure.

The peculiarities of diesel generators, an assessment of existing variable speed technologies and their evaluation according to a number of performance criteria are described in detail in [12]. The authors consider harmonics, frequency stability, voltage, etc., which are the main indicators of electricity quality, and discuss the impact of inverter control algorithms on these indicators.

In [13], the developers propose technical and system solutions (monitoring of diagnostic symptoms) to minimize the likelihood of power supply failure and its timely restoration. In [14], the authors propose to use the electrical parameters of a generator as an indicator of the technical condition of an energy source, which may be relevant for autonomous low-power systems, for example, in microgrids or backup systems.

3. Formulation of the goal of the paper

The aim of this paper is to conduct experimental studies of the main indicators of power quality of low-power autonomous synchronous and inverter generators. Such a study is necessary to assess the possibility of connecting electrical consumers that are sensitive to the content of higher harmonic components, frequency deviations, and supply voltage. To increase the reliability of the results obtained, it is necessary to use the hardware and software complex developed by the authors, which is based on the technology of virtual devices, simultaneously with the specialized power quality analyzer Metrel MI2892. It is worth noting that for the completeness of the research, it is necessary to measure the quality of electricity at the terminals of autonomous power generators with a power range from 3 to 10 kVA, both single-phase and three-phase, including inverter ones.

4. Presentation and discussion of the research results

The research methodology involved measuring and recording instantaneous voltage values at the terminals of autonomous generators in the idle mode, as well as in the mode close to the nominal active load. Household heating appliances such as electric convectors and electric kettles were used as a load. The set of electrical appliances used provided a power range of 0.7 - 0.9 of the rated power of the autonomous generators. A Metrel MI2892 power quality analyzer was used to measure the frequency, rms voltage, harmonic content, and total harmonic distortion.

The disadvantage of this Metrel MI2892 device is the difficulty of obtaining oscillograms with instantaneous voltage values. Therefore, we used primary voltage converters CV3-1000 from LEM, an analog-to-digital converter NI USB-6210, and a laptop with software developed by the authors for the rapid recording of instantaneous voltage values with the ability to save them to a hard disk. The ADC sampling rate is 10 kHz (200 points per period of 50 Hz industrial frequency for each channel), the bit depth is 16 bits of bipolar signal (±32768 discrete samples), the bandwidth of the measuring channels is in the range from 0 to 2 kHz. This made it possible to obtain informative voltage waveforms at the terminals of autonomous generators (Figures 2, 3).

Metrel MI2892 device uses digital signal processing, in particular the fast Fourier transform, to determine the higher harmonic voltages contained in the voltage at the terminals of autonomous generators, as well as the voltage frequency, its rms value, and total harmonic distortion according to EN 50160:2022 [15].

As a result of the experimental studies, it was found that the main indicators of the power quality of autonomous inverter generators fully comply with the EN 50160:2022 standard [15]. However, attention should be paid to the voltage spectral composition of low-power autonomous synchronous generators, which contains an unacceptably high total

harmonic distortion and significant odd harmonic voltages in the off-load mode (Table 1). In Table 1, the models of synchronous generators are shown conventionally, indicating the value of the rated total power and the number of phases.

In particular, Table 1 shows that the voltage and frequency deviations, total harmonic distortion, and higher harmonic components of all the studied generators, except for the Gen8500 generator, are within the permissible limits according to EN 50160-2022 [15]. However, the total harmonic distortion of the Gen8500 single-phase synchronous generator with a rated full power of 8.5 kVA in the no-load mode is 16.2%, which is twice the value allowed by EN 50160-2022 [15].

Table 1. Power Quality parameters of single-phase autonomous generators (idle mode).

Name of parameter	Measured Values				Allowed Values EN 50160:2022
	Gen8500 single-phase	Gen3000 single-phase Invertor	Gen6000 three-phase	Gen10000 three-phase	
U, V	226.9	230.9	235.0	226.7	207-253
f, Hz	54.1	50.1	52.6	53.3	42.5-57.5
Total Harmonic Distortion (THD), %	16.2	0.3	6.6	7.8	8
$U_{(3)}$, %	4.0	0.16	1.5	2.9	5.0
$U_{(5)}$, %	5.4	0.11	5.4	4.4	6.0
$U_{(7)}$, %	0.6	0.1	1.0	2.4	5.0
$U_{(9)}$, %	1.5	0.05	0.6	2.1	1.5
$U_{(11)}$, %	1.1	0.04	1.1	1.8	3.5

Table 2 shows the results of measuring the above-mentioned power quality indicators when supplying consumers with an active load and power close to the nominal value.

Table 2. Power Quality parameters of single-phase autonomous generators (nominal active load mode).

Name of parameter	Measured Values				Allowed Values EN 50160:2022
	Gen8500 single-phase	Gen3000 single-phase Invertor	Gen6000 three-phase	Gen10000 three-phase	
U, V	229.1	224.7	240.0	224.2	207-253
f, Hz	48.9	50.1	52.0	51.8	42.5-57.5
Total Harmonic Distortion (THD), %	17.7	2.6	9.9	6.7	8
$U_{(3)}$, %	17.2	0.9	7.5	2.5	5.0
$U_{(5)}$, %	2.0	0.1	5.0	3.8	6.0
$U_{(7)}$, %	0.58	1.9	1.0	2.1	5.0
$U_{(9)}$, %	0.9	0.8	0.7	1.4	1.5
$U_{(11)}$, %	0.76	0.8	1.0	1.2	3.5

Table 2 shows that when operating under load in autonomous low-power generators, except for the inverter generator, the content of higher-order harmonics decreases, but the percentage of the third harmonic voltage and, accordingly, the total harmonic distortion increase. This is probably due to the peculiarities of the stator winding schemes and their design, changes in the saturation of the magnetic system when operating under load, as well as the settings of automatic excitation controllers.

The voltage waveforms at the terminals of the studied generators in the idle mode are shown in Fig.1. As can be seen, the voltage curve of the inverter generator has practically no nonlinear distortions, the voltage curve of the single-phase generator with a capacity of 8.5 kVA contains higher-order harmonics, and the voltage curve of the three-phase generator with a capacity of 6 kVA contains higher harmonic distortions, approximately the same in the frequency spectrum that was studied.

The voltage waveforms at the terminals of the investigated generators under an active load are shown in Fig.2. As can be seen, the voltage curve of the inverter generator contains minor nonlinear distortions, the voltage curve of the single-phase generator with a capacity of 8.5 kVA does not contain higher-order harmonics, and the voltage curve

of the three-phase generator with a capacity of 6 kVA contains higher harmonic distortions, approximately the same in the frequency spectrum under study.

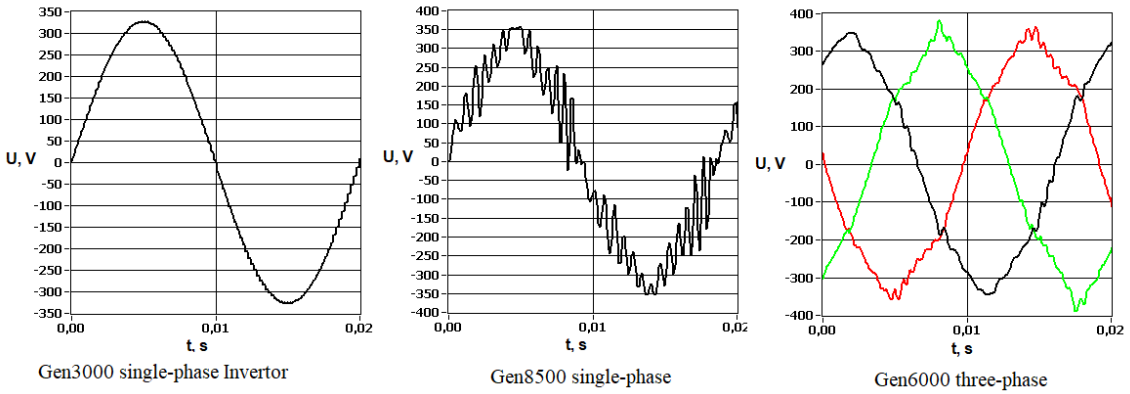

Fig.1. Waveforms of generator voltages in idle mode.

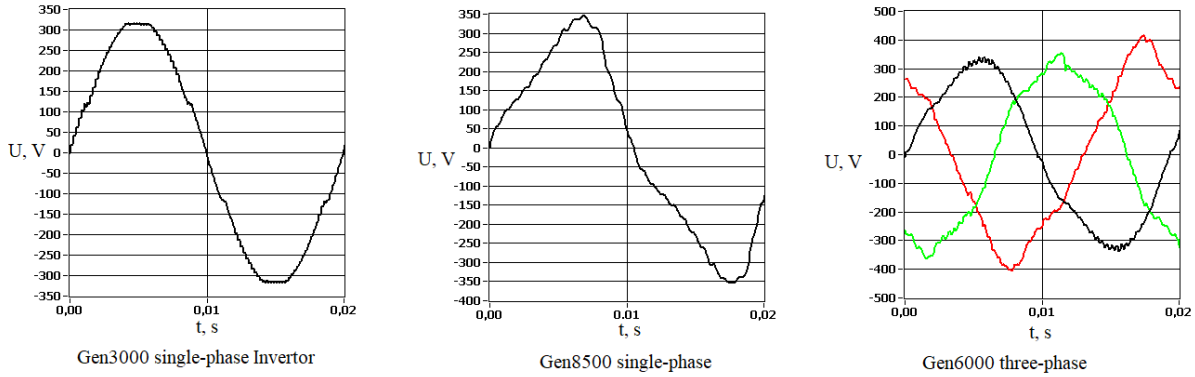

Fig.2. Waveforms of generator voltages in nominal active load mode.

Also, Fig.2 shows that a three-phase synchronous generator with a capacity of 6 kVA does not provide sufficient symmetry of phase voltages when operating with a load, so in the future it will be advisable to conduct experimental studies to determine the asymmetry factor and its impact on the power consumer.

5. Conclusion

The publication highlights the results of experimental studies of low-power autonomous synchronous and inverter generators. For this purpose, the measurement methodology used with the Metrel MI2892 power quality analyzer, CV3-1000 high-precision voltage converters, NI USB-6210 ADC, and specialized software made it possible to perform a detailed spectral analysis of the voltage with the determination of higher harmonics, frequency, and rms value.

The results of the analysis showed that inverter generators provide high power quality indicators that fully meet the requirements of EN 50160-2022 with a load ranging from idle to rated. At the same time, low-power synchronous generators demonstrate significant voltage quality violations in the idle mode: elevated values of total harmonic distortion and unpaired harmonic voltages were found, which can negatively affect the operation of sensitive electronic equipment.

The results obtained indicate the feasibility of optimizing the winding design, excitation schemes, or implementing filtration measures to improve the quality of electricity in synchronous generators. In particular, the connection of an active load reduces the content of higher harmonic components in low-power autonomous synchronous generators.

References

[1] Mugarra, A.; Guerrero, J.M.; Mahtani, K.; Platero, C.A. Synchronous Generator Stability Characterization for Gas Power Plants Using Load Rejection Tests. Appl. Sci. 2023, 13, 11168. https://doi.org/10.3390/app132011168.

[2] Varetsky, Y.; Gajdzica, M. Power Compatibility of Induction Motors in Industrial Grids Containing Synchronous Generators. Energies 2024, 17, 1066. https://doi.org/10.3390/en17051066.

[3] Khezri, Rahmat & Oshnoei, Arman & Yazdani, Amirmehdi & Mahmoudi, Amin. (2020). Intelligent coordinators for automatic voltage regulator and power system stabiliser in a multi-machine power system. IET Generation, Transmission and Distribution. 10.1049/iet-gtd.2020.0504.

[4] Gavrilyuk R. B. Secrets that preserve the harmonics of the magnetizing force of symmetrical multiphase winding circuits (2009) Electrotekhnika i Elektromechanika. 2009. No. 1, National Technical University "KhPI", P. 5-8.

[5] Rasilo, Paavo. (2007). Low-Voltage Synchronous Generator Excitation Optimization and Design. PP. 1-70. https://www.researchgate.net/publication/27516626.

[6] Shpenst, Vadim & Belsky, Aleksey & Orel, Evgeny. (2023). Improving the efficiency of autonomous electrical complex with renewable energy sources by means of adaptive regulation of its operating modes. Journal of Mining Institute. 261. 479-492.

[7] Kosareva IV, Shcherbak IE Analysis and practice of voltage control in distribution networks. Electric power engineering, electromechanics and technologies in the agro-industrial complex: materials of the International scientific and practical conference, December 22, 2022, State Biotechnology University, Kharkiv: 2022. C. 9-10.

[8] Hai-Chao Li et al 2023 J. Phys.: Conf. Ser. 2452 012032. DOI 10.1088/1742-6596/2452/1/012032.

[9] Solomchak O.V., Solomchak A.O. Measurement of higher harmonics of currents and voltages at the points of joint connection of distribution electrical networks. P. 194-201. DOI https://doi.org/10.32782/2663-5941/2024.4/29.

[10] A. Tayyebi, D. Groß, A. Anta, F. Kupzog and F. Dörfler, "Frequency Stability of Synchronous Machines and Grid-Forming Power Converters," in IEEE Journal of Emerging and Selected Topics in Power Electronics, vol. 8, no. 2, pp. 1004-1018, June 2020, doi: 10.1109/JESTPE.2020.2966524.

[11] Y. Fediv, O. Sivakova, V. Lysiak, M. Korchak. Switching overvoltages protection of power electronics converters with gate turn-off thyristors. Energy Engineering and Control Systems, 2021, Vol. 7, No. 2, pp. 103 – 110. https://doi.org/10.23939/jeecs2021.02.103.

[12] Grzeczka, Grzegorz & Piłat, Tomasz & Polak, Adam. (2017). The parameters of excitation current of ship synchronous generator as the diagnostic symptoms of the propelling IC engine. Journal of Marine Engineering & Technology. 16. P. 1-5. 10.1080/20464177.2017.1381063.

[13] Mobarra, M.; Rezkallah, M.; Ilinca, A. Variable Speed Diesel Generators: Performance and Characteristic Comparison. Energies 2022, 15, 592. https://doi.org/10.3390/en15020592.

[14] Y. Shelekh, M. Sabat, V. Lysiak, L. Parashchuk. Enhancing safety and reliability of electric power supply to consumers through safe electricity networks of up to 1 kV. Energy Engineering and Control Systems, 2021, Vol. 7, No. 2, pp. 97 – 102. https://doi.org/10.23939/jeecs2021.02.097.

[15] EN 50160:2022 Voltage characteristics of electricity supplied by public electricity networks. Online: https://standards.iteh.ai/catalog/standards/clc/083c552d-f4b8-4373-a5ec-8a27b6c8d37d/en-50160-2022?srsltid=AfmBOoq4zJRM8sYUfwnN2YpKAha3Rv57nlK5kZ2Qb6kvVkLsSbhaUAs-.

Експериментальні дослідження показників якості електричної енергії автономних генераторів малої потужності

Іван Гладь, Віталій Цих, Ярослав Бацала

Івано-Франківський національний технічний університет нафти і газу,
вул. Карпатська, 15, Івано-Франківськ, 76019, Україна

Анотація

Проведено експериментальні дослідження основних показників якості електричної енергії на затискачах автономних генераторів малої потужності. Визначено вміст вищих гармонік напруги, а також відхилення напруги і частоти від номінального значення. В ході досліджень використано технічні засоби збору та аналізу даних компанії National Instruments. Показано, що основні показники якості електроенергії автономних інверторних генераторів повністю відповідають стандарту EN 50160-2022. Встановлено, що напруги парних гармонік автономних генераторів, які досліджувалися, відсутні у всіх режимах роботи. В результаті проведених експериментальних досліджень виявлено, що при зростанні підключеного навантаження в інверторних генераторах дещо збільшується вміст вищих гармонік, однак величина спотворень не перевищує допустимих значень. Також встановлено, що при збільшенні електричного навантаження синхронних генераторів, величина спотворень кривої напруги суттєво знижується, порівняно із напругою неробочого ходу. На основі проведених досліджень показано, що для зменшення вмісту вищих гармонік напруги доцільно приєднувати електроспоживачі із активним характером навантаження, що дозволить живити паралельно приєднані чутливі до вищих гармонік пристрої.

Ключові слова: якість електроенергії; вимірювання; синхронний генератор; інвертор; гармоніки.

Volume 11, Number 1, 2025

Application of CFD Numerical Simulations and Shape Optimization to Modify the Flow Characteristics of Throttle Valves

Alicja Dykas, Urszula Warzyńska*

Wrocław University of Science and Technology, Faculty of Mechanical Engineering, 5 Łukasiewicza St., Wrocław, 50-371, Poland

Received: April 17, 2025. Revised: May 31, 2025. Accepted: June 23, 2025.

Abstract

The aim of the study was to perform a numerical analysis using the CFD method of oil flow through a hydraulic valve gap and to perform an optimisation of the gap shape with a view to linearising the valve characteristics. As part of the work, a flow analysis of the valve was carried out using numerical simulations. This made it possible to develop the characteristics of the studied valve. The optimisation process started with a shape sensitivity analysis to determine the effect of geometry on key flow parameters such as pressure drop. One of the resulting solutions selected on the basis of its functionality and technological manufacturing possibility was further analysed. The flow characteristics determined for the optimised design were compared with those of the original valve using statistical tools. It was shown that optimised geometry achieved a more linear characteristic, which will enable more precise throttle control using this valve.

Keywords: shape optimisation; computational fluid dynamics; pressure valve; pressure drop; flow characteristics; finite volume method; hydraulic systems.

1. Introduction

The development of modern hydraulic power systems is associated with increasing demands for control precision, energy efficiency and compactness of design solutions. A key role in achieving these goals is played both by new valve concepts and the development of numerical methods – primarily computational fluid mechanics (CFD), which supports the design and optimization of hydraulic components. In the technical literature, several major areas of research can be distinguished that are part of these issues.

Innovative approaches to valve design are an important direction in the development of power hydraulics. Ongoing research focuses, inter alia, on control valves [1] for which a method of active control of differential pressure in control valves has been proposed, which allows for a significant improvement in their accuracy and dynamic performance, or on proportional valves [2] where a flow coefficient analysis has been carried out using the CFD method, identifying the effect of internal geometry on flow characteristics. Both approaches show that properly selected design and numerical support can significantly improve the functionality of hydraulic valves.

Numerical simulations have also been successfully used in the analysis of flows in hydraulic pumps, motors and actuators, for example for the aerospace industry [3], where an electro-hydraulic pump was studied, focusing on the analysis of dynamic flow properties. Studies using simulation are also applicable to pumps in the automotive industry [4], where very high speeds are involved. Also, simulations using deforming mesh and mesh replacement [5] show possibilities to accurately represent geometry and boundary conditions for realistic flow analyses. Another example is the possibility of studying fluid-structure interactions, which increase the accuracy of the representation of real operating conditions [6].

* Corresponding author. Email address: urszula.warzynska@pwr.edu.pl

This paper should be cited as: A. Dykas, U. Warzyńska. (2025) Application of CFD numerical simulations and shape optimization to modify the flow characteristics of throttle valves. *Energy Engineering and Control Systems*, Vol. 11, No. 1, pp. 33 – 43. https://doi.org/10.23939/jeecs2025.01.033

2. Analysis of recent research and publications

An important area of research is the application of shape and topology optimization methods in the design of hydraulic components. Studies of the effect of the diameter of the inlet nozzle on the efficiency of fluid exchange in a hydraulic cylinder [7] show that optimizing the shape of the inlet elements significantly improves the efficiency of the actuator. Also exemplified is a comprehensive approach to the design of gerotor and orbital hydraulic machines [8], which uses advanced reverse engineering, 3D modelling and flow analysis to improve performance. This approach is in line with current trends of combining simulation techniques with geometric optimization, which is the foundation of modern design.

Shape optimisation became one of the most popular directions in components design thanks to many modern calculation tools many of which contain optimisation modules already built in. One of the examples that used CFD method to optimise shape is spool valve grove optimisation [9] using method of inner surface response checking. Shape optimisation of the valves may be used in many fields and may have many different objective functions, such as improving the electromagnetic force in electromagnetic valves [10] or temperature distribution efficiency [11] that can be used in heat control valves. The next advantage of shape optimisation is a fact that multiple objectives can be set for one optimisation, so that a compromise between several desirable properties is reached. Examples can be multi-objective optimization to improve structural safety and sealing performance of butterfly valves [12] or optimization of channel shape with Tesla valve [13] taking into account both temperature uniformity and pressure drop.

3. Formulation of the goal of the paper

On the background of the above studies, the present work focuses on using CFD methods and shape optimization to modify the flow characteristics of a throttling valve. The goal is to improve its efficiency and match its precise operating conditions by analysing the velocity distribution, pressure losses and the effect of geometry on hydraulic parameters.

4. Theoretical analysis

The velocity of the receiver in a hydrostatic drive system is dependent on the rate of fluid supplied to it. The use of throttling valves in the hydrostatic drive system in a suitable arrangement allows us to control the speed of the receiver when using a fixed displacement pump (throttle control or throttle regulation). The efficiency of systems with such a solution is low, because of power loss caused by intentionally draining part of the fluid flow back to the tank. The second solution for controlling the speed of the receiver is the use of a variable displacement pump (volumetric control or regulation). However, variable displacement pumps are often much more expensive than fixed-displacement. Throttle control is more often selected in low-power systems and in cases of long downtimes of the throttle-controlled receiver or in the case of a short period of time in the operating cycle that requires choking the flow.

To describe the behaviour of a fluid and its parameters within a throttle valve, two extreme cases of throttling gaps are considered: a sharp-edged orifice and a capillary. In the first case, the flow is turbulent, whereas in the second, it is laminar. Laminar flow through a circular cross-section, such as a capillary, can be described using the Hagen-Poiseuille equation, which is expressed as follows [14]:

$$Q = k_1 f_d \Delta p, \tag{1}$$

where k_1 is proportionality coefficient depending on the viscosity of the liquid; f_d is flow area of the capillary (m^2); Δp is pressure difference between the inlet and outlet of the capillary (Pa).

We can describe the coefficient k_1 as [14]:

$$k_1 = \frac{d^2}{32\mu l}, \tag{2}$$

where d is diameter of the capillary (m); μ is dynamic viscosity of the liquid (Pa·s); l is length of the capillary (m).

Turbulent flow, which occurs when the fluid flows through an orifice, can be described for this case by the equation [14]:

$$Q = k f_d \sqrt{\Delta p}. \tag{3}$$

In this case, the k-factor can be described by the equation [9]:

$$k = \sqrt{\frac{2}{\zeta \varrho}}, \tag{4}$$

where ζ is flow resistance coefficient for the local resistances, which depends, among other things, on the geometry of the orifice; ϱ is the density of the fluid (kg/m^3).

Based on equations (1) and (3), the general equation for flow through any type of throttling gap may be determined. This equation is as follows [14]:

$$Q = k_1 f_d \Delta p^n. \tag{5}$$

In this equation, the power exponent n will take the value $n = 1$ for a capillary, while $n = 1/2$ for a sharp-edged orifice. Creating from these equations the flow characteristics for both these types of flow resistances as a function of pressure difference Δp, it can be concluded that the greater variability will be characterized by the flow through the capillary. The slots of actual throttling valves, which are most often the geometric connection of an orifice and a capillary, will be characterized by flows whose characteristics will lie between these two extremes, their power exponents n will be in the range of $½ > n > 1$.

Obtaining the desired flow characteristic of a throttle valve depends mainly on the shape of the flow gap, which can be improved by shape optimization methods. Modern optimization methods, based on algorithms and numerical techniques, make it possible to identify the optimal solution more efficiently without having to analyse all possible alternatives. Optimization is a separate theory that lies within the field of applied mathematics. It aims to adequately formulate the object of optimization with a set of solution searches and to define the objective function. Once this problem has been formulated, the next step is to find the optimal solution that satisfies the accepted criterion. The following steps of optimization can be presented as [15]:

- Development of a mathematical model of the problem under analysis.
- Determination of the objective function.
- Searching for the optimal solution using the selected optimization method.

There are some basic concepts associated with optimization, which are discussed below.

- The set of admissible solutions $X_d \subset X$ is defined as the set of points $x \in X$ that are taken into account in the optimization process. It is defined by specifying conditions that must be satisfied by a vector x in order for it to belong to the set X_d. When no constraints are specified and $X_d = X = R_n$, where R_n is an n-dimensional space of real vectors, optimization without constraints occurs. Otherwise, there is optimization with constraints.
- The objective function is as follows:

$$f : X \rightarrow R$$

For each solution $x \in X$ there is assigned some numerical value $f(x) \in R$ from the set of admissible solutions. This gives the possibility to compare different solutions, since this assigned value expresses the quality of the solution against the specified optimization criterion. Depending on the problem, one seeks maximization or minimization. In minimization problems, the objective function is often referred to as the cost function. The goal of optimization in such cases is to identify, among the possible options defined by the given constraints, the solution that minimizes this cost, which may be, for example, the pressure output.

Any optimization problem requires finding a solution x that minimizes (or maximizes) the value of the objective function while satisfying certain constraints that define the set of feasible solutions. For the vast majority of practical applications of optimization methods, it is unlikely to find an exact minimum (or maximum) solution. This is due to the limited accuracy of numerical methods. Therefore, a solution x close to assumed is sufficient, which is determined by satisfying the stop conditions. Stop conditions are most often convergence tests, when the point obtained in successive iterations differs little from the previous one, it can be assumed that subsequent iterations will not lead to a much closer solution [15].

There are many optimization methods and criteria for their division. However, the remainder of this paper focuses only on the methods used by the optimization module of Ansys Fluent software in conjunction with Adjoint Solver. These are gradient methods. They use not only knowledge of the current values of the objective function, but also its gradient and associated values. Therefore, the objective function in the case of gradient methods must be defined and differentiable throughout space. When searching for the minimum solution, gradient methods analyse- -the upward

trend of the objective function, since the gradient $\nabla f(x)$ indicates the direction of the greatest increase in the objective function, while the vector- $\nabla f(x)$ indicates the direction of the greatest decrease.

In general, the optimization problem can involve both minimization and maximization of observable shapes, as well as constraints localized in space. This requires an approach that can provide a deformation field that is well-behaved and consistent with production requirements, while allowing locally sharper deformations when required to satisfy the imposed constraints. For Adjoint solver, Fluent provides three different morphing techniques: polynomial-based, using direct interpolation and using a radial basis function. These methods are based on different design spaces and therefore produce different morphing results. Key information about them is presented below [16]:

- The polynomial method uses polynomial functions to model changes in the geometry in the design space. In this technique, shape modifications are defined using low-order polynomials, which preserves the smoothness and continuity of geometric surfaces. The advantage of this method is its simplicity and low computational requirements, making it suitable for relatively simple geometries or preliminary stages of optimization. However, a limitation is the difficulty in accurately representing complex shape changes, which may require the use of higher-order polynomials, increasing computational complexity.
- The direct interpolation method involves directly displacing selected points on a geometric surface based on specified displacement values. In this technique, displacement values at intermediate points are calculated by linear or higher order interpolation. This method is intuitive and allows for precise control of changes in selected areas of the geometry, making it useful for local optimizations. However, the lack of global control over shape smoothness can lead to discontinuities, especially with large changes in geometry.
- The radial basis function (RBF) method uses mathematical functions that are defined with respect to the distance from a central point (known as a node). These functions are used to smoothly transform the entire geometric mesh based on the displacement values at selected nodes. RBF is very flexible and does a good job of mapping complex shape changes while keeping the geometry smooth and continuous. This makes the method particularly effective for complex geometries and global optimizations. The disadvantage of this technique is its higher computational cost compared to other methods, especially for large meshes.

5. Results of the study

5.1. Original valve flow characteristics

The CFD flow simulations were performed in Ansys Fluent software with the use of finite volume method. The original geometry of the valve was prepared based on technical documentation [17] using SpaceClaim software. Based on 2D technical drawings, the internal 3D domain of the fluid filling the interior of the valve structure was modelled (Fig.1 and Fig.2). The discrete model was composed of tetrahedral elements on surface mesh and poly-hexcore elements in the interior domain with the maximum size of 2 mm, and mesh refinement rate of 1.2 in small gaps (Fig.3).

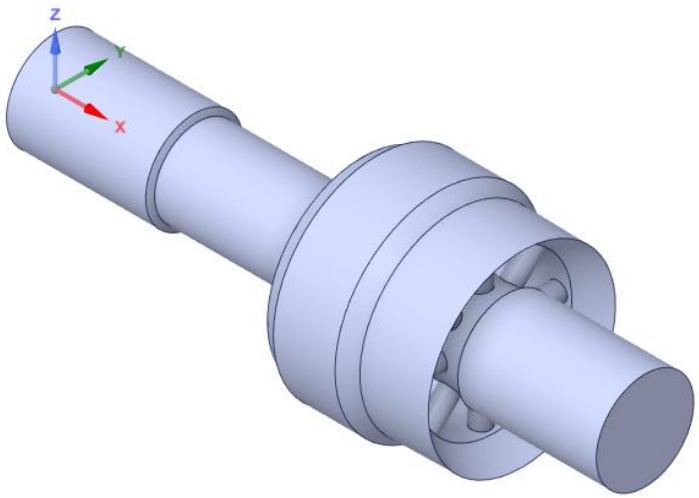

Fig.1. Geometrical model of the original valve fluid domain geometry.

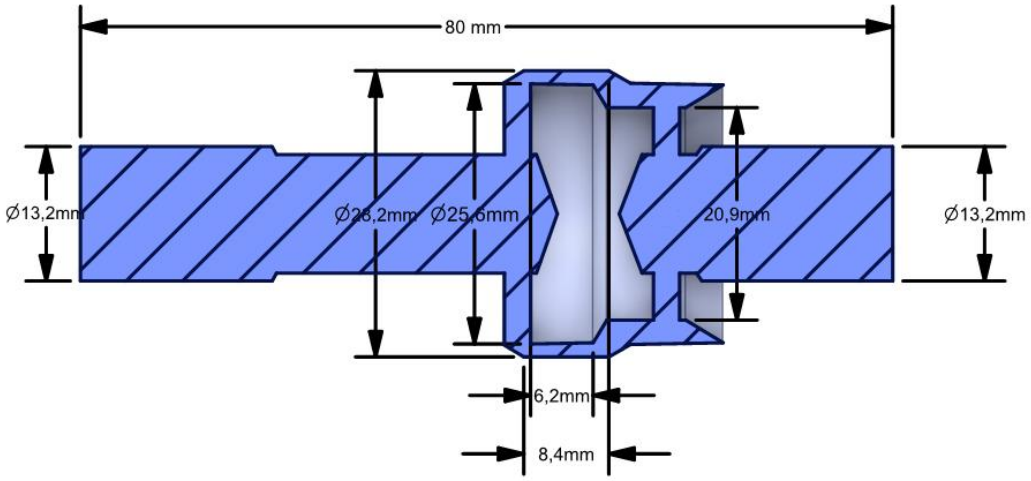

Fig.2. Basic dimensions of the original valve fluid domain geometry.

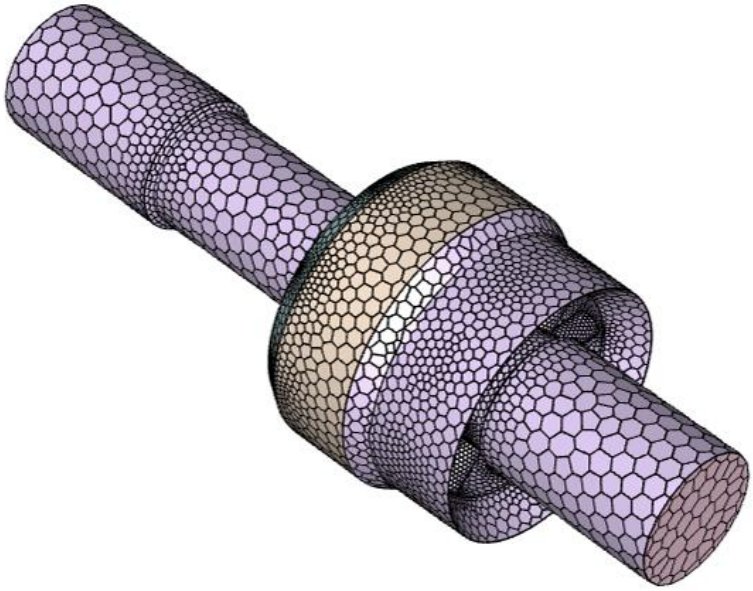

Fig.3. Discrete model of the original valve fluid domain geometry.

In the flow simulations, hydraulic oil Hydrol L-HL 46 was used with constant parameters of density equal to 864.7 kg/m^3 and viscosity 0.0393 Pa·s [18]. The inlet boundary condition was set to velocity varying with the analysed case. Pressure and flow velocity distributions were analysed for five flow rates, ranging from 10 to 50 l/min, with a step of 10 l/min, which translated into inlet flow velocities ranging from 1.2 to 6.1 m/s. The outlet was set to a pressure outlet with free outflow. The standard k-ε turbulence model was chosen because of reported reliable results in engineering applications [19]. The following k-ε model parameters values were used. For Cmu, which is the k-ε turbulence model constant associated with the modeling of turbulent viscosity the value Cμ=0.09 is a standard value calibrated experimentally and theoretically for most turbulent flows. For C1-Epsilon which is the calibration constant in the transport equation for ϵ, the turbulence dispersion rate the standard value is C_{ϵ}^{1}= 1.44 and it results from calibration for fully turbulent flows. C2-Epsilon is the damping constant in the transport equation for ϵ. It controls the decay of turbulence where the production rate of ϵ is low, such as near the laminar-turbulent flow boundary. The standard value is C_{ϵ}^{2} = 1.92. The first step of the study was to perform steady-state flow simulations in the original geometry of the valve. The results of pressure and velocity fields in the example of the highest flow rate of 50 l/min are shown in Fig.4 and Fig.5. The simulation results for all tested cases (with different flow rates) allowed us to develop the flow characteristics $\Delta p = f(Q)$ for the original geometry of the valve. Convergence was reached after about 70 iterations. During this time, the values of the finite residuals declined. The residuals for velocities in the x, y, and z directions and

the continuity equation decreased to values on the order of 10^{-4}. In addition to the residuals, the stability and consistency of physical parameters such as wall forces, pressure losses and flow development were monitored. Finite residuals of 10^{-4} are acceptable for most engineering applications, suggesting that the solution is accurate, and further iterations would not result in significant changes in the results. The reliability of these results is also affected by the quality of the grid, the choice of the turbulence model and the use of second-order schemes, which makes it possible to accurately represent the distribution of flow parameters in sensitive zones.

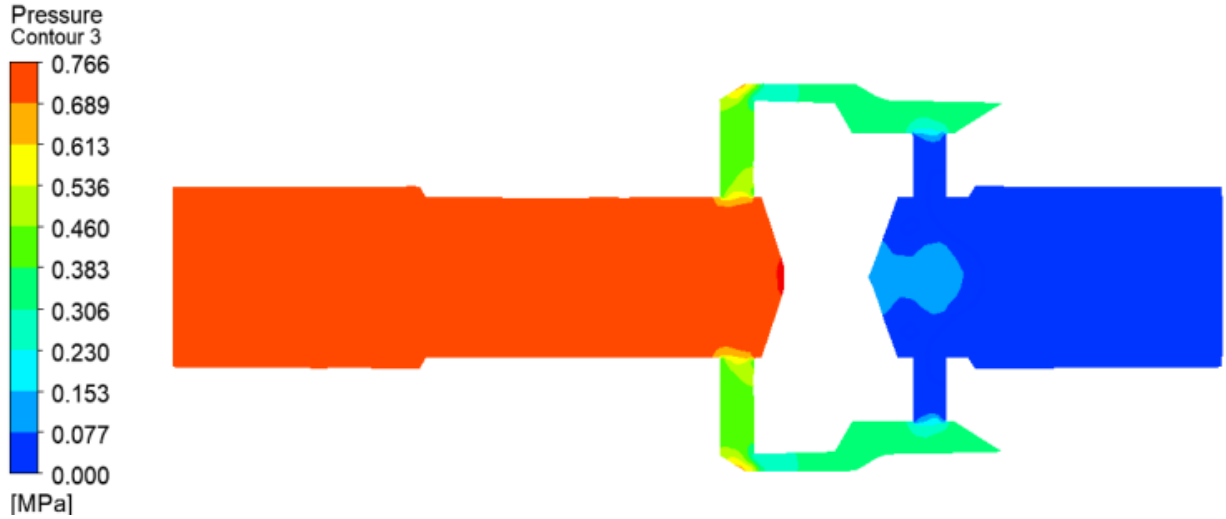

Fig.4. Contour pressure diagram for a flow rate of 50 l/min.

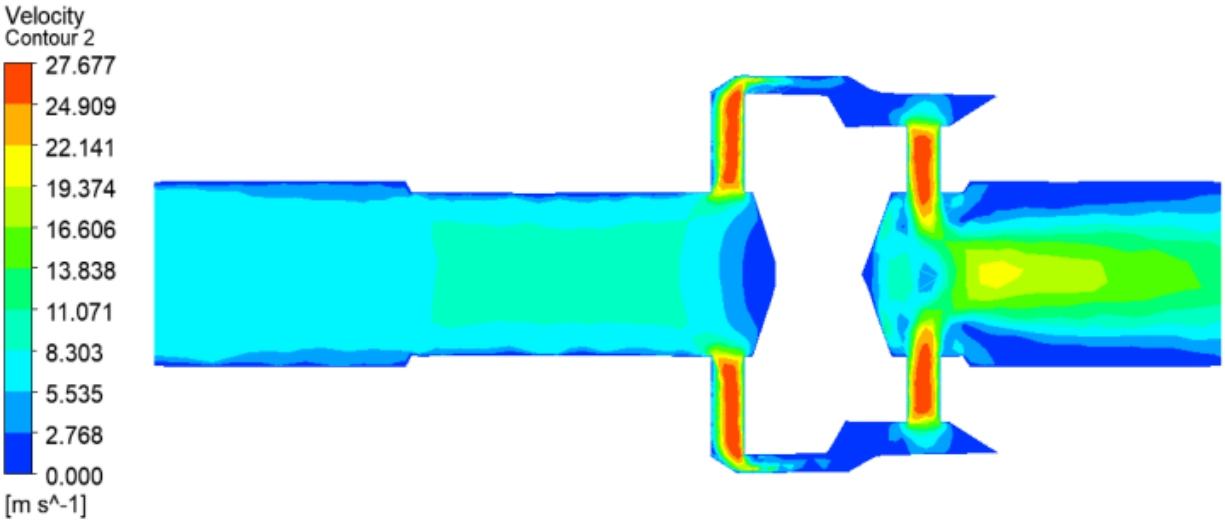

Fig.5. Contour flow velocity diagram for a flow rate of 50 l/min.

Fig.6, in addition to the characteristic itself, shows the value of the R^2 coefficient. This is the coefficient of determination used to evaluate the fit of the linear regression model to the data. The value of the coefficient R^2= 0.9718 indicates high agreement of the studied characteristics with the characteristics determined by linear regression. However, to determine the reliability of this coefficient, it is worth supplementing it with the value of the root mean square error RMSE, which gives information about the difference between actual and predicted values. For this case, the calculated value was RMSE = 0.04234. The RMSE value representing less than 10% of the spread of characteristic values can be considered low. With this information, the reliability of the coefficient of determination R^2 has been confirmed, so further analysis and comparison of subsequent characteristics can be carried out on its basis.

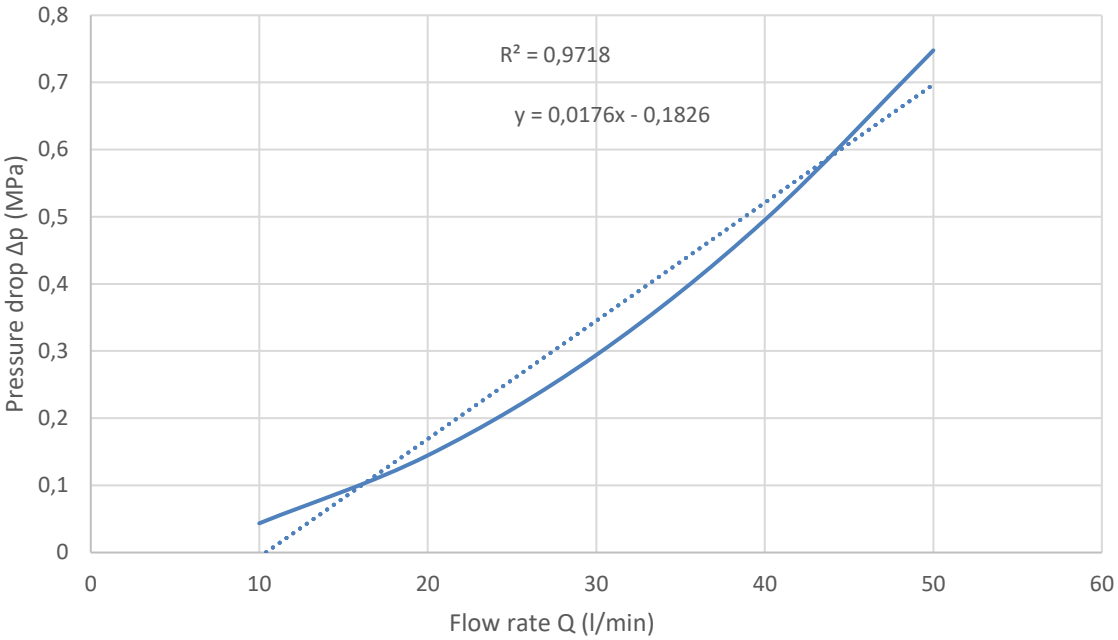

Fig.6. Flow characteristics of the original geometry of the valve.

5.2. Valve shape modification

Modification started on calculating the sensitivities of the observable variable to individual flow parameters. These are used as input data for the optimization module in the further step. Pressure drop was chosen as an observable.

Fluent's shape optimization module – Design Tool – based on the coupled sensitivities determined by Adjoint Solver performs shape optimization of the user-selected part of the geometry to achieve the optimization goal. A change in pressure drop is chosen as the optimization goal. At this stage, the desired value of this drop will be determined. However, the first step is to determine the method of morphing, that is, changing the mesh.

Part of geometry that was chosen to be modified is inner surface of the throttling gap. Defined value of change in pressure drop was set as -6% and -8% for each morphing method. Achieved geometries are compared in Table 1 along with analysis of functionality of changes and technological feasibility. The technological feasibility of the valve modification was determined by analysing its geometry, the materials used for such components and the available processing methods, taking into account the applicable tolerances and parameters of the manufacturing processes.

Table 1. Comparison of modification methods and resulting geometries.

Morphing method	Percentage of change in pressure drop	Functionality	Technological feasibility	Selection for further analysis
Polynomials	-6%	No information- invisible change	Mesh displacement values too small, below possible manufacturing tolerances	Rejected
	-8%	No information- invisible change	Mesh displacement values too small, below possible manufacturing tolerances	Rejected
Radial basis function	-6%	Operation for one valve setting only	The need for complex operations	Rejected
	-8%	Operation for one valve setting only	The need for complex operations	Rejected
Direct interpolation	-6%	Change in the whole circuit, influence in the whole range of the valve setting	Mesh displacement values close to manufacturing tolerances	Rejected
	-8%	Change in the whole circuit, influence in the whole range of the valve setting	Mesh displacement values within the manufacturing tolerances of CNC lathes	**Chosen**

As a result of modification by Direct interpolation by the value of the change in pressure drop of -8%, a gap surface geometry technologically feasible in a simple operation of turning the rounded surface of the valve inner sleeve was obtained. Displacements on the order of tenths to hundredths of a millimetre are also within the manufacturing tolerances for CNC lathes [20]. The functionality of this solution also extends to the remaining valve settings. For these reasons, the geometry was further analysed. The geometry before optimisation is shown in Fig.7. And the optimised geometry selected for further analysis is shown in Fig.8.

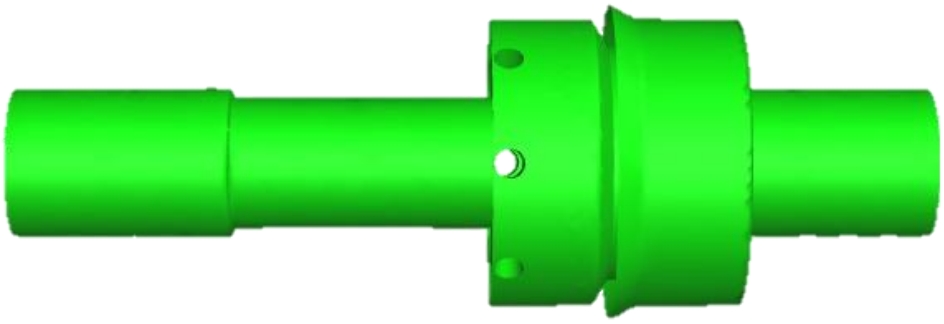

Fig.7. Geometry of the original valve (inner surface shown).

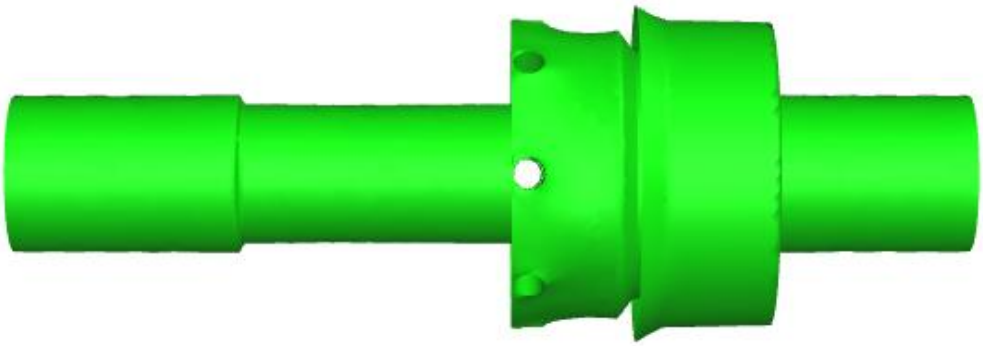

Fig.8. Geometry obtained in the modification (inner surface shown).

For the optimised geometry, flow calculations were performed again to determine its flow characteristics. Boundary conditions were the same as for the original geometry to achieve meaningful comparison. Results in the form of contour plots of pressure and velocity fields are presented in Table 2. The flow characteristics of the optimised geometry are shown in Fig.8.

Table 2. Pressure and velocity charts for optimised valve geometry.

Flow rate	Pressure charts	Velocity charts
$10\ \frac{l}{min}$	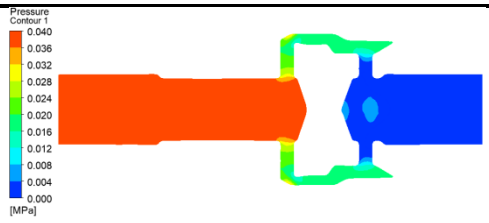	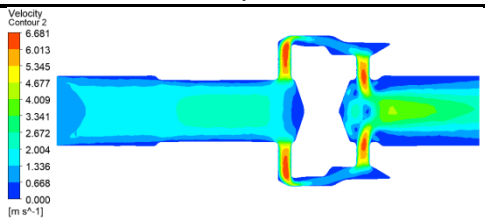
$20\ \frac{l}{min}$	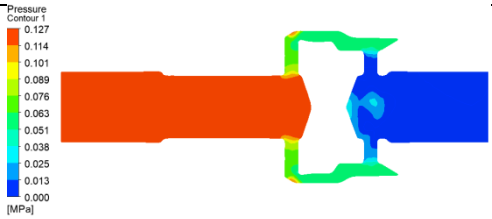	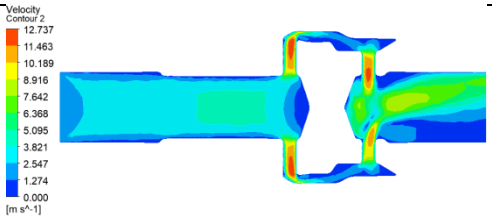

Table 3 (continued)

Flow rate	Pressure charts	Velocity charts
$30\ \frac{l}{min}$	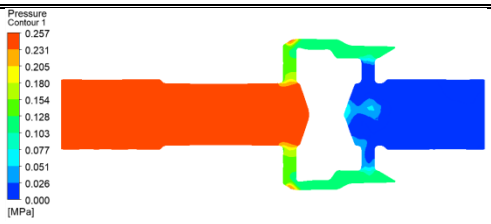	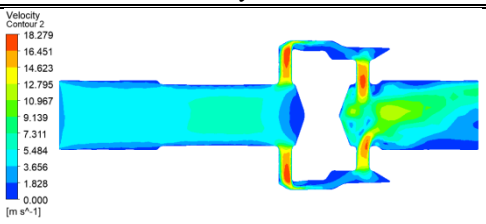
$40\ \frac{l}{min}$	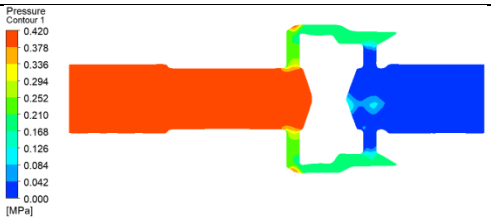	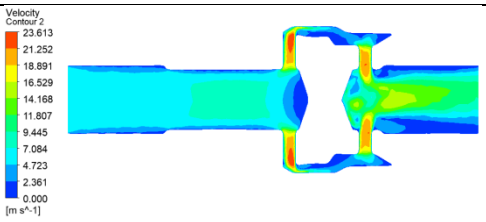
$50\ \frac{l}{min}$	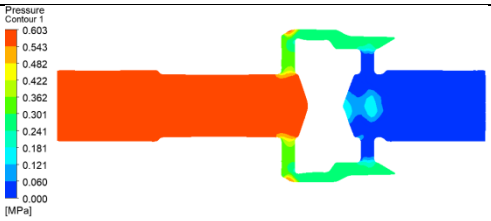	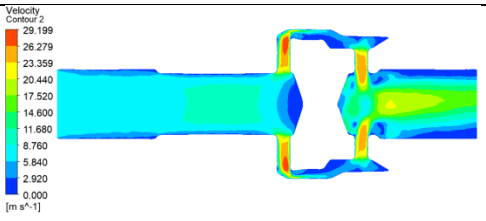

In order to compare the obtained characteristics (Fig.9), the coefficient of determination R^2 was determined. For the optimised case, it was equal to 0.9825 with RMSE = 0.026059, while for the original geometry R^2 = 0.9718 with RMSE = 0.04234.

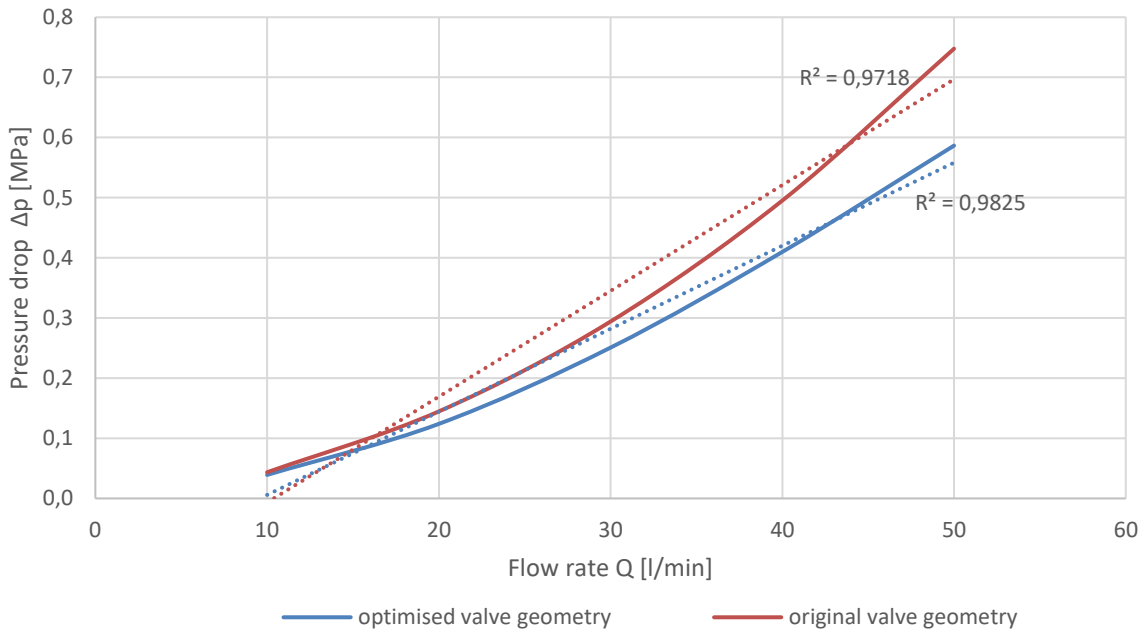

Fig.9. Flow characteristics of the optimised and original geometry of the valve.

6. Conclusion

The study demonstrates that optimizing the shape of the throttling gap in a throttle valve significantly improves the linearity of its flow characteristics. By employing computational fluid dynamics simulations and optimization algorithms, the geometrical modifications that reduce flow nonlinearity and enhance control precision were identified.

The valve with the original geometry has an R^2 of 0.9718, indicating that its characteristics are well matched to linear characteristics, but not perfectly. There is some nonlinearity in the performance of the valve in this configuration.

The valve with the modification of the internal gap area has a higher R^2 value, equal to 0.9825. This indicates that the change in the internal gap geometry improves the fit of the valve's characteristics to the linear characteristic, which may mean a more stable and predictable performance.

Compared to using complex mechanical compensation mechanisms, shape optimization offers a simpler and more economical solution, reducing manufacturing and maintenance costs. Further research could explore adaptive shape control and real-time optimization techniques to enhance valve efficiency under varying operating conditions.

References

[1] Wang, B., Zhao, X., Quan, L., Li, Y., Hao, Y., & Ge, L. (2023). *A method for improving flow control valve performance based on active differential pressure regulation*. *Measurement, 219*, 113271. https://doi.org/10.1016/j.measurement.2023.113271

[2] Lisowski, E., & Filo, G. (2017). *Analysis of a proportional control valve flow coefficient with the usage of a CFD method*. *Flow Measurement and Instrumentation, 53*(Part B), 269–278. https://doi.org/10.1016/j.flowmeasinst.2016.12.008

[3] Zhu, D., Fu, Y., Han, X., & Li, Z. (2020). Design and experimental verification on characteristics of electro-hydraulic pump. *Mechanical Systems and Signal Processing, 144*, 106771. https://doi.org/10.1016/j.ymssp.2020.106771

[4] Milani, M., Montorsi, L., & Paltrinieri, F. (2024). Experimental investigation of the suction capabilities of an innovative high speed external gear pump for electro-hydraulic actuated automotive transmissions. *International Journal of Fluid Power, 25*(2), 243–272. https://doi.org/10.13052/ijfp1439-9776.2527

[5] Castilla, R., Gamez-Montero, P. J., Ertürk, N., Vernet, A., Coussirat, M., & Codina, E. (2010). Numerical simulation of turbulent flow in the suction chamber of a gear pump using deforming mesh and mesh replacement. *International Journal of Mechanical Sciences, 52*(10), 1334–1342. https://doi.org/10.1016/j.ijmecsci.2010.06.001

[6] Pellegri, M., Manne, V. H. B., & Vacca, A. (2020). *A simulation model of Gerotor pumps considering fluid–structure interaction effects: Formulation and validation*. Mechanical Systems and Signal Processing, 140, 106720. https://doi.org/10.1016/j.ymssp.2020.106720

[7] Siwulski, T., & Warzyńska, U. (2021). Numerical investigation of the influence of the inlet nozzle diameter on the degree of fluid exchange process in a hydraulic cylinder. *Engineering Applications of Computational Fluid Mechanics, 15*(1), 1243–1258. https://doi.org/10.1080/19942060.2021.1958379

[8] Stryczek, J., & Stryczek, P. (2021). Synthetic approach to the design, manufacturing and examination of gerotor and orbital hydraulic machines. *Energies, 14*(3), 624. https://doi.org/10.3390/en14030624

[9] Li, R., Wang, Z., Xu, J., Yuan, W., Wang, D., Ji, H., & Chen, S. (2024). *Design and optimization of hydraulic slide valve spool structure based on steady state flow force*. Flow Measurement and Instrumentation, 96, 102568. https://doi.org/10.1016/j.flowmeasinst.2024.102568

[10] Zhang, C., Zhao, Y., Jiang, C., Guo, J., & Li, W. (2024). *Structure optimization of electromagnetic valve to improve electromagnetic force*. Journal of Magnetism and Magnetic Materials. https://doi.org/10.1016/j.jmmm.2024.171600

[11] Moayedi, H., Chen, Y.-C., Liu, C.-Y., & Weng, C.-I. (2024). *Geometry optimization of a vortex tube for use as a throttling device in natural gas liquefaction process*. Cryogenics. https://doi.org/10.1016/j.cryogenics.2024.103366

[12] Meng, H., Zuo, S., Ren, W., & Li, Z. (2024). *Multi-objective optimization design of triple-eccentric butterfly valve considering structural safety and sealing performance*. Engineering Failure Analysis. https://doi.org/10.1016/j.engfailanal.2024.107280

[13] Xie, B., Guo, S., Zhang, Q., Zhang, X., & Chen, H. (2025). *Multi-objective optimization of Tesla valve channel battery cold plate*. Results in Engineering, 100052. https://doi.org/10.1016/j.rineng.2025.1006826

[14] Stryczek, S. (2017). *Hydrostatic drive. Vol. 2: Systems* (2nd ed.). Polish Scientific Publishers PWN (in Polish)

[15] Danielewska-Tułecka, A., Oprocha, P., & Kusiak, J. (2009). *Optimization*. Warsaw: Wydawnictwo Naukowe PWN. (in Polish)

[16] ANSYS Inc. (2017). *ANSYS Fluent User's Guide* (Version 18.2). ANSYS Inc.

[17] https://www.ponar-wadowice.pl/!uploads/attachments_prod/mg_wk496290_pl_11.2020.pdf

[18] Orlen Oil, „HYDROL L-HL", Wersja 1 / 2023.07.17

[19] Blazek, J. (2005). *Computational fluid dynamics: Principles and applications* (2nd ed.). Elsevier

[20] Zalewski A., Grzesik W., Deja M., et al., *CNC Machine Tools: Fundamentals of Operation and Programming*, WNT, Warsaw 2024. (in Polish)

Застосування чисельного CFD моделювання та оптимізації форми для модифікації витратних характеристик дросельних клапанів

Аліція Дикас, Урсула Важинська

Вроцлавський університет науки і техніки, факультет машинобудування,
вул. Лукасевича, 5, Вроцлав, 50-371, Польща

Анотація

Метою дослідження було виконати числовий аналіз потоку оливи через прохідний отвір гідравлічного клапана за допомогою методу CFD та виконати оптимізацію профілю клапана з метою лінеаризації його характеристик. В рамках роботи було проведено аналіз витратних характеристик клапана за допомогою числового моделювання. Це дозволило розробити характеристики досліджуваного клапана. Процес оптимізації розпочався з аналізу чутливості форми, щоб визначити вплив геометрії на ключові параметри потоку, такі як перепад тиску. Одне з отриманих рішень, вибране на основі його функціональності та технологічної можливості виробництва, було додатково проаналізовано. Характеристики потоку, визначені для оптимізованої конструкції, були порівняні з характеристиками вихідного клапана за допомогою статистичних методів. Було показано, що оптимізована геометрія досягла більш лінійної характеристики, що дозволить забезпечити точніше керування процесом дроселювання за допомогою цього клапана.

Ключові слова: оптимізація форми; обчислювальна гідродинаміка; напірний клапан; перепад тиску; характеристики потоку; метод скінченних об'ємів; гідравлічні системи.

Volume 11, Number 1, 2025 44

Application of Thermal Imaging Diagnostics for Technical Maintenance of Electrical Centralization Devices in Railway Automation Systems

Maksym Silnyk*, Vasyl Fedynets

Lviv Polytechnic National University, 12 S. Bandery St., Lviv, 79013, Ukraine

Received: April 09, 2025. Revised: April 28, 2025. Accepted: May 05, 2025.

Abstract

This article examines the use of thermal imaging diagnostics for the maintenance of electrical centralization devices in railway automation. It analyzes traditional diagnostic methods, their limitations, and the risks associated with the late detection of faults (overheating). The effectiveness of thermal imaging control in detecting overheating of relay contact groups, conductor joints, transformers, and other crucial elements of electrical centralization has been proven. Mathematical models for analyzing thermal deviations are proposed, which allow predicting failures before the equipment malfunctions. The economic effectiveness of implementing thermal imagers in railway infrastructure is substantiated. The use of this technology enhances safety, reduces maintenance costs, minimizes emergency situations, shortens repair time, and improves overall equipment condition control.

Keywords: thermal imaging diagnostics; railway automation; electrical centralization; fault prediction; maintenance.

1. Definition of the scientific problem chosen for research

Railway transport is a key element of infrastructure in Ukraine and many other countries, and its uninterrupted operation depends on the reliability of electrical centralization (EC) systems. Failure of these systems may lead to train delays, disruptions to transport schedules, and, in some cases, to serious emergency situations [1], [2].

The main problem with checking the technical condition of elements is that most modern EC system diagnostic methods are based on regular inspections and reactive repairs, which do not allow for timely detection of hidden faults [3]. For example, overheating of contact groups or insulation damage in transformers may remain undetected during standard checks and lead to emergency situations [17].

Therefore, more attention is being paid to predicting faults in EC system elements using thermal imaging diagnostics. Thermal imagers allow for the quick and non-contact identification of overheating elements, which is a critical indicator of insulation wear or defects in relay contact surfaces [4].

This article analyzes classic methods of monitoring the condition of EC devices and modern trends in technical diagnostics, as well as the prospects for further research.

2. Analysis of recent publications and studies related to the problem

An analysis of recent publications and studies in the field of diagnostics and maintenance of railway automation devices indicates insufficient development of the general theoretical foundations for implementing EC control

* Corresponding author. Email address: maksym.y.silnyk@lpnu.ua

This paper should be cited as: M. Silnyk, V. Fedynets. (2025) Application of thermal imaging diagnostics for technical maintenance of electrical centralization devices in railway automation systems. *Energy Engineering and Control Systems*, Vol. 11, No. 1, pp. 44 – 52. https://doi.org/10.23939/jeecs2025.01.044

methods. Some aspects, such as improving reliability and efficiency in maintenance, have been studied in the context of specific operating conditions [1], [2].

The paper [1] discusses the issue of improving maintenance for electrical signaling and centralization devices through comprehensive monitoring of their technical condition. The author emphasizes the lack of sufficient theoretical justification for methods to determine the timing of maintenance tasks based on the actual state of EC devices, as well as the need to adjust their operating modes considering specific operating conditions.

The study [2] proposes a new approach to evaluating the effectiveness of the railway automation maintenance system. A criterion is proposed that is an integrated indicator considering both the labor intensity of maintenance and the effect achieved from its implementation. This approach can be used to select the most effective option for organizing maintenance.

Particular attention is drawn to the use of thermal imaging diagnostics in the maintenance of railway automation devices. For example, research [3] discusses the development of an automated thermal imaging system for monitoring the condition of underground heat networks [18].

The proposed system combines the use of thermal cameras and automatic data processing algorithms to detect temperature anomalies, indicating potential damage or heat leaks. Although this system was developed for heat networks, its methods can be adapted for monitoring EC devices [19].

Publication [4] describes a study of the technical diagnostics of electrical installations using a thermal imager. Special attention is paid to monitoring contact connections and transformer radiators, allowing timely detection of defects and preventing emergency situations. The author demonstrates the effectiveness of thermal imaging control in the technical diagnostics of electrical equipment.

Studies from the 1990s show that thermal imaging systems were first used to detect areas of elevated heat in electrical power supply devices [5]. However, the results indicated that the proposed thermal imaging systems had limited application for diagnosing electrical devices due to low resolution and other technical limitations. The authors argue that with further development and improvement of thermal imaging technologies, defects in contact connections, uneven loads, and other anomalies that may lead to emergency situations will be detected.

The use of thermal imaging diagnostics in the maintenance of electrical equipment and railway automation began to develop in the 1990s [9]. At early stages, the method had limitations, such as low resolution and dependence on external factors. However, modern thermal imaging systems have significantly improved, which has allowed for their wider use in various industries, including railway transport.

In work [5], the authors studied the possibilities of using thermal imaging control for diagnosing electrical networks. They note that infrared diagnostics not only allows evaluating the condition of equipment without interrupting operations but also predicts the need for repairs, which improves system reliability.

Another important research area is the development of methods for automated analysis of thermal images. Paper [6] discusses algorithms for processing thermograms to detect potential defects in electrical installations. The use of such methods combined with machine learning allows for reducing human error in diagnostic accuracy.

Based on the analysis, it can be concluded that thermal imaging diagnostics is an effective method for monitoring the condition of EC devices. However, its application in railway automation requires further research, particularly regarding the adaptation of existing technologies to specific operating conditions.

3. Aim and objectives of the research

The aim of this research is to analyze the possibilities of using thermal imaging diagnostics for the maintenance of EC devices. To achieve this, the following tasks must be solved:

- Investigate the existing methods of equipment condition monitoring and their limitations [7];
- Evaluate the effectiveness of thermal imaging control in comparison to traditional approaches [8];
- Develop mathematical models for analyzing temperature changes in EC devices [9];
- Analyze the economic efficiency of implementing thermal imagers in railway infrastructure [10].

4. Analysis of previous research and modern diagnostic methods

4.1. Traditional methods of monitoring the condition of EC devices

The maintenance of EC devices is traditionally based on the following approaches [11]:

1) Preventive maintenance – regular inspections and component replacements regardless of their actual condition;
2) Functional control – testing devices under load, assessing operation based on signals and relay conditions;
3) Electrical measurement methods – checking voltage, insulation resistance, and current levels in the electrical circuits of EC systems.

The methods mentioned above have significant disadvantages:

- They do not allow the detection of early defects (e.g., contact degradation or metal fatigue) [12];
- They require system downtime for testing, which may affect train operations [13];
- There is a considerable human factor influence, which can lead to errors during inspections [14].

4.2. Modern trends in technical diagnostics

To improve the effectiveness of diagnosing the technical condition of EC elements, automated monitoring systems are being considered, with thermal imaging diagnostics playing an important role here.

Thermal imaging control is based on the analysis of infrared radiation from heated facilities. Temperature changes in facilities are the key indicators for detecting such malfunctions [15]:

- Overheating of contacts indicates increased resistance or mechanical problems;
- Temperature anomalies in relay cabinets suggest possible short circuits;
- Increased temperature in transformer windings signals overload or insulation degradation.

Modern railway automation systems use smart algorithms to analyze thermal images to predict malfunctions and prevent accidents [16]. A comparative analysis of traditional and thermal imaging diagnostic methods is presented in Table 1.

Table 1. Comparative analysis of traditional and thermal imaging diagnostic methods.

Parameter	Traditional methods	Thermal imaging diagnostics
Diagnostic Method	Contact-based	Non-contact
Diagnostic Time	Long	Fast (up to 10 minutes)
Detection of Hidden Defects	Limited	High accuracy
Human Factor Influence	Significant	Minimal
Implementation Cost	Low	Relatively high, but cost-effective

The comparative analysis in Table 1 shows that the use of thermal imaging control allows reducing the number of emergency situations and improving the effectiveness of EC device maintenance.

5. Methods of thermal imaging diagnostics research

5.1. General principles of thermal imaging analysis

Thermal imaging control is based on the analysis of infrared radiation from the facilities, which enables determining their temperature without contact [17].

The main stages of studying the condition of EC devices using a thermal imager include:

1) Preliminary thermography – capturing thermal images in normal operating conditions;
2) Analysis of thermal deviations – comparing the obtained temperatures with reference values;
3) Recording anomalous zones – detecting overheating of contacts, connections, or power supply units;
4) Predicting possible malfunctions – assessing the temperature change dynamics using mathematical models.

Compared to traditional methods, thermal imaging analysis has several advantages:

- It does not require system shutdown for inspection;
- It allows for rapid evaluation of the condition of all components;
- It detects overheating before equipment failure.

5.2. Use of thermal maps to assess the condition of devices

Thermal maps are color images that show the temperature distribution on the surface of equipment. In the case of EC devices, the most critical areas are as follows:

- Contact groups – increased resistance causes local heating;
- Relay blocks – contact wear can lead to overheating beyond normal levels;
- Power supply units – voltage stabilization issues lead to overheating of components.

Identifying such anomalies enables the timely planning of maintenance work and helps avoid emergency shutdowns.

6. Mathematical models for analyzing temperature anomalies

6.1. Calculation of normal temperature regime

To effectively analyze the technical condition of a component, it is necessary to know the optimal operating temperature of each system component. The contact temperature under normal operating conditions is determined by the heat balance equation:

$$T_{norm} = T_{average} + \frac{P \cdot R}{k}, \tag{1}$$

where T_{norm} is expected element temperature under normal conditions; $T_{average}$ is average ambient temperature; P is electrical power at the contacts; R is contact resistance; k is heat transfer coefficient.

If the actual temperature exceeds the calculated value by 5-10%, it may indicate a potential malfunction.

Using formula (1) with the following parameters at an ambient temperature of $T_{average}$ = 25 °C, contact electrical power P = 50 W, contact resistance R = 0.02 Ohm and heat transfer coefficient k = 0.8, the normal contact temperature will be as follows:

$$T_{norm} = 25 + \frac{50 \cdot 0.02}{0.8} = 26.25°\text{C}.$$

If a temperature of 30°C is recorded during diagnostics, which exceeds the norm by ≈15 %, this indicates the potential development of a malfunction.

6.2. Determining critical temperature deviations

The critical temperature deviation, which indicates a potential failure, is determined by the following equation:

$$\Delta T_{critical} = T_{max} - T_{norm}, \tag{2}$$

where T_{max} is maximum recorded temperature on the component.

If T_{max} > 15 °C, an urgent technical inspection is required.

During the analysis of the transformer thermogram, T_{max} = 72 °C was recorded. The maximum permissible value according to the method is 15 °C above the norm. Provided that the normal temperature T_{norm} = 50 °C, an excess of 22 °C indicates the need for urgent technical inspection of the transformer.

6.3. Fault prediction based on thermal deviations

For long-term analysis, it is advisable to use a thermal degradation model for contacts, which is expressed by the equation:

$$T(t)=T_0+\alpha\cdot e^{\beta t}, \quad (3)$$

where $T(t)$ is temperature of the element at time t; T_0 is initial temperature of the element; α is initial thermal deviation; β is degradation rate coefficient; t is operating time.

If the temperature exceeds the acceptable values faster than predicted, it signals the need for contact or relay node replacement.

The initial temperature of the contact group is set to T_0 = 30 °C, the degradation coefficient β = 0.02 °C/h, and the initial thermal deviation α = 2 °C. The temperature forecast after 100 hours of operation is made using formula (3): $T(100) \approx 44.78$ °C.

If the actual thermogram readings show a temperature of 50 °C, this indicates accelerated contact aging.

6.4. Use of machine learning algorithms for analyzing temperature trends

Modern thermal imaging systems can use artificial intelligence for automatic detection of problem areas. This is possible through the analysis of temperature graphs over time.

Main algorithms used:

- Linear regression – for predicting temperature growth;
- Neural networks – for detecting abnormal temperature values;
- Principal Component Analysis – for identifying the most at-risk areas in the system.

Such approaches allow for the automatic determination of the likelihood of equipment failure before the problem becomes critical.

7. Discussion of thermal imaging diagnostics results

Traditional methods of diagnosing devices (EC) often do not allow for early detection of malfunctions due to their limited accuracy. For example, electrical measurement methods can only detect anomalies after significant wear of the contacts, while thermal imaging allows for the identification of early stages of degradation through temperature change analysis.

Research results show that thermal imaging diagnostics reduce the number of emergency failures by 35-50%, significantly improving the safety of railway automation.

The main advantages of thermal imaging control include:

- Detection of hidden faults – contact groups, relays, and wiring may overheat long before mechanical failure occurs;
- Automation of the diagnostic process – the ability to connect thermal imagers to remote monitoring systems;
- Speed of inspection – studies show that a single thermal imaging inspection takes on average 5-10 minutes, whereas traditional methods take 2-4 hours.

8. Examples of using thermal imagers in EC device diagnostics

In our study, we analyzed the condition of contact relay cabinets at railway stations using infrared cameras. It was found that:

- 10% of relays had elevated temperatures (>70 °C), indicating contact wear;
- 15% of connections had excessive heating (>50 °C) due to loosening of connections;
- Cases of early-stage insulation burning not detected by traditional inspection methods were identified.

This allowed for timely problem resolution and helped avoid system failure.

As a result of implementing thermal imaging control of switch point electric drives on mainline railways, it was found that in 8% of cases, the heating elements of electric drives were operating with reduced efficiency, leading to the formation of frost on the automatic switch contacts and further deterioration of electrical contact during the winter period.

Thanks to thermal imagers, heating heterogeneity was identified, and defective heaters were promptly replaced, reducing train delays during the winter period.

The condition of power supply units and transformers at electric centralization stations was also studied. It was found that:

- 30% of devices had localized overheating zones due to the loss of insulation properties;
- 20% of transformers were operating in overload mode, which could lead to emergency shutdown.

The use of thermal imaging monitoring enabled the implementation of an automated control system that alerted maintenance personnel in real-time about overheating risks [20], [21].

The heat map of the overheated wire connection is shown in Fig.1. The image of transformer overheating due to overload is shown in Fig.2.

Fig.1. Thermal map of wire connections with excessive heating.

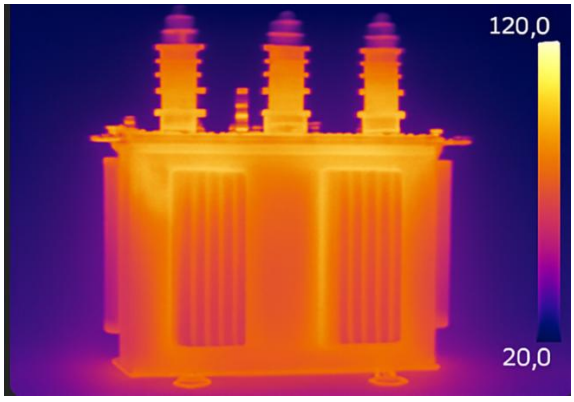

Fig.2. Transformer overheating due to overload.

9. Analysis of the economic efficiency of implementing thermal imaging diagnostics

To assess the feasibility of implementing thermal imaging control, it is necessary to compare the operating costs of traditional diagnostic methods and the costs of introducing infrared monitoring.

According to studies, the costs of traditional control of EC devices include:

- Personnel: each electromechanic engineer performs approximately 4 inspections per day, requiring labor costs and significant personnel expenses;
- Diagnostic time: one inspection takes about 3 hours, while thermal imaging inspection takes 10-20 minutes;
- Repair costs: due to late detection of faults, the number of emergency repairs increases, which are 2-3 times more expensive than planned work.

Table 2 below compares the costs of traditional methods and thermal imaging diagnostics as of 2020.

Table 2. Comparison of costs for traditional and thermal imaging control.

Parameter	Traditional methods	Thermal imaging diagnostics
Inspection time (1 facility)	≈3 hours	10-20 minutes
Average inspection cost	UAH 2,000	UAH 700
Detection of hidden defects	Limited	High accuracy
Frequency of failures due to late diagnosis	High	Reduced by 35-50%
Repair costs (per facility)	≈ UAH 50,000	≈ UAH 20,000

The results show that the use of thermal imagers allows reducing diagnostic and repair costs by more than half.

To evaluate the economic feasibility of implementing thermal imaging control, we use the payback period formula:

$$T_{payback} = \frac{C_{implementation}}{C_{savings}}, \quad (4)$$

where $T_{payback}$ is payback period (in years); $C_{implementation}$ is total costs for purchasing thermal imagers and training personnel; $C_{savings}$ is annual savings due to reduced diagnostic and emergency repair costs.

According to [11], the average total cost of implementing a thermal imaging control system for 10 facilities is ≈ UAH 500,000. The annual savings from reduced emergency repairs and quick diagnostics amount to ≈ UAH 250,000. Accordingly, the payback period of the thermal imaging monitoring system will be $T_{payback} = 2$ years.

In addition to cost savings, thermal imaging diagnostics has several additional advantages:

- Reduction of operational risks – early detection of overheating of various elements helps prevent accidents;
- Improved safety of operations – reducing the number of unexpected system failures in centralization systems;
- Reduced energy consumption – eliminating problematic contacts helps optimize energy usage;
- Automation of the diagnostic process – integrating thermal imaging systems with digital service platforms.

10. Conclusion

The conducted research confirmed that thermographic diagnostics is an effective method for technical control of electric signaling and centralization (EC) devices.

The main results of the work are as follows:

1) The advantages of thermographic control compared to traditional diagnostic methods have been established:
   - Non-contact detection of faults at early stages;
   - 5-10-fold reduction in diagnostic time;
   - Reduction in the probability of emergency failures by 35-50 %.
2) Mathematical models for analyzing temperature deviations have been developed, allowing the prediction of the risks of overheating in contact groups and relay blocks.

3) The economic feasibility of implementing thermal imagers has been determined, according to which the payback period is approximately 2 years due to reduced maintenance and repair costs.

4) Real cases of using thermal imagers for the control of relay cabinets, turnout switches, and transformers have been reviewed, confirming the effectiveness of this method in railway automation.

Further research can be focused on:

- Integrating thermographic monitoring with artificial intelligence systems for automatic analysis of temperature anomalies;
- Optimizing software for processing thermograms and integrating them with existing digital platforms for managing railway infrastructure;
- Reducing energy consumption – eliminating problematic contacts helps optimize energy usage;
- Expanding the use of thermal imagers to other types of equipment, including traction substations and high-voltage power lines.

References

[1] Moroz V.P. Improving the technical maintenance of electrical signaling and centralization devices through comprehensive control of technical condition. – K.: Tekhnika, 2010. – 250 p. (in Ukrainian)

[2] Lapko A.O. An approach to assessing the effectiveness of the railway automation device maintenance system. – Lviv: Svit, 2012. – 180 p. (in Ukrainian)

[3] Yuzvak O.O. Automated thermal imaging system for monitoring the condition of underground heating networks. – Kharkiv: Prapor, 2015. – 200 p. (in Ukrainian)

[4] Vnukov V.D. Thermal imaging control of contact connections and transformer radiators. – Odesa: Astroprint, 2011. – 220 p. (in Ukrainian)

[5] Control of heating of contact joints. – Donetsk: Donbas, 1998. – 150 p. (in Ukrainian)

[6] Petrenko I.M., Sydorenko O.V. Application of thermal imaging diagnostics in electric power industry. Electrical Engineering and Electromechanics. 2018. No. 2. Pp. 45–50. (in Ukrainian)

[7] Kovalenko P.S., Ivanchenko R.M. Using thermal imaging for diagnostics of electrical networks. Technical diagnostics and non-destructive testing. 2019. No. 3. pp. 32–38. (in Ukrainian)

[8] Semenov A.V., Kravchenko D.O. Thermal imaging diagnostics of electrical equipment: automated image analysis. Kyiv: Tekhnika, 2020. – 240 p. (in Ukrainian)

[9] Smith J., Brown K. Application of infrared thermography in railway signaling maintenance. – Railway Technical Journal, 2020. – Vol. 12, No. 4. – P. 45-52.

[10] European Rail Agency Report. Predictive maintenance in railway infrastructure using thermal imaging. – ERA Publications, 2021. – 134 p.

[11] Johnson L., Kettering D. Cost analysis of implementing infrared thermography in railway diagnostics. – Journal of Railway Engineering, 2019. – Vol. 28, No. 3. – P. 112-125.

[12] National Transport Safety Board. Failure analysis of railway signaling systems due to thermal degradation. – NTSB Technical Report, 2022. – 78 p.

[13] Gonzalez R., Patel S. AI-driven thermal monitoring for railway automation. – Smart Rail Technologies, 2023. – Vol. 5, No. 2. – P. 88-97.

[14] ISO 18434-1:2008. Condition monitoring and diagnostics of machines – Thermography – Part 1: General procedures.

[15] Jones M., White P. Advances in thermal imaging for industrial applications. – Applied Infrared Journal, 2022. – Vol. 15, No. 1. – P. 99-115.

[16] Railway Standards Board. Best practices for infrared inspection of railway infrastructure. – Technical Manual, 2023. – 200 p.

[17] Bagavathiappan S., Lahiri B.B., Saravanan T., Philip J., Jayakumar T. Infrared thermography for condition monitoring – A review. – Infrared Physics & Technology, 2013. – Vol. 60. – P. 35–55. https://doi.org/10.1016/j.infrared.2013.03.006

[18] Maldague X.P.V. Theory and Practice of Infrared Technology for Nondestructive Testing. – New York: Wiley-Interscience, 2001. – 684 p.

[19] Wang K., Zhang J., Ni H., Ren F. Thermal Defect Detection for Substation Equipment Based on Infrared Image Using Convolutional Neural Network. – Electronics, 2021. – Vol. 10, No. 16. – Article 1986. https://doi.org/10.3390/electronics10161986

[20] Stypułkowski, K., Gołda, P., Lewczuk, K., & Tomaszewska, J. (2021). Monitoring System for Railway Infrastructure Elements Based on Thermal Imaging Analysis. *Sensors*, *21*(11), 3819. https://doi.org/10.3390/s21113819

[21] Anand R., Ansari M.A. Intelligent Condition Monitoring of Electrical Assets Using Infrared Thermography and Image Processing Techniques. – In: Sharma D.K. (ed.) Micro-Electronics and Telecommunication Engineering (ICMETE 2021). Lecture Notes in Networks and Systems, vol. 373. Singapore: Springer, 2022. – P. 47–59. https://doi.org/10.1007/978-981-16-8721-1_5

Застосування тепловізійної діагностики для технічного обслуговування пристроїв електричної централізації в системах залізничної автоматики

Максим Сільник, Василь Фединець

Національний університет «Львівська політехніка», вул. С. Бандери, 12 , Львів, 79013, Україна

Анотація

У статті розглянуто дослідження застосування тепловізійної діагностики для технічного обслуговування пристроїв електричної централізації залізничної автоматики. Проаналізовано традиційні методи діагностики, їхні обмеження та ризики, пов'язані з несвоєчасним виявленням несправностей (перегрівання). Доведено ефективність тепловізійного контролю у виявленні перегрівання контактних груп реле, з'єднань струмопровідних частин, трансформаторів та інших важливих елементів електричної централізації. Запропоновано математичні моделі аналізу теплових відхилень, що дають змогу прогнозувати несправності ще до виходу обладнання з ладу. Обґрунтовано економічну ефективність впровадження тепловізорів у залізничну інфраструктуру. Використання цієї технології підвищує безпеку руху, зменшує витрати на технічне обслуговування, мінімізує аварійні ситуації, скорочує час ремонту та покращує загальний контроль стану обладнання.

Ключові слова: тепловізійна діагностика; залізнична автоматика; електрична централізація; прогнозування несправностей; технічне обслуговування.

Volume 11, Number 1, 2025

Analysis of Methods for Training Robotic Manipulators to Perform Complex Motion Trajectories

Yurii Senchuk*, Fedir Matiko

Lviv Polytechnic National University, 12 Stepana Bandery St., Lviv, 79013, Ukraine

Received: April 16, 2025. Revised: June 23, 2025. Accepted: June 27, 2025.

Abstract

The article examines current approaches to training robotic manipulators for executing complex tasks in dynamic and changing environments. It provides a comparative analysis of modern training methods, highlighting their advantages and disadvantages. Additionally, the paper outlines the typical areas in which these methods are applied. Particular attention is given to approaches that involve human instructors, self-learning, and reinforcement learning. Special emphasis is placed on training efficiency, robot adaptability to new conditions, human-robot interaction, and the transfer of skills from virtual training environments to the real world. Based on the analysis, the authors recommend imitation learning — specifically, the learning from demonstration approach — as it enables the rapid and safe transfer of skills from humans to robots without the need for task formalization. The article also highlights the challenges of adapting trained models to real-world conditions and ensuring effective human-robot collaboration. It identifies key challenges faced by modern robot training systems. Based on these challenges, the article offers recommendations for selecting optimal training strategies according to the specific task type and available resources.

Keywords: robotics; robotic manipulators; teaching methods; adaptability.

1. Definition of the problem to be solved

In the context of today's rapid advancements in robotics and industrial automation, there is a growing demand for robotic manipulators to perform tasks that require high accuracy, adaptability, and autonomy. At the same time, traditional programming methods that rely on hard-coded scripts and predefined trajectories often do not permit rapid adaptation of the system to environmental changes. Additionally, these methods require considerable time and highly skilled personnel.

The challenge of teaching robotic manipulators to follow complex trajectories is particularly relevant today. These trajectories often involve multiple stages, interactions with various objects, and operation in dynamic or partially uncertain environments. One promising direction for solving this issue is the use of intelligent learning methods. These methods include approaches based on environmental interaction, action demonstration, and adaptive generalization of prior experience. However, the limitations, capabilities, and suitability of these methods for complex trajectory formation tasks still require further analysis and comparison.

Therefore, there is a need for an approach to training robotic manipulators that ensures rapid learning of new motion paths. This approach should minimize dependence on manual programming, allow adaptation to environmental changes, and reduce implementation time and cost. This need is particularly important for next-generation flexible robotic systems, where self-learning capabilities are a key performance factor.

* Corresponding author. Email address: yurii.m.senchuk@lpnu.ua

This paper should be cited as: Y. Senchuk, F. Matiko. (2025) Analysis of methods for training robotic manipulators to perform complex motion trajectories. *Energy Engineering and Control Systems*, Vol. 11, No. 1, pp. 53 – 61. https://doi.org/10.23939/jeecs2025.01.053

2. Analysis of the recent publications and research works on the problem

Recent research in the field of robotics demonstrates a growing interest in intelligent methods for training robotic manipulators. The objective is to enhance system flexibility and adaptability while reducing reliance on manual programming.

Papers [1]–[3] provide an overview of imitation learning methods based on demonstrations, along with practical considerations for implementing these systems in industrial settings. Articles [6], [7] introduce the fundamentals of reinforcement learning, while studies [9], [10] focus on deep learning algorithms designed for continuous monitoring. The inverse reinforcement learning approach — which enables the recovery of expert goals from observational data, is presented in [11]. The implementation of collaborative learning and the organization of agent interactions in real-world industrial environments are discussed in [12]–[14].

A number of publications [15]–[22] explore alternative approaches that demonstrate potential for reducing the need for training data and enhancing adaptability. However, these methods remain insufficiently studied in the context of using robotic manipulators for training, particularly for tasks involving the reproduction of complex trajectories in dynamic environments.

Despite significant theoretical progress, the practical application of these methods — especially in reproducing complex trajectories in dynamic environments — remains an open challenge. This underscores the need for further analysis of their effectiveness in relation to the demands of the requirements of modern robotic production.

3. Formulation of the goal of the paper

The aim of this article is to review and compare modern methods for training robotic manipulators. It seeks to identify their advantages and limitations and to develop recommendations for their application based on the types of tasks being addressed. In particular, the authors focus on analyzing the use of current approaches in imitation learning, reinforcement learning, collaborative learning, self-learning, and hybrid strategies. These methods are examined in the context of training robotic manipulators to execute complex motion trajectories.

4. Analysis of methods for teaching robot manipulators

The following section provides an overview of current approaches aligned with the stated objective. It focuses on investigating the capabilities of modern learning methods to reproduce complex motion trajectories. Special attention is given to methods that enable robotic manipulators to acquire skills with minimal human intervention.

Imitation learning refers to the transfer of skills from a human to a robot through the demonstration of required actions. As noted in [1], during imitation training, a robotic manipulator learns to perform tasks by replicating the movements of an expert — either a human or another agent — who has demonstrated the actions in advance. Demonstrations may be provided in various forms, including direct control (e.g., via a joystick), physical guidance of the manipulator (kinesthetic teaching), or observation through video or sensor data.

This approach enables the acquisition of skills without the need for a formal algorithmic description. Consequently, it significantly reduces the level of user expertise required and simplifies the process of programming the robot. This technique is particularly effective in scenarios where formulating an optimal action strategy is difficult, yet demonstrating the desired behavior is relatively straightforward.

The primary advantage of this method is its ability to enable rapid skill acquisition by a robot through direct demonstration. This significantly reduces the time required for system training compared to alternative approaches. The method is particularly effective for tasks in which constructing an optimal algorithm and formalizing its individual steps is challenging. For example, robots can learn manipulation tasks that require fine motor skills by observing human actions. This approach minimizes the likelihood of errors during the initial stages of system operation, as the learning process is based on demonstrated and validated behaviors [2].

One of the key challenges associated with this approach is its limited generalization capability. A robot may fail to handle situations that differ from those encountered during training. Addressing this limitation often requires additional demonstrations or integration with other learning methods. Furthermore, the effectiveness of the approach largely depends on the quality and precision of the expert's demonstrated actions.

Depending on the mode of interaction between the operator and the robot, the demonstration of the desired behavior can be carried out using different approaches. The most common of these include:

a) **Kinesthetic teaching**, in which the operator physically guides the manipulator, and the system records the movements using its internal sensors.

b) **Teleoperation**, where the robot is operated remotely through specialized interfaces such as joysticks, motion trackers, tactile gloves, or external manipulators.

c) **Passive observation**, where information about the operator's actions is obtained through external sensors — such as video cameras — without direct physical contact with the robot.

The classification of demonstration methods proposed in [3] is relevant for industrial environments. In these settings, factors such as integration flexibility, minimal disruption to existing workflows, and safety are critically important. The second and third approaches — telerobotic control and passive observation — are especially practical for industrial applications, as they enable robot training in scenarios where direct physical contact is either undesirable or technically constrained.

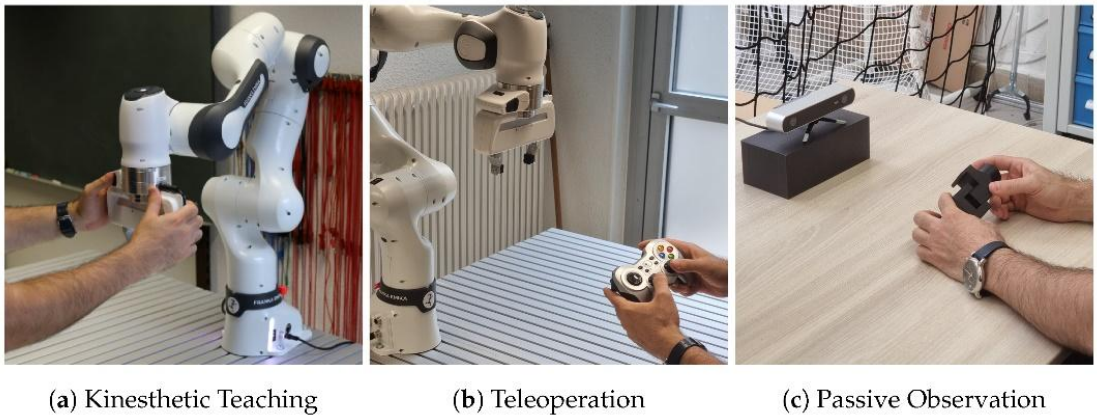

Fig.1. Examples of approaches to demonstrating desired actions during robot training [3].

Among the most commonly used imitation learning algorithms are Behavioral Cloning (BC) and Dataset Aggregation (DAgger). Behavioral Cloning treats the learning process as a classical supervised learning task with a teacher. In contrast, DAgger addresses the issue of error accumulation that is typical of the standard Behavioral Cloning method.

According to [4], BC is a fundamental approach in which a training dataset is constructed from expert demonstrations in the form of situation–action pairs. These pairs consist of input data from sensors and the corresponding actions performed by the operator. Based on this data, a model is trained to replicate the expert's behavior. The algorithm is relatively simple to implement and can produce quick results, particularly when the demonstrations are of high quality and sufficiently cover the range of possible behaviors.

However, a significant limitation of this approach is the phenomenon known as **covariate shift**. Even a slight deviation of the robot from the demonstrated trajectory may cause the system to enter a state that is not represented in the training data. In such cases, the robot is unable to determine the correct course of action.

To address this limitation, the DAgger algorithm was introduced in 2011 [5]. It employs an iterative learning process in which the robot performs actions autonomously, while an expert provides optimal action suggestions for each encountered state. As a result, a new dataset is generated that includes situations the robot experiences during its execution. This data is incrementally added to the initial training set, which significantly expands the coverage of possible states and reduces the impact of error accumulation during execution.

This approach substantially improves the robot's behavioral stability and its ability to operate in previously unencountered situations. However, DAgger requires the continuous involvement of an expert at each iteration, which can be burdensome in real-world applications — particularly when real-time precision is necessary.

Reinforcement Learning (RL) is based on the principle that a system learns through interactions with its environment, receiving rewards or penalties depending on the outcomes of its actions. The primary objective of this approach is to maximize cumulative reward, thereby encouraging the development of effective behavior [6]. As a result, the robot can gradually learn optimal actions to achieve its goals, even without prior knowledge of the environment.

Figure 2 illustrates the interaction scheme between the agent and the environment in the context of reinforcement learning for a robotic manipulator. Based on observations from the current state S_t, the agent generates an action A_t and sends it to the environment. In response, the environment returns a new state S_{t+1} and a reward R_t, which are then used to update the agent's action policy.

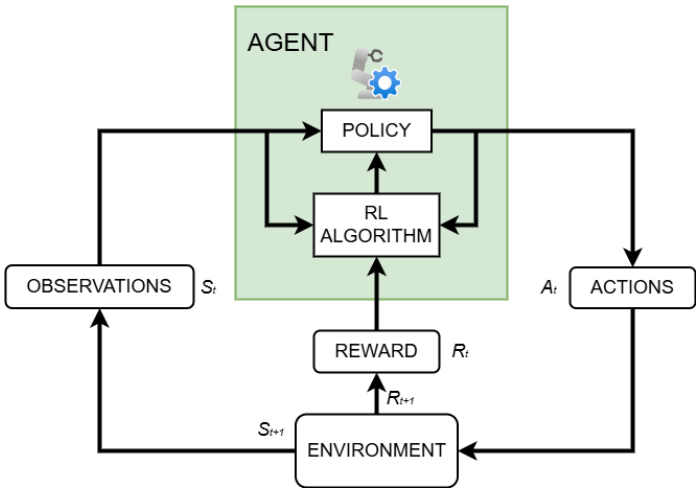

Fig.2. Scheme of interaction between the agent and the environment in the method of reinforcement learning of a robot manipulator.

The key advantages of RL include its capacity for autonomous learning, adaptability to new conditions, and the ability to operate without requiring demonstrations or pre-labeled data. However, the learning process typically demands a large number of episodes, substantial computational resources, and significant time. An additional challenge is ensuring the stability and convergence of RL algorithms, which often requires careful tuning of parameters [7].

Additionally, the risk of hardware damage during real-world experimentation must be considered. For this reason, RL is usually first implemented in simulation environments. However, this practice introduces the well-known problem of sim-to-real transfer — that is, the difficulty of transferring learned behaviors from simulation to physical systems [7].

Article [8] discusses the integration of reinforcement learning with deep neural networks, which led to the emergence of the field known as **Deep Reinforcement Learning**. This approach allows agents to operate in complex state spaces and manage continuous action domains.

The practical reinforcement learning algorithms include Proximal Policy Optimization (PPO) [9] and Soft Actor-Critic (SAC) [10]. PPO promotes stable learning by constraining abrupt changes in the robot's behavior during model updates, thereby increasing the reliability of the training process. In contrast, SAC is based on the principle of maximum entropy, encouraging the robot not only to perform actions with high precision but also to actively explore alternative behaviors. This enhances the system's ability to adapt to complex and unpredictable environmental conditions.

Inverse Reinforcement Learning (IRL) is a method that enables the training of a robot manipulator by observing the actions of an expert, without requiring a predefined reward function [11]. In contrast to classical Reinforcement Learning (RL), where the system receives explicit feedback indicating which actions are desirable, IRL seeks to deduce the expert's underlying objective solely from observed behavior.

This approach is particularly useful in situations where it is difficult or even impossible to explicitly formalize the desired behavior using a clear reward function. In such cases, manually defining all necessary criteria becomes a major challenge. For example, a human can easily demonstrate how to handle a fragile object with care. However, mathematically specifying all the relevant parameters for this task is extremely difficult. IRL allows the system to learn from such demonstrations. This reduces the need for manual reward function design and enables flexible reproduction of behavior, even under changing conditions.

The primary advantage of this method is its ability to enable learning without explicitly defining the objective. This is particularly valuable for tasks that depend on intuitive human experience. At the same time, Inverse Reinforcement Learning (IRL) has several significant limitations. First, multiple reward functions can explain the same observed behavior, leading to an ambiguity problem. Second, the implementation of IRL is computationally complex and often requires substantial computational resources. In addition, the quality of the results strongly depends on the accuracy and completeness of the expert demonstrations.

Collaborative Learning (CL) involves interaction among multiple robotic manipulators or between a robot and a human, with the aim of acquiring shared skills for performing tasks. The core concept of this method is that the experience gained by one agent during training can be transferred to others through knowledge exchange, observation of partners' actions, or direct interaction [12].

Such knowledge transfer can be organized in two ways: centrally, through a shared memory or control module, or in a decentralized manner, via message passing, signaling, or by interpreting the actions of other agents [12]. Additionally, CL often includes human–robot interaction, which enables more intuitive and comprehensible cooperation from the perspective of the human participant.

This approach is especially valuable for tasks that require coordinated actions. Examples include collective assembly, the manipulation of large or heavy objects, and scenarios that involve close interaction with a human operator.

In such cases, CL enhances efficiency by supporting role distribution, joint action planning, and the use of complementary capabilities among agents. Furthermore, human involvement contributes to a more intuitive and natural learning environment, which in turn enhances the overall performance of the system [13].

The advantages of the approach include accelerated learning through shared experience, a reduction in the number of required training episodes, and increased system robustness to environmental changes.

However, the implementation of CL presents several challenges. The most critical among them are the need for effective communication between agents, alignment on shared goals, prevention of action conflicts, and resolution of possible discrepancies in environmental perception or task interpretation.

One example of a modern approach to CL is the DEEPCOBOT project (Collective Efficient Deep Learning and Networked Control for Multiple Collaborative Robot Systems) [14]. This platform focuses on developing decentralized deep learning techniques for groups of collaborative robots that interact with one another and with human operators in real time.

A distinctive feature of the approach is local training performed by each agent, followed by knowledge exchange across the network without relying on a central server. This architecture supports scalability, fault tolerance, and accelerated collective learning. DEEPCOBOT robots are capable of adapting to changes in the production environment, coordinating their actions, and safely cooperating with human operators.

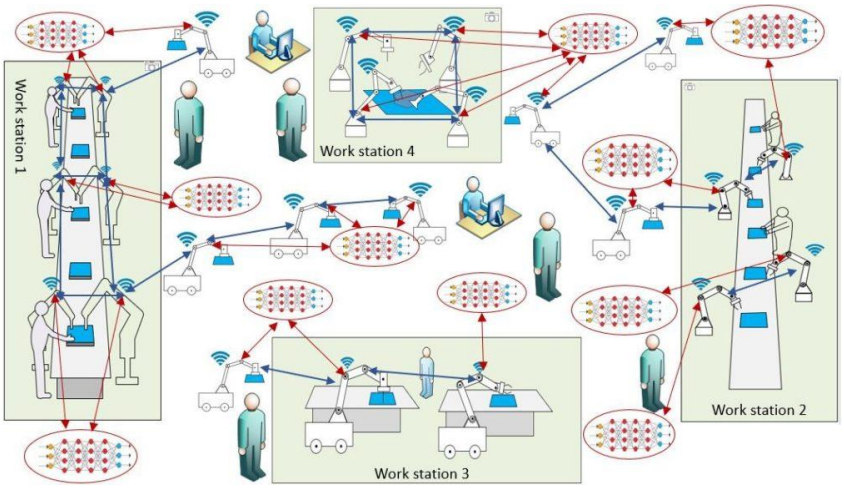

Fig.3. Collaborative interaction of robots in a production environment with decentralized deep learning [14].

Modern robotics tasks increasingly require systems that are not only accurate but also flexible, adaptable, and capable of rapid learning in complex and dynamic environments. No single training method can fully satisfy all of these requirements. As a result, there is growing interest in **combined** and **hybrid** approaches that integrate the strengths of multiple learning paradigms. These strategies for training robotic manipulators aim to enhance overall system efficiency, adaptability, and robustness. Such hybrid methods are currently being investigated in research and practical applications, particularly in environments characterized by high uncertainty and variability.

For example, in [15], the authors propose a combination of imitation learning and reinforcement learning. In this approach, the robot first acquires initial skills through expert demonstrations. Subsequent improvement is achieved through autonomous interaction with the environment using RL algorithms.

Another common strategy involves integrating classical control methods, such as PID controllers, with neural network models. This hybrid approach enables effective adaptation of robot behavior to changing environmental conditions [16].

The primary advantage of hybrid approaches lies in their ability to eliminate or mitigate the limitations of individual learning methods. These approaches can accelerate the training process, decrease computational requirements, and simultaneously provide the flexibility and adaptability needed for robotic manipulators to perform diverse tasks under varying operating conditions.

However, the use of combined methods presents specific challenges. One of the primary difficulties is selecting appropriate methods for integration and optimizing their interaction. Additionally, hybrid systems often result in increased architectural complexity, which demands a high level of expertise in system design and implementation.

Another promising and emerging area is **few-shot learning** and **unsupervised learning**, which are particularly relevant in environments where collecting large amounts of labeled data are complex, costly, or impractical. These methods allow robotic manipulators to adapt to new situations using only minimal prior information or without any explicit supervision.

In the case of few-shot learning, a robot can acquire a new skill based on only a few demonstrations [17]. This capability is enabled by meta-learning approaches [18], which allow systems to "learn how to learn" — that is, to leverage prior experience from previously solved tasks in order to rapidly adapt to new ones. This method is particularly effective in scenarios where quick adaptation is required, for example, when learning novel actions or interacting with unfamiliar objects that the system has not previously encountered.

Unsupervised learning, as described in [19] and [20], enables a system to learn the structure of its environment without relying on pre-labeled examples. Instead of using manually prepared data, the robot analyzes raw observations to identify patterns, group similar states, or perform clustering. These capabilities form a foundation for subsequent goal-directed learning. As a result, unsupervised learning is considered a promising approach for developing autonomous robotic systems. Such systems are capable of exploring their environment independently and gradually improving their behavior over time.

Despite their significant potential, these methods still face several challenges. Few-shot learning requires complex models that can rapidly adapt with minimal data. Designing and training such models remains a non-trivial task. On the other hand, unsupervised learning offers limited mechanisms for evaluating and controlling the quality of learning, especially in the absence of clearly defined goals or external feedback. These limitations hinder its direct application in tasks that require high levels of reliability and precision.

One of the most important aspects in the context of training robotic manipulators is the use of **simulation environments** for preliminary training. Simulations help reduce the consumption of physical resources and prevent potential equipment damage during the early stages of learning.

Thanks to advanced platforms such as Gazebo, MuJoCo, and PyBullet, researchers can conduct experiments in a virtual space. This significantly accelerates the development and testing of new algorithms and training approaches. Moreover, high-fidelity simulations that accurately model the physical properties of the real world facilitate a smooth transition from virtual to physical deployment without compromising the effectiveness of the trained model.

However, a persistent challenge is the so-called "reality gap" — the discrepancy between the simulated and real environments. This gap can lead to reduced accuracy or instability in the robot’s performance when transferring trained behaviors to real-world conditions [21].

To address this issue, researchers apply **transfer learning** techniques, as described in [22]. These methods aim to preserve learning efficiency when moving from a virtual to a physical space. The main advantages of transfer learning include reduced training time and resource consumption, fewer required demonstrations or training episodes, and improved system adaptability to new conditions.

Nonetheless, transfer learning is not without limitations. If there is a substantial mismatch between the simulated and real tasks, the system may experience negative transfer, which can degrade performance or even lead to failure [22].

A comparative analysis shows that no single method is universally applicable. Each approach has its strengths and limitations, depending on the specific context.

For example, imitation learning enables the rapid acquisition of basic skills but often demonstrates limited generalization to new or unforeseen situations. In contrast, reinforcement learning offers flexibility and autonomy, but it requires substantial computational resources and time. Inverse reinforcement learning provides a deeper understanding of the expert's intentions, but it is complex to implement and computationally demanding. Combined and collaborative approaches deserve particular attention. They enable the integration of complementary advantages from multiple learning paradigms, supporting the development of more robust and adaptive robotic systems.

Ultimately, the choice of an optimal learning strategy should be guided by several factors. These include the nature of the task, environmental complexity, the availability of training data, and technical constraints. A brief comparative overview of the discussed methods is presented in Table 1.

Table 1. Brief comparative characteristics of teaching methods.

Method	Advantages	Disadvantages	Typical scenarios of possible application
Imitation Learning	1) Fast learning without complex setup 2) No reward function required 3) Suitable for clear demonstrations 4) Low risk of hardware damage	1) Poor generalization to new situations 2) Requires many high-quality demonstrations 3) Hard to teach complex or error-prone behaviors	1) Simple motions and action sequences 2) Industrial tasks in controlled settings 3) Social robotics with human-like behavior
Reinforcement Learning	1) Learns through trial and error 2) No demonstrations or labels needed 3) Works well in complex, dynamic environments 4) Optimizes long-term strategies.	1) High computational cost and long training 2) Requires many training episodes 3) Risk of hardware damage in real-world training 4) Sim-to-real transfer issues (reality gap)	1) Autonomous learning in dynamic settings 2) Real-time control optimization 3) Complex behaviors hard to program manually
Inverse Reinforcement Learning	1) Learns expert's hidden goals 2) Useful when reward is hard to define 3) Flexible generalization to new situations	1) High complexity and computational cost 2) Reward ambiguity for the same behavior 3) Requires many expert demonstrations	1) Intuitive tasks hard to formalize 2) Manual or medical skills (e.g., surgery)
Collaborative Learning	1) Faster learning via collaboration or knowledge sharing 2) Enables teamwork and human–robot interaction 3) Task distribution reduces individual agent load	1) Complex coordination between agents 2) Requires communication protocols 3) Risk of goal or action conflicts	1) Multi-robot collaboration in cooperative systems 2) Human–robot cooperation 3) Joint manipulation of large or complex objects
Hybrid / Combined Learning	1) Combines strengths of multiple methods 2) Flexible and scalable solutions 3) Improved stability for complex tasks	1) Complex implementation and integration 2) Requires deep customization and testing 3) Higher hardware and software demands	1) Error correction and policy refinement 2) Low-data or high-risk domains
Transfer Learning	1) Reduces training time and data requirements 2) Reuses prior knowledge for new tasks 3) Effective for sim-to-real transfer	1) Risk of negative transfer with dissimilar tasks 2) Requires good task alignment 3) May need model architecture adaptation	1) Transferring grasping skills across objects 2) Retraining after sim-to-real deployment

5. Conclusion

Based on the conducted analysis, imitation learning is the most suitable choice for training robotic manipulators. In particular, training through demonstration proves effective in tasks where high-quality expert demonstrations are feasible.

This method enables fast and safe acquisition of basic skills, which is particularly important when working with robotic manipulators, as it minimizes the risk of equipment damage during experimentation. It is especially well suited for tasks involving well-defined trajectories or repetitive actions. In such cases, imitation learning significantly reduces the time and resources required at the training stage. This is particularly useful when an operator intuitively knows how to perform a task but is unable to formalize it in the form of a program.

Moreover, demonstration-based learning supports safe training in real-world environments and lowers computational demands compared to methods relying solely on autonomous exploration, such as reinforcement learning. These characteristics make imitation learning an optimal choice for training robotic manipulators in applications that require high levels of reliability and repeatability.

References

[1] Argall, B. D., Chernova, S., Veloso, M., & Browning, B. (2009). A survey of robot learning from demonstration. Robotics and Autonomous Systems, 57(5), 469–483. https://doi.org/10.1016/j.robot.2008.10.024

[2] Billard, A., Calinon, S., Dillmann, R., & Schaal, S. (2008). Robot programming by demonstration. In Springer handbook of Robotics (pp. 1371-1394). Springer. https://doi.org/10.1007/978-3-540-30301-5_60

[3] Barekatain, A., Habibi, H., & Voos, H. (2024). A practical roadmap to learning from demonstration for robotic manipulators in manufacturing. Robotics, 13(3), 100. https://doi.org/10.3390/robotics13070100

[4] Underactuated Robotics. (n.d.). Ch. 21 – Imitation Learning. Retrieved from https://underactuated.mit.edu/imitation.html.

[5] Ross, S., Gordon, G., & Bagnell, D. A reduction of imitation learning and structured prediction to no-regret online learning. *AISTATS*. 2011. – P. 627–635.

[6] Sutton, R. S., & Barto, A. G. (2018). *Reinforcement Learning: An Introduction (2nd Edition)*. MIT Press.

[7] Kober, J., Bagnell, J. A., & Peters, J. (2013). Reinforcement learning in robotics: A survey. International Journal of Robotics Research, 32(11), 1238–1274. https://doi.org/10.1177/0278364913495721

[8] Lillicrap, T. P., Hunt, J. J., Pritzel, A., et al. (2015). Continuous control with deep reinforcement learning.

[9] Schulman, J., Wolski, F., Dhariwal, P., Radford, A., & Klimov, O. (2017). Proximal policy optimization algorithms.

[10] Haarnoja, T., Zhou, A., Abbeel, P., & Levine, S. (2018). Soft actor-critic: Off-policy maximum entropy deep reinforcement learning with a stochastic actor.

[11] Ng, A., & Russell, S. (2000). Algorithms for inverse reinforcement learning. Proceedings of the 17th International Conference on Machine Learning (ICML), 663–670.

[12] Panait, L., & Luke, S. (2005). Cooperative multi-agent learning: The state of the art. Autonomous Agents and Multi-Agent Systems, 11(3), 387–434. https://doi.org/10.1007/s10458-005-2631-2

[13] Nikolaidis, S., & Shah, J. A. (2013). Human-robot cross-training: computational formulation, modeling and evaluation of a human team training strategy. ACM/IEEE International Conference on Human-Robot Interaction. https://doi.org/10.1109/HRI.2013.6483499

[14] DEEPCOBOT – Collective Efficient Deep Learning and Networked Control for Multiple Collaborative Robot Systems. UiA WISENET Lab. 2024. URL: https://deepcobot.uia.no/about

[15] Zhu, Y., Mottaghi, R., Kolve, E., et al. (2018). Reinforcement and imitation learning for diverse visuomotor skills. Proceedings of Robotics: Science and Systems (RSS), 33–40. https://doi.org/10.15607/RSS.2018.XIV.009

[16] Levine, S., Finn, C., Darrell, T., & Abbeel, P. (2016). End-to-End Training of Deep Visuomotor Policies. Journal of Machine Learning Research, 17(39), 1–40.

[17] Yaqing Wang, Quanming Yao, James Kwok, Lionel M. Ni (2019). Generalizing from a Few Examples: A Survey on Few-Shot Learning. Science, 53(3), 1–34. https://doi.org/10.1145/3386252

[18] Finn, C., Abbeel, P., & Levine, S. (2017). Model-Agnostic Meta-Learning for Fast Adaptation of Deep Networks. Proceedings of the 34th International Conference on Machine Learning (ICML), 1126–1135.

[19] Naeem, S., Ali, A., & Anam, S. (2023). An unsupervised machine learning algorithms: Comprehensive review. International Journal of Computing and Digital Systems, 12(1), 1–10. https://doi.org/10.12785/ijcds/130172

[20] Hjelm, R. D., Fedorov, A., Lavoie, E., et al. (2019). Learning deep representations by mutual information estimation and maximization. International Conference on Learning Representations (ICLR).

[21] James, S., Davison, A. J., & Johns, E. (2019). "Sim-to-Real via Sim-to-Sim: Data-efficient Robotic Grasping via Randomized-to-Canonical Adaptation Networks." Proceedings of the IEEE/CVF Conference on Computer Vision and Pattern Recognition (CVPR), 2019. https://doi.org/10.1109/CVPR.2019.01291

[22] Pan, S. J., & Yang, Q. (2010). "A Survey on Transfer Learning." IEEE Transactions on Knowledge and Data Engineering, 22(10), 1345–1359. https://doi.org/10.1109/TKDE.2009.191

Аналіз методів навчання роботів-маніпуляторів для виконання складних траєкторій руху

Юрій Сенчук, Федір Матіко

Національний університет «Львівська політехніка», вул. С. Бандери, 12 , Львів, 79013, Україна

Анотація

У статті розглянуто актуальні підходи до навчання роботів-маніпуляторів, які застосовуються для виконання складних завдань у динамічних та змінних умовах середовища. Проведено порівняльний аналіз сучасних методів, визначено їхні основні переваги, недоліки, а також окреслено типові сфери їхнього практичного застосування, зокрема методи із залученням людини-інструктора, самонавчання та навчання з підкріпленням. Особливу увагу приділено питанню ефективності навчання, адаптивності роботів до нових умов, взаємодії з людиною та перенесення навичок з віртуального навчального середовища у реальне. На основі аналізу рекомендованим визначено імітаційне навчання, зокрема підхід навчання за демонстрацією, що дозволяє швидко та безпечно передавати навички від людини до робота без необхідності формалізації завдань. Крім того, в статті акцентовано увагу на проблемах адаптації навчених моделей до реальних умов і взаємодії роботів із людиною. Визначено ключові виклики, що стоять перед сучасними системами навчання роботів та сформульовано рекомендації щодо вибору оптимальних стратегій навчання залежно від типу завдань і доступних ресурсів.

Ключові слова: робототехніка; робот-маніпулятор; система керування; методи навчання; траєкторія руху; адаптивність.

Volume 11, Number 1, 2025 62

Peculiarities of Application of Contact Methods for Measuring the Temperature of Technological Objects

Vasyl Fedynets*, Ihor Vasylkivskyi

Lviv Polytechnic National University, 12 S. Bandery St., Lviv, 79013, Ukraine

Received: April 18, 2025. Revised: May 13, 2025. Accepted: May 20, 2025.

Abstract

Contact methods are usually used to measure the temperature of industrial technological objects. When using the contact method to create the necessary conditions for heat exchange, thermal transducer must be in direct contact with the object of study, the temperature of which must be measured. When measuring stationary temperatures, the readings must be taken after a certain time interval from the moment of contact of the thermal transducer with the object of study, when a state of thermal equilibrium is established between them. Measurement of non-stationary temperatures by contact methods is always associated with the occurrence of dynamic errors over time due to the thermal inertia of the thermal transducer. The complexity of the processes of interaction of thermal transducers with heat flows of different nature of the objects of study necessitates the construction of simplified models to obtain practical estimates of the measurement results. Therefore, the article proposes the principles of choosing a thermal transducer to reduce possible methodological errors and estimate the actual errors of measuring the temperature of the objects of study. The conditions that must be met when setting up and conducting experiments to obtain reliable temperature measurement results are given. The article contains reference and methodological materials on measuring the temperature of technological objects by contact methods.

Keywords: temperature; contact measurement methods; thermal transducer; measurement errors; heat flows.

1. Definition of the scientific problem chosen for research

A contact thermal transducer is any transducer based on a certain principle of converting temperature into another physical quantity that can be measured directly. In this case, its thermal interaction with the object of study (solid, liquid, gas flow, etc.) is based on direct thermal contact. The quality of this thermal contact is a determining factor that characterizes the error of temperature measurement by this thermal transducer.

To assess the measurement error of a contact thermal transducer, it is necessary to consider all thermal processes in which the thermal transducer participates, from the point of view of the theory of heat transfer. It is advisable to consider heat flows of various nature supplied to the thermal transducer from the object of study and flows removed from it into the environment.

The complexity of the processes of interaction of the thermal transducer with heat flows necessitates the construction of simplified models to obtain practical estimates of the measurement error. But with all simplifications, it is necessary to consider the conditions of use of thermal transducers and the thermophysical properties of their structural materials, which is not always possible. Therefore, based on the above, it is advisable to offer an approximate scheme for the correct selection of a thermal transducer to reduce the measurement error to a practically possible value.

* Corresponding author. Email address: vasyl.o.fedynets@lpnu.ua

This paper should be cited as: V. Fedynets, I. Vasylkivskyi. (2025) Peculiarities of application of contact methods for measuring the temperature of technological objects. *Energy Engineering and Control Systems*, Vol. 11, No. 1, pp. 62 – 68. https://doi.org/10.23939/jeecs2025.01.062

2. Analysis of recent publications and research works on the problem

The authors' analysis of publications and research on contact methods of temperature measurement of various technological objects shows that the most widely used in modern temperature measurement systems are thermal transducers based on electrical temperature conversion, i.e. resistance thermal transducers and thermoelectric transducers (thermocouples) [1]-[5].

Currently, there are no general theoretical foundations for the development and application of contact methods of temperature measurement, although some issues of designing contact thermal transducers for some specific conditions of application and the possibility of reducing the measurement error have been worked out [6]. Therefore, in this article we offer the necessary reference and methodological materials on the correct choice of contact methods of temperature measurement to achieve the minimum possible value of the temperature measurement error.

3. Formulation of the purpose of the article

The article aims to familiarize scientists, research engineers and designers involved in temperature measurements with the theoretical foundations and practical implementation of contact thermal transducers while ensuring the minimum value of the measurement error in various application conditions.

The article identifies the following main research objectives: the correct choice of the measurement method and ways to reduce methodological errors in temperature measurement.

4. Presentation and discussion of the research results

4.1. Thermal processes during contact temperature measurement

The quality of thermal contact between the thermal transducer and the object of study determines the time of establishing its readings and in most cases is a determining factor characterizing the error of temperature measurement by this thermal transducer. Therefore, an important property of a contact thermal transducer is its suitability for ensuring sufficient heat exchange under the conditions of installation on the object of study so that the temperature difference between it and the object under study is minimal. This difference determines the methodological error of the thermal transducer for these measurement conditions. Given that a contact thermal transducer is any transducer based on an arbitrary principle of converting temperature into a directly measured physical quantity, the thermal interaction of which with the object under study (solid, liquid, gas, etc.) is based on direct thermal contact.

To assess the methodological error of a contact thermal transducer, it is necessary to consider all thermal processes in which the thermal transducer participates, from the point of view of the theory of heat transfer [7,8]. To do this, it is first necessary to determine the heat flux dissipated (at elevated temperatures) into the environment by the protruding parts of the thermal transducer. This heat flux is continuously removed from the thermal transducer and, when thermal equilibrium is established, the same heat flux is continuously supplied to it from the object of study, the temperature of which is measured through the thermal resistance placed between them. That is, a contact thermal transducer in principle always has a lower temperature than the object of study that is in thermal contact with it.

If the heat transfer coefficient of the thermal transducer during operation at the object has a constant value, then this temperature difference can be considered in the calibration process. When the heat transfer coefficient changes under operating conditions, such a type of methodological error occurs.

It is also necessary to consider that heat transfer occurs through radiation from the surface of a heated solid object of study. Therefore, the temperature of its surface is often significantly lower than the temperature inside of it. This difference will be determined by the ratio of heat flows. If the heat flow dissipated by the thermal transducer is greater than the heat flow lost by the surface of the object of study because of heat transfer through radiation, then the temperature of this surface area measured by the thermal transducer will be lower than the temperature of neighboring areas. If the reverse ratio of heat flows occurs, then the temperature of the surface area under the thermal transducer will be higher than that of neighboring areas.

A continuous and constant flow of heat from the object of study to the thermal transducer is possible only when the object has a practically unlimited supply of heat. In many cases of industrial temperature measurements, this condition is met. However, in practice, there are often cases when the thermal transducer and the object of study have

comparable masses. Then the thermal contact of the thermal transducer and the object under study with significant differences in their initial temperatures will lead to a significant change in the temperature of the latter. This type of error can be reduced by pre-equalizing their temperatures before their thermal contact.

Therefore, for these conditions, the criterion for the suitability of a thermal transducer for measuring temperature in the given conditions should be the change in the temperature of the object under study, which occurs because of its heating (or cooling) of the thermal transducer from the initial to the final temperature. For such cases, it is advisable to take one third of the value of the instrumental error of the measuring system as the permissible change in the temperature of the object under study [1]. This determines the limit of application of contact methods for measuring the temperatures of small objects under study.

Another circumstance that may limit the application of contact methods is the possible disruption of the course of physicochemical processes in the object under study, caused by the installation of a thermal transducer in it.

Measurement of non-stationary temperatures by contact methods is always associated with the emergence of constantly present and time-varying dynamic errors, which are due to the thermal inertia of the thermal transducer [9]. This type of error can be considered and excluded by introducing appropriate calculation corrections.

The above analysis shows the complexity of the processes of interaction of thermal transducers with heat flows of various nature under complex initial and boundary conditions. Therefore, to obtain practical estimates of the temperature measurement error, simplified mathematical models of processes are usually built. But with such simplifications, it is imperative to consider the conditions of use of thermal transducers and the main thermophysical characteristics of materials, which is not always achievable using simple means.

In this regard, an approximate scheme for selecting a thermal transducer is proposed to reduce methodological errors to a practically possible or necessary value and to estimate real or permissible errors.

1) Based on the analysis of measurement tasks, operating conditions, requirements for technical means of the measuring path, make a choice of possible temperature meters according to the principle of operation. At the same time, determine the measurement locations and ensure conditions for maximum reduction of systematic errors.

2) Substantiate the values of permissible measurement errors based on tasks, the solution of which requires information about temperature values with a given reliability.

3) Pre-evaluate the heat exchange conditions that will determine the operation of the temperature transducer. Based on the worst possible conditions (minimum heat exchange intensity, maximum possible temperature change rate, maximum temperature difference between the object under study and the environment surrounding the thermal transducer, etc.), evaluate the possible maximum errors for each of the thermal transducers proposed for use. In this case, it is advisable to choose the temperature change rate for that section of the temperature curve that is of greatest interest. This may be a transitional mode or a mode of smooth monotonic temperature change. Preference should be given to that thermal transducer that has a certain margin of accuracy or some operational advantages over others.

4) If the heat transfer conditions and the requirements for the values of permissible errors are such that none of the proposed thermal transducers meet them, then it is advisable to choose the most suitable thermal transducer for the given measurement conditions and to introduce appropriate corrections into the results obtained with its help. Note that to be able to introduce corrections, it is necessary to perform additional measurements to obtain the necessary information about the thermal operating conditions of the thermal transducer. The volume of this information may vary, but data on heat transfer coefficients and on the temperature difference between the object under study and the environment surrounding the thermal transducer at the place of its installation is necessary. If the operating mode of the object under study is relatively stable from experiment to experiment, then after a single receipt of information, there is no need for repeated measurements. Under variable conditions, these measurements must be repeated.

5) Carry out measurements and, depending on the type of the obtained temperature curve in time, evaluate the corrections calculated for the values of the parameters of the thermal transducer that correspond to the thermal conditions of measurement. The need to introduce corrections depends on their numerical value, the overall accuracy of the measuring path and the value of the permissible measurement error based on the general rules of the theory of errors.

In general, it is necessary to strive for the measuring instruments to have the necessary margin of accuracy for the given measurement conditions and the need to introduce corrections to exist only in exceptional cases. But in

cases where the margin of accuracy is absent, it is necessary to use either corrections or limit estimates of methodological errors.

4.2. Distribution of permissible errors

When measuring the temperature of the object under study, it is first necessary to distinguish from the total permissible error, which is normalized by the requirements for the accuracy of the study of this process, those of its components that can be defined as:

- permissible instrumental error of the entire measuring path Δ_i;
- permissible methodological measurement error Δ_m;
- permissible dynamic measurement error Δ_d.

If we consider a stationary temperature process and the duration of the measurement operation is not significantly limited, then the dynamic error will be absent and the total permissible error will be distributed between the instrumental and methodological errors.

All three components Δ_i, Δ_m and Δ_d can contain both systematic and random parts. Systematic parts that are subject to evaluation are subject to exclusion by introducing appropriate corrections and they cannot be considered as components of the permissible error. The uncertainty of these corrections, estimated by calculation or experiment, does not exclude systematic errors, and they are attributed to random errors.

When isolating the components of the total permissible error, it is advisable to consider the following considerations. If the total permissible error is normalized correctly, then it should be considered as a characteristic of the expected random errors of measurements and a certain probability should be attributed to it, for example, 95%, which corresponds to the confidence interval 2σ. Then all components Δ_i, Δ_m and Δ_d should have the same confidence probability. Since all these three components are mutually independent, then the following relation is valid [10], [11]:

$$\Delta = \sqrt{\Delta_i^2 + \Delta_m^2 + \Delta_d^2}\,. \tag{1}$$

In temperature measurements, methodological errors are the most difficult to reduce. Therefore, it is advisable to first try to reduce the instrumental Δ_i and dynamic Δ_d components of the measurement error as much as possible by appropriate selection of measuring instruments, and then, using their values, determine the value of the methodological component Δ_m using formula (1).

It should be considered that increasing the accuracy class of the measuring equipment used leads to an increase in its cost and quite often to a decrease in its reliability. Therefore, the desire to reduce the instrumental component Δ_i of the error is not always justified and the task of reducing the measurement error requires finding an optimal solution.

4.4. Selection of the measurement method and measuring equipment

To obtain reliable results from measuring the temperature of technological objects, the design and conduct of experimental studies must ensure the fulfillment of the following conditions:

- correct choice of measurement method and measuring instruments;
- correct consideration of methodological errors that arise in the given conditions of temperature measurement.

It should be noted that the task of selecting the measurement method and measuring instruments is quite complex, since it is necessary to look for the optimal solution considering many often contradictory factors. Quite often, there are cases when the task cannot be successfully solved and the desired temperature values are found indirectly using the results of measurements of other physical parameters of the object under study, related to temperature by certain dependencies.

Below are the main factors that determine the choice of the measurement method and measuring instruments.

4.4.1. Range of measured temperatures

This factor is quite important. Thus, if for measuring low and high temperatures it is possible to choose contact methods, then with an increase in the temperature range, the number of methods becomes more and more limited. This limitation arises in relation to primary transducers because high temperatures significantly affect the systematic

change in their calibration characteristics. Therefore, the question of the possibility of using this transducer should be resolved considering the duration of its operation and the rate of change in the calibration characteristic when measuring high temperatures. The upper temperature range of applications is the value of the measured temperature at which, during the required time of operation of the transducer, the change in its calibration characteristic will not exceed the permissible value. Using the transducer when measuring temperatures that are too high for it leads to its destruction.

4.4.2. Chemical interactions

A significant influence on the stability of the thermotransducer at high temperatures is its chemical interaction with the environment whose temperature it measures, as well as the interaction of various materials that make up its composition. Chemical interaction is especially pronounced at high temperatures, when some of the constituent materials of the thermotransducer become quite active.

This group of influences also includes the catalytic effect that occurs on the surface of platinum group metals when measuring temperature in combustible gas mixtures. Therefore, the readings of thermotransducers that have parts that are in direct contact with such mixtures do not characterize the temperature established between the thermotransducer and the medium under study, but a higher one due to catalytic heating.

The chemical interaction of the environment under study and the thermotransducer is often the main reason for the instability of its calibration characteristic when measuring high temperatures. Therefore, to ensure reliable operation in aggressive, and sometimes oxidizing environments, it is necessary that the protective housing of the thermal transducer, which separates the sensitive element from the medium under study, be practically gas-proof.

4.4.3. Dynamics of the studied process

When choosing a thermal transducer for the study of non-stationary temperature processes, special attention should be paid to its dynamic characteristics and the characteristics of the elements of the measuring path. First, it is necessary to determine whether the process is stationary or non-stationary. Such a determination can be made only by focusing on a certain measurement time interval. A stationary process should be considered one in which, over a sufficiently large time interval, the temperature change does not exceed the limits of random measurement errors.

From the point of view of the coordination of the dynamic characteristics of the thermal transducer and the entire measuring path with the time characteristics of the measurement process, the degree of stationarity should be determined in relation to the duration of a separate measurement, that is, the time required to obtain a separate reference. Therefore, a stationary process should be considered one in which, over the time required to perform one measurement of the temperature change, the random error of the measuring path does not exceed the total. Since the assessment of such a random error is probabilistic, the degree of process stationarity is also a probabilistic characteristic, and for the correct qualification of the process, a certain confidence probability should be considered. Therefore, for measuring stationary temperatures, the thermal transducer and the entire measuring path should be selected with such dynamic characteristics that the time for establishing readings for a single reference meets the requirements of the experiment.

When selecting a thermal transducer and elements of the measuring path for measuring a non-stationary temperature process, it is necessary that the dynamic error due to the thermal inertia of the thermal transducer does not exceed that part of the permissible total error that can be interpreted as the permissible dynamic error.

4.4.4. Accuracy class of measuring system links

When determining the required accuracy class of measuring and recording measuring instruments, it should be borne in mind that the accuracy class is determined by the value of the permissible basic and additional errors, expressed as a percentage in relation to the entire measurement range [10]. The corresponding relative error, attributed to the measured temperature itself, will be the greater the closer its value is to the beginning of the scale. For example, in a measuring device of accuracy class 0.5 with a scale from 100 to 500 °C, the absolute value of the permissible error is 2 °C at any point on the scale. Its relative value for this case can vary from 2/500 (0.4%) at the end of the scale to 2/100 (2.0%) at the beginning of the scale. Therefore, it is advisable to choose measuring instruments with such measurement ranges that the expected value of the measured temperature falls into the last

third of the scale for stationary and smoothly varying temperatures. For measuring fluctuating temperatures - in 2/3, and in the presence of strong temperature pulsations - in 1/2 of the scale.

If the calculation of relative errors is performed in relation to temperature, then it is advisable to conduct it not to the absolute value of the temperature, but only to the temperature interval that covers the process under study.

Since depending on the scale (Kelvin or Celsius) in which the given temperature is expressed, the relative measurement error will have a different value, which cannot be considered acceptable.

4.4.5. Sensitivity of the measuring device

Depending on the required measurement accuracy, it is necessary to ensure the appropriate sensitivity of the measuring path, which characterizes the change in the output value of the thermal transducer when the measured temperature changes by one degree.

It is incorrect to state that the most sensitive measuring device can provide the highest measurement accuracy, which is sometimes not even necessary for this study. The use of a measuring device with excessively high sensitivity can create a false idea of the dynamics of the process under study. Such a device may be difficult to maintain in these operating conditions, its readings may be affected by adverse factors, which can lead to an increased and not typical spread of readings for this measurement.

The use of a measuring device with low sensitivity will not allow for recording small, but characteristic temperature fluctuations for this process. As a result, a false idea of high temperature stability in this technological process may arise.

Measurement of small quantities (for example, small temperature differences) can be complicated at values close to the sensitivity threshold, which is taken as the minimum value of the change in the measured quantity, which causes a noticeable change in the instrument readings. Note that when measuring deterministic signals, the sensitivity threshold of the measuring instrument should be 2-3 times smaller than the minimum value of the measured quantity. In measuring systems with information transmission in code form, the signal-quantization step is taken as the sensitivity threshold of the system by level [10], [11].

5. Conclusion

The article provides reference and methodological information on measuring the temperature of technological objects by contact methods. Thermal processes during contact temperature measurement are considered, which are the determining factors of the measurement error.

An approximate algorithm for selecting a thermal transducer to reduce methodological errors in temperature measurement is proposed. The main factors that determine the choice of temperature measurement method and measuring instruments are presented, depending on the measurement range, chemical interaction with the studied environment, dynamics of the studied process, accuracy class and sensitivity of measuring instruments.

References

[1] Lutsyk, Ya.T., Huk, O.P., Lakh, O.I., Stadnyk, B.I. (2006) Temperature measurement: theory and practice. – Lviv. Beskyd Bit Publishers. (in Ukrainian).

[2] Metrology. Resistance thermoconverters made of platinum, copper and nickel. General technical requirements and test methods: DSTU GOST 6651:2014. - K.: Ministry of Economic Development of Ukraine, 2015. - 26 p. (in Ukrainian).

[3] Thermoelectric temperature transducers. Part 1. Performance specification and tolerance of the electromotive force (EMF): DSTU EN 60584-1:2016 (EN 60584-1:2013, Idt). – [Effective 2016–11–01]. – Kyiv: State Committee of Ukraine for Technical Regulation and Consumer Policy, 2016. – 90 p. – (National Standards of Ukraine). (in Ukrainian).

[4] Pistun Y., Vasylkivskyi I., Fedynets V., Krykh H., Matiko H. (2024) Automated system for measuring thermal conductivity of solid materials. *Metrology and Measurement Systems*. **31**, iss. 1. 179–193. (SciVerse SCOPUS, Web of Science). http://dx.doi.org/10.1109/9.402235

[5] Fedynets V., Yusyk Ya., Vasylkivskyi I., Guk N. (2019) Primary converters for temperature measurement in metallurgy. *Measuring Technology and Metrology*. **80**, No. 2. 41-48. (in Ukrainian). http://dx.doi.org/10.23939/istcmtm2019.02.041

[6] O. Kochan, R. Kochan, V. Kochan and J. Su. (2017) Thermocouple with adjustable error. *9th IEEE International Conference on Intelligent Data Acquisition and Advanced Computing Systems: Technology and Applications (IDAACS)*, Bucharest, Romania, 684-689. http://dx.doi.org/10.1109/IDAACS.2017.8095178.

[7] Bulyandra O. F. (2006) Technical thermodynamics. K.: Technika. (in Ukrainian).

[8] Shinkaryk M.M., Kravets O.I. (2024) Basics of heat engineering. Ternopil: individual entrepreneur Palyanitsa V.A. (in Ukrainian).

[9] Fedynets V., Vasylkivskyi I. (2024) Research of thermal inertia of thermotransducers for measuring the temperature of gas flows. *Energy Engineering and Control Systems*. Vol. 10, No. 2, pp. 96–101. https://doi.org/10.23939/jeecs2024.02.096

[10] Kucheruk V.Yu., Kukharchuk V.V. (2024) Fundamentals of metrology and electrical measurements/ - K: University book. (in Ukrainian).

[11] Podzharenko V.O., Kulakov P.I., Ignatenko O.G., Voytovych O.P. (2006) Fundamentals of metrology and measuring equipment. Vinnytsia: VNTU. (in Ukrainian).

Особливості застосування контактних методів для вимірювання температури технологічних об’єктів

Василь Фединець, Ігор Васильківський

Національний університет «Львівська політехніка», вул. С. Бандери, 12, м. Львів, Україна

Анотація

Для вимірювання температури промислових технологічних об’єктів зазвичай застосовують контактні методи. При застосуванні контактного методу для створення необхідних умов теплообміну термоперетворювач повинен знаходитися в безпосередньому контакті з об’єктом дослідження, температуру якого необхідно виміряти. При вимірюванні стаціонарних температур відлік показів необхідно здійснювати через деякий інтервал часу з моменту контакту термоперетворювача з об’єктом дослідження, коли між ними встановиться стан теплової рівноваги. Вимірювання нестаціонарних температур контактними методами завжди пов’язано з виникненням в часі динамічних похибок, обумовлених термічною інерцією термоперетворювача. Складність процесів взаємодії термоперетворювачів з тепловими потоками різної природи об’єктів дослідження обумовлює побудову спрощених моделей для отримання практичних оцінок результатів вимірювання. Тому в статті запропоновано принципи вибору термоперетворювача для зменшення можливих методичних похибок і оцінки дійсних похибок вимірювання температури об’єктів дослідження. Наведено умови, які необхідно виконати при постановці і проведенні експериментів для отримання достовірних результатів вимірювання температури. Стаття містить довідковий і методичний матеріали з вимірювання температури технологічних об’єктів контактними методами.

Ключові слова: температура; контактні методи вимірювання; термоперетворювач; похибки вимірювання; теплові потоки.

Volume 11, Number 1, 2025

Simulation of Minefield Installation in a Video Game Engine

Maksym Maksymov[a], Oleksii Neizhpapa[a], Oleksandr Toshev[a,*], Maksym Kiriakidi[b]

[a]*Odesa Polytechnic National University, 1 Shevchenka Ave., Odesa, 65044, Ukraine*
[b]*National University "Odesa Maritime Academy", 8 Didrikhson St., Odesa, 65029, Ukraine*

Received: April 22, 2025. Revised: May 31, 2025. Accepted: June 20, 2025.

Abstract

In the evolving world of modern digital gaming, particularly within tactical war-game strategies and realistic naval combat environments, the demand for accurate simulation and immersive experience is growing. The design and simulation of naval warfare must integrate more complex systems, including the impact of underwater minefield effectiveness. The research goal is to develop a framework and model that accurately predicts the tactical and operational impact of naval minefields on vessels across diverse gameplay scenarios. The simulation is designed to consider many variables, such as different mine and ship types, different landing strategies, varying environmental parameters and weather. The first objective of this research is to improve damage prediction algorithms, enabling the simulation to more accurately estimate the consequences of ships passing through a minefield. The second objective is to enhance mine allocation logic, developing algorithms that calculate the optimal quantity, type, and distribution of mines needed to halt or delay enemy advances.

Keywords: underwater mines; computer game; simulation framework; game engines; tactical strategy games.

1. Introduction

As computer games continue to evolve, players increasingly seek out highly realistic and deeply immersive experiences. Across various game genres, there is a growing appeal for simulations that let users take control of vehicles, ranging from sports cars to aircraft and naval vessels, and immerse themselves in diverse combat environments.

Within the broader category of simulation games, military-themed titles stand out for their complex modeling of armed forces, equipment, and operational roles. These war-games enable players to step into the shoes of field commanders, operators, or specialized military units, reimagining real-world conflicts or exploring fictional combat scenarios.

In this context, our focus turns to naval strategy, with particular attention to the placement and operational impact of naval minefields installation during sea-based confrontations [1], [2]. Game developers are tasked with building robust simulation frameworks that can realistically portray the mechanics and consequences of mine deployment. This includes the creation of intelligent systems that can determine effective mine-laying patterns, estimate disruption zones for enemy ships, and simulate activation conditions when opposing vessels enter the mine field [3].

Moreover, modeling must account for the logistical and tactical decisions behind minefield planning, including environmental constraints and mission-specific goals. Incorporating these elements not only increases the strategic

* Corresponding author. Email address: toshev.oleksandr@outlook.com

This paper should be cited as: M. Maksymov, O. Neizhpapa, O. Toshev, M. Kiriakidi. (2025) Simulation of minefield installation in a video game engine. *Energy Engineering and Control Systems*, Vol. 11, No. 1, pp. 69 – 78. https://doi.org/10.23939/jeecs2025.01.069

depth of gameplay but also helps players make better-informed choices while managing limited defensive resources in dynamic maritime scenarios.

Our game development framework is structured to simulate a broad spectrum of maritime combat scenarios, each presenting unique strategic challenges. The game features a detailed collection of naval mines, categorized by type, functionality, and deployment effectiveness [1], [4]. We also experiment with different deployment strategies to observe how the positioning of minefields affects the flow and outcome of naval engagements. The game further includes a variety of ship classes, each assigned specific roles and operating doctrines. Using our simulation model, we can analyze how different ship formations perform when navigating mined waters under various tactical conditions.

Moreover, the engine integrates detection systems and countermeasure technologies such as mine-hunting vessels and drones, allowing us to assess their performance in neutralizing underwater threats. This comprehensive approach enables precise modeling of the effects of waterborne minefields in multiple combat environments, delivering a highly detailed and engaging simulation of naval defense operations.

Within the framework of strategy-focused video games, players assigned to defend coastal or strategic maritime zones must carefully plan minefield deployment to counter advancing enemy fleets. Success relies on a thorough evaluation of multiple elements, including the opposing force's composition, tactics, and likely paths of approach [5]. Defenders must also assess their own available resources, mine types, and optimal placement zones, while factoring in game environment variables such as sea depth, currents, and weather each of which can affect detection, activation, and navigational hazards.

The primary objective for players managing mine warfare is to create an efficient, sustainable defense strategy that adapts to dynamic threats over time. These simulation-heavy strategy games push players to anticipate enemy maneuvers and respond with calculated precision. The fidelity of the simulation is key to fostering a rich and realistic gameplay experience, promoting strategic innovation and thoughtful decision-making.

In designing a game that accurately portrays naval mine warfare, we draw from real-world military documentation and historical conflict data to set credible baseline parameters for all elements in the simulation. This includes defining activation radius, explosive yield, survivability against clearance operations, and the detection likelihood for each mine type. Similarly, we establish operational characteristics for mine-laying vessels and their limitations. These foundational values ensure that the simulation mirrors real-world operational behavior, providing players with a deep and authentic understanding of tactical engagements shaped by underwater minefields.

2. Analysis of the recent publications and research works on the problem

By analyzing a wide range of scholarly and technical literature on naval mine warfare, we establish a solid foundation for our research. This approach enables us to adopt and refine existing models and methodologies, using them as reference points for developing a robust and effective simulation framework.

The reviewed sources highlight advanced strategies for coordinated deployment of naval minefields, designed to maximize coverage and strategic disruption. One such method emphasizes synchronized mine-laying across multiple zones to ensure that enemy vessels encounter obstacles simultaneously, thereby increasing the likelihood of damage and reducing the chances of successful navigation through the area. These tactics involve precise control over placement timing and spatial distribution, even under variable conditions such as shifting currents or limited communication between mine-laying units. Simulations demonstrate that such coordination significantly improves the effectiveness of minefields in contested environments, especially when considering differing vessel approaches and dynamic sea conditions.

Further literature introduces mathematical models that describe ship behavior when navigating through both safe and mined waters [5], [6]. These models apply an Estimation-Before-Modeling approach, in which key variables, such as ship speed, maneuverability, and hydrodynamic responses are estimated individually before analyzing patterns of vessel movement. The results allow comparison between the maneuvering performance of ships in unaffected conditions versus those affected by mine detonations or near-miss scenarios [7]. These insights provide a deeper understanding of how ships respond under pressure and how damage affects their tactical flexibility.

We use these established studies to define core baseline parameters for our simulation, such as ship attributes, mine trigger mechanisms, explosive yields, and detection probabilities. These parameters allow for a realistic portrayal of tactical interactions within the game environment, from both defensive and offensive standpoints.

Moreover, several works draw upon differential game theory to design optimal strategies for laying minefields in scenarios involving a defender, an intruder, and protected zones. These strategies enable the defender to hinder the attacker's movement while avoiding premature detection or engagement [8], [9]. Notably, these models do not require precise knowledge of the attacker's decisions or path, instead relying on probabilistic patterns and strategic positioning. Simulation results validate the effectiveness of these methods across varying initial conditions and battlefield constraints [4], [10]. Additional research outlines how defenders can preemptively structure minefield networks to reduce the success rate of enemy operations, even in the presence of mine countermeasure technologies.

Drawing on tactical doctrines and strategies outlined in naval warfare literature and operational manuals, we can establish a set of core interactions for our simulation model. These interactions define key gameplay scenarios involving water minefield deployment, segmented into several operational phases:

1) Naval Transit and Amphibious Approach: In this phase, enemy landing fleets transport personnel, vehicles, and equipment toward the target coastline. These vessels are engineered for shore landings under varied sea and weather conditions, often without prior coastal preparation. Ensuring disruption at this stage is critical for delaying or disorganizing the initial wave of the amphibious assault.

2) Deployment of Landing Forces: This stage involves the unloading of troops and materiel from larger transports and landing craft into designated coastal zones or shallow water staging areas. Strategic minefield placement near these drop zones can significantly hinder the safe disembarkation of forces and equipment.

3) Approach Under Fire and Combat Support: As landing vessels move into range of the target shoreline, they provide covering fire to neutralize defensive assets and secure landing zones. Minefields, especially influence or intelligent variants, placed near fire support routes or expected anchor positions can limit maneuverability and disrupt coordination.

4) Sustainment and Extraction Operations: Landing forces rely on logistical support from the sea to maintain combat effectiveness, including the delivery of ammunition, supplies, and medical evacuation. Mines placed along supply lanes or extraction routes serve to constrain movement and impose long-term pressure on sustained enemy operations.

The defending player has strategic freedom to initiate mine-laying operations or rely on pre-deployed fields during any of these phases. Timing is critical, decisions must weigh resource availability, real-time battlefield intelligence, environmental conditions, and enemy fleet behavior. Choosing the most impactful moment to activate or reinforce minefields can be decisive in preventing a successful enemy landing and turning the tide of the operation.

3. Objectives and tasks of the research

The core gameplay scenario is structured around two opposing players. The first, acting as the attacker, is tasked with escorting a squadron of landing ships to enemy-controlled waters to initiate an amphibious landing. The attacking force is composed of landing vessels, protective escort ships and minesweeper ships. The defending player, on the other hand, primarily relies on naval mines and supporting detection and disruption systems to halt the enemy advance.

The main objective for the defending player is to deploy and manage underwater minefields in a way that maximizes damage to the incoming landing fleet and effectively disrupts or halts the amphibious operation. This requires high levels of operational readiness, where mine-laying vessels, surveillance units, and crew are well-prepared and positioned strategically to execute their mission with precision and speed.

The initial focus of the research is to develop and refine a simulation model that can estimate the potential impact of minefield deployment on invading landing ships, taking into account all relevant factors including mine type, density, placement pattern, and detection probability.

The second goal is to establish a method for calculating the optimal number and configuration of mines required to successfully block or degrade a landing operation. This would provide valuable decision-making tools for both players and AI systems, enhancing their ability to make strategic choices under varying conditions and mission parameters within the game environment.

4. Model and methods

The simulation model centers on the strategic task of employing underwater minefields to disrupt and neutralize enemy landing operations, with an emphasis on identifying optimal deployment tactics for common gameplay scenarios.

The arrangement of the defending player's forces is fine-tuned to meet mission-specific objectives, guided by criteria that define effective minefield utilization. To configure these forces properly, the player must assess the operational capabilities of mine-laying vessels, available mine types, and the prevailing tactical context. This includes calculating the ideal density and layout of mine placements, grouping mine-laying units for coordinated deployment, and determining the sequencing and timing of their actions.

The positioning and use of minefield zones are also influenced by the attacking player's escort fleet configuration, as its defensive strength directly affects the survivability of incoming landing vessels. Exploring different configurations of defensive forces, such as varying the number, type, or quality of mines and deployment platforms is vital for understanding how these variables shape the overall success of the mission. In the base scenario, an increase in the number or complexity of escort ships in the attacking player's formation requires a corresponding escalation in the scale and sophistication of minefield defenses.

Determining the appropriate quantity and type of deployed mines, along with the necessary support infrastructure, involves detailed tactical analysis. To aid players in making informed decisions, these findings must be presented in a way that clearly demonstrates how minefield effectiveness shifts under different operational conditions. This process requires comprehensive modeling, scenario-based comparisons, and conclusions that highlight the advantages and limitations of each potential setup.

Once the player receives a mission directive, they can draw on prior calculations to choose a suitable configuration or refine their strategy in response to evolving in-game factors.

To make an estimate for an effectiveness of a minefield we need to calculate multiple values, such as:

- The expected number of destroyed ships when passing through a minefield consisting of a certain number of mines.

- The expected number of mines requires to form a minefield to destroy a certain number of ships which are passing through.

- The expected combat resistance of the minefield against various mine countermeasures.

To calculate mathematical expectation for the number of destroyed ships from a group of N ships, we can use a formula:

$$M_N = m\frac{A}{A_p}RS\alpha, \tag{1}$$

where m is a number of columns in the convoy; A is a mine hit area; A_p is a mine response area on a ship; R is a minefield density; S is an area of mine barrier, based on a fairway; α is a relative part of an S area affected by passing ships.

The area of a mine barrier S could be calculated using the following formula:

$$S = A + l_s E_k, \tag{2}$$

where E_k is a mean deviation of the ship's position dispersion relative to the general course of the column; l_s is a stochastic coefficient which depends on environment conditions.

α value is a statistical coefficient which depends on a number of columns in the convoy, number of ships in each column and an area which convoy covers.

The average deviation of the ship's position dispersion relative to the general course of the column E_k could be calculated by the formula:

$$E_k = \sqrt{(rD_k)^2 + V_k^2}, \tag{3}$$

where D_k is a distance between ships in a convoy; V_k is an estimated speed of a convoy.

Minefield density R could be calculated by the following formula:

$$R = \frac{M_N}{m\frac{A}{A_p}S\alpha} K_i, \tag{4}$$

where M_N is a required mathematical expectation of a number of destroyed ships from a total number of N ships in a convoy; K_i is a statistical coefficient which defines effectiveness of used mines and mine installing equipment.

The number of required mines to build an effective minefield N could be calculated by the formula:

$$N = \frac{RA}{K_i}. \tag{5}$$

To enable mine ships to deploy the required number of naval mines, it is important to calculate the mine placement interval. Different type mines have varying effective trigger ranges. The interval must ensure that adjacent mines' activation zones either overlap or leave minimal gaps to avoid safe passages. The mine placing ships velocity during deployment determines the time between drops. For example, at higher speeds, a shorter time interval is needed to maintain a consistent spacing.

To calculate an interval, we can use the below formula:

$$I = \frac{A}{N}. \tag{6}$$

To evaluate the combat resistance of a minefield, we will define it as the amount of time it takes for opposing mine countermeasure forces to breach the minefield and establish a navigable, safe corridor for the convoy. This measurement will account for the complexity and density of the mine distribution, the types of naval mines used (contact, influence, or smart mines), and their spatial layout across the waterway.

The total clearance time required to establish a secure passage through the minefield will serve as a quantitative metric of its combat resistance. A longer clearance time indicates higher resistance and greater effectiveness in delaying or disrupting enemy maritime operations.

As an example for our model, we will make calculations for one of the basic types for naval mines countermeasures – naval minesweeper with a mine-clearing line charge.

To calculate number of required mine-clearing line charges N_c we can use the following formula:

$$N_c = \frac{W_f}{M\sigma} * \frac{L_f}{l\sigma}, \tag{7}$$

where W_f and L_f are width and length of a fairway required for the safe passage of a convoy; M is a width of a line cleared of mines when cord charges explode; σ is a statistical error for setting up a line charge before exploding; l is a length of a mine-clearing line charge.

Time t_c required for minesweepers for traveling and setting up line charges could be calculated by the following formula:

$$t_c = t_t + \frac{2L}{V} + t_s, \tag{8}$$

where t_t is a time needed for arming minesweepers with a required number of charges; t_s is a time required to setup all mine-clearing line charges; L is a distance to the fairway from a doc station of a minesweepers; V is a speed of a minesweepers.

The time T_s needed for destroying mines by a mine-clearing line charges is calculated using the formula:

$$T_s = N_c t_c, \tag{9}$$

where N_c is a number of a setups of a line charges, required to clear a fairway of a certain size; t_c is a time required for a minesweepers for preparations, traveling, setting up and exploding required amount of a line charges.

The range of combat stability of a minefield T_r is the range of the total time T of completing the task, which is calculated from a working time required to working days according to the formula and rounded to a whole number in the higher direction:

$$T_r = T_s\tau + (\frac{T_s\tau}{n_a} - 1)t_r, \tag{10}$$

where τ is a statistical coefficient which depends on an outside factors, such as weather; n_a is a time during which a minesweeper could operate without an additional service, depends on a type of a minesweeper; t_r is a time required for a full service of a minesweeper, also depends on a type of a minesweeper ship.

5. Experiments

Experiment 1. Determine the number of mines required to install naval minefield against enemy landing convoy. Enemy convoys consist of 60 ships. To effectively stop enemy landing operation, it is required to destroy at least 12 ships and ensure combat resistance of a minefield more than 96 hours. Possible passing area is 15 miles wide and 5 miles long. It is expected for ships to be divided into 5 columns. The distance between ships is 0.4 miles. Speed of ships in convoy 12 knots.

In the experiment, we are using mines of "M1" type which have 35m hit radius and 40m response radius.

Opposing convoys is supported by 4 minesweepers of type "MS1".

For the ships which are placing mines we will define coefficient: $K_i = 0.95$.

For a mines of type "M1": $A = 35,\ A_p = 40$.

Columns in a convoy: $m = 5$.

Statistical coefficient: $r = 6.25$.

Using formula (3) we can calculate the average deviation of the ship's position dispersion relative to the general course of the column:

$$E_k = \sqrt{(6.25 * 0.4)^2 + 12^2} = 29.816.$$

Statistical coefficient which depends on a number of columns in the convoy, number of ships in each column and an area which convoy covers: $\alpha = 0.488$.

The statistical coefficient for the environment: $l_s = 10$.

The area of a mine barrier we can calculate with formula (2):

$$S = 35 + 10 * 29.816 = 333.$$

We can calculate minefield density with the formula (4):

$$R = \frac{12}{5 * \frac{35}{40} * 333 * 0.488} * 0.95 = 0.01685.$$

Using formula (5) we can calculate the number of required mines to build an effective minefield:

$$N = \frac{0.01685 *\ 15 * 1852}{0.95} = 492.$$

With a calculated required number of mines, we can calculate an interval at which mines should be placed with the below formula (6):

$$I = \frac{15*1852}{492} \approx 56.5.$$

Using the same formula, we can make different calculations for the same environment setup and enemy forces, for different mine placing intervals and variable number of columns in a convoy to get the mathematical expectation for a number of destroyed ships (Fig.1).

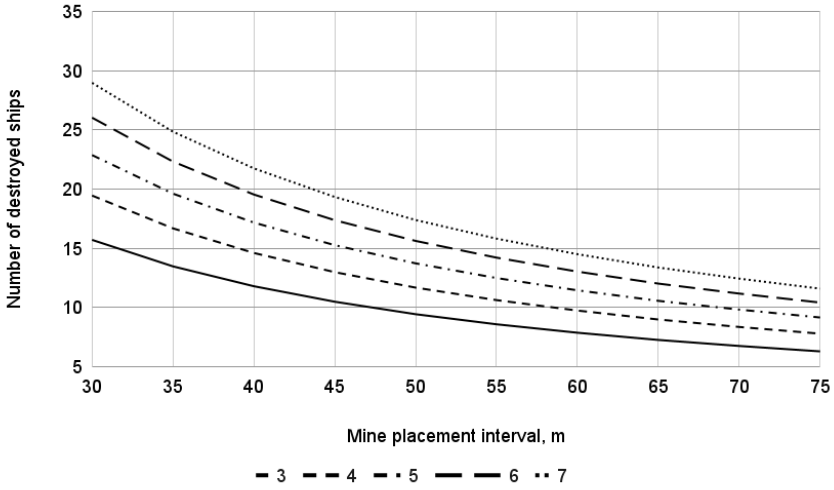

Fig.1. Estimated number of destroyed ships for a set interval for mines placement for experiment 1.

The results of our calculations provide a better understanding of how different minefield configurations affect the outcome of enemy landing operations. This information enables us to make highly optimized strategic decisions that balance maximum defensive effectiveness with efficient resource utilization.

For the chosen type of minesweeper and supporting equipment, we can define required variables, such as width of a line cleared of mines when cord charges explode $M = 185$, and the length of a mine-clearing line charge $l = 1000$.

Number of required mine-clearing line charges could be calculated with the formula (7):

$$N_c = \frac{15*1852}{185\sigma} * \frac{5*1852}{1000\sigma} = 48.$$

Time needed for arming minesweepers with a required number of charges $t_t = 1$, time required to setup all mine-clearing line charges $t_s = 1$, distance to the fairway from a doc station of a minesweepers $L = 15$, speed of a minesweepers $V = 10$.

To calculate (8) time t_c required for minesweepers for traveling and setting up line charges:

$$t_c = 1 + \frac{2*15}{10} + 1 = 5.$$

The time T_s needed for destroying mines by a mine-clearing line charges we can calculate with the formula (9):

$$T_s = \frac{48*5}{12} = 20.$$

For the chosen types of minesweepers: time during which a minesweeper could operate without an additional service $n_a = 5$, t_r is a time required for a full service of a minesweeper $t_r = 2$, and statistical coefficient which is $\tau = 1.43$.

The range of combat stability of a minefield we can calculate with the formula (10):

$$T_r = 20 * 1.43 + \left(\frac{20*1.43}{5} - 1\right) * 2 = 5 * 24h = 120h.$$

Experiment 2. For the second experiment, let's define the setup with smaller landing forces and smaller area of possible passage. Enemy convoys consist of 12 ships. To effectively stop enemy landing operation, it is required to destroy at least 4 ships and ensure combat resistance of a minefield more than 48 hours. Possible passing area is 4 miles wide and 2 miles long. It is expected for ships to be divided into 3 columns. The distance between ships is 0.5 miles. Speed of ships in convoy is 14 knots.

For this experiment, we will use the same types of mines, ships and minesweepers.

$K_i = 0.95, A = 35,\ A_p = 40.$

Columns in a convoy: $m = 3$.

Statistical coefficient: $r = 6.25$.

Using formula (3), we can calculate the average deviation of the ship's position dispersion relative to the general course of the column:

$$E_k = \sqrt{(6.25 * 0.5)^2 + 14^2} = 35.84.$$

Statistical coefficient $\alpha = 0.314$.

The statistical coefficient for the environment: $l_s = 10$.

The area of a mine barrier we can calculate with formula (2):

$$S = 40 + 10 * 35.84 = 393.4.$$

We can calculate minefield density with the formula (4):

$$R = \frac{4}{3 * \frac{35}{40} * 393 * 0.314} * 0.95 = 0.0123.$$

We can calculate the number of required mines to build an effective minefield:

$$N = \frac{0.0123 *\ 4 * 1852}{0.95} = 96.$$

With a calculated required number of mines we can calculate an interval at which mines should be placed using the below formula (6):

$$I = \frac{4*1852}{96} \approx 77.$$

Let's make the same calculations for the same environment setup and enemy forces, for different mine placing intervals and variable number of columns in a convoy (Fig.2).

Let's calculate the number of required mine-clearing line charges with the formula (7):

$$N_c = \frac{4*1852}{185\sigma} * \frac{2*1852}{1000\sigma} =\ 24.$$

With the same setup for the minesweepers we got variables $t_t = 1,\ t_s = 1, L = 15, V = 10$.

$$t_c = 3.5.$$

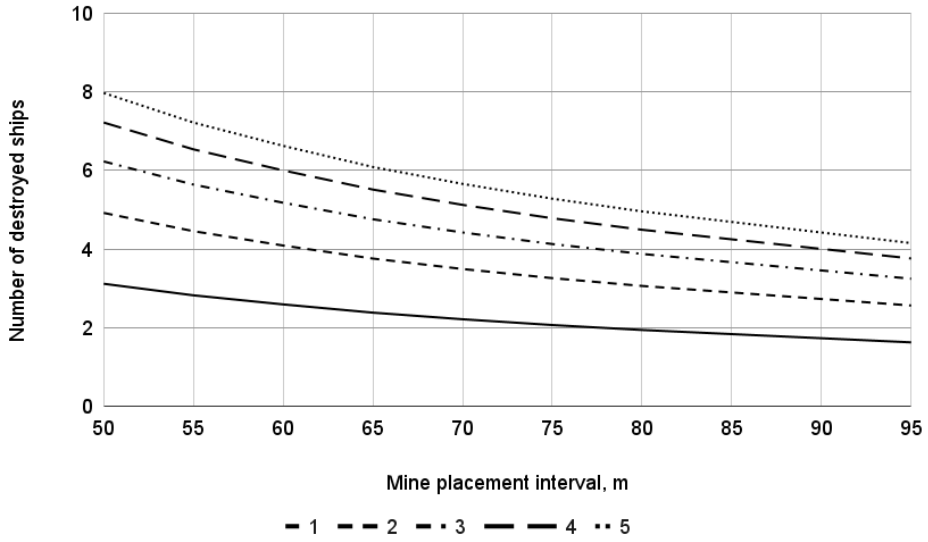

Fig.2. Estimated number of destroyed ships for a set interval for mines placement for experiment 2.

The time T_s needed for destroying mines by a mine-clearing line charges:

$$T_s = 7.$$

For the chosen types of minesweepers: $n_a = 5, t_r = 2, \tau = 1.43$.

The range of combat stability of a minefield:

$$T_r = 3 * 24h = 72h.$$

6. Conclusion

A simulation model has been developed to assess the effectiveness of naval minefields in countering naval landing operations. This model incorporates all critical components typically involved in such operations, including landing vessels transporting troops and equipment, escort and supply ships of various classes, and different tactical compositions of the opposing player's naval task force.

The model identifies the optimal density and configuration of minefields necessary to fulfill the objective of halting the adversary's landing attempt by neutralizing or obstructing elements of their amphibious group. It enables the selection and evaluation of multiple defensive configurations, helping players determine the most effective layout based on the specific tactical situation in the game scenario.

Experimental simulations validate the model's versatility, demonstrating its application across a wide range of enemy fleet configurations. By comparing outcomes for different setups of the attacking player's naval group, including variations in ship classes, support elements, the model provides insights into the contribution of each component to the success or failure of a landing attempt.

This modeling tool empowers both human players and game AI to rapidly devise and implement effective mine warfare strategies. It enables accurate scenario forecasting and supports critical planning decisions such as minefield size, deployment timing, type of mines to be used, and placement zones, all aimed at preventing or severely disrupting the rival player's naval landing operation.

References

[1] Kazuki Sakai, Ryusuke Hohzaki, Emiko Fukuda, Yutaka Sakuma, "Risk evaluation and games in mine warfare considering ship counter effects", European Journal of Operational Research, Volume 268, Issue 1, 2018, Pages 300-313, ISSN 0377-2217, https://doi.org/10.1016/j.ejor.2018.01.030.

[2] Sun-Kyung Jung, Myung-Il Roh, Ki-Su Kim, "Arrangement method of a naval surface ship considering stability, operability, and survivability", Ocean Engineering, Volume 152, 2018, Pages 316-333, ISSN 0029-8018, https://doi.org/10.1016/j.oceaneng.2018.01.058.

[3] Wonjune Chang, Joonmo Choung, "Sensitivity analysis of damage extent in naval ship compartments due to internal airborne explosions", International Journal of Naval Architecture and Ocean Engineering, Volume 16, 2024, 100622, ISSN 2092-6782, https://doi.org/10.1016/j.ijnaoe.2024.100622.

[4] Hyunwoo Kim, Burak Can Cerik, Joonmo Choung, "Effects of fracture models on structural damage and acceleration in naval ships due to underwater explosions", Ocean Engineering, Volume 266, Part 3, 2022, 112930, ISSN 0029-8018, https://doi.org/10.1016/j.oceaneng.2022.112930.

[5] Myungjun Jeon, Hyeon Kyu Yoon, Jongyeol Park, Shin Hyung Rhee, Jeonghwa Seo, "Identification of 4-DoF maneuvering mathematical models for a combatant in intact and damaged conditions", International Journal of Naval Architecture and Ocean Engineering, Volume 14, 2022, 100480, ISSN 2092-6782, DOI: https://doi.org/10.1016/j.ijnaoe.2022.100480.

[6] Myo Jung Kwak, Joon Young Yoon, Sayyoon Park, Seungmin Kwon, Yun-Ho Shin, Yoojeong Noh, "Extent of damage analysis of naval ships subject to internal explosions", International Journal of Naval Architecture and Ocean Engineering, Volume 15, 2023, 100514, ISSN 2092-6782, https://doi.org/10.1016/j.ijnaoe.2023.100514.

[7] S. N. Ghawghawe and D. Ghose, "Pure proportional navigation against time-varying target manoeuvres," in IEEE Transactions on Aerospace and Electronic Systems, vol. 32, no. 4, pp. 1336-1347, Oct. 1996, DOI: https://doi.org/10.1109/7.543854.

[8] Yasukawa, H. Yoshimura, Y. 2015/03/01 "Introduction of MMG standard method for ship maneuvering predictions" Journal of Marine Science and Technology Volume 20 Issue 1437-8213 DOI: https://doi.org/10.1007/s00773-014-0293-y.

[9] Tianle YAO, Run MIAO, Weili WANG, Zhirong LI, Jun DONG, Yajuan GU, Xuefei YAN, "Synthetic damage effect assessment through evidential reasoning approach and neural fuzzy inference: Application in ship target", Chinese Journal of Aeronautics, Volume 35, Issue 8, 2022, Pages 143-157, ISSN 1000-9361, DOI: https://doi.org/10.1016/j.cja.2021.08.010.

[10] P. R. Mahapatra and U. S. Shukla, "Accurate solution of proportional navigation for maneuvering targets," in IEEE Transactions on Aerospace and Electronic Systems, vol. 25, no. 1, pp. 81-89, Jan. 1989, DOI: https://doi.org/10.1109/7.18664.

Симуляція встановлення мінного поля у відеоігровому рушієві

Максим Максимов[a], Олексій Неїжпапа[a], Олександр Тошев[a], Максим Кіріакіді[b]

[a]*Національний університет «Одеська політехніка», Пр. Шевченка, 1, 65044, м. Одеса, Україна*
[b]*Національний університет «Одеська морська академія», вул. Дідріхсона, 8, 65029, м. Одеса, Україна*

Анотація

У світі сучасних цифрових ігор, особливо в рамках тактичних військових стратегій та реалістичних морських бойових середовищ, зростає попит на точне моделювання та захопливий досвід. Проектування та моделювання морських бойових дій повинні інтегрувати складніші системи, та включно вплив ефективності підводних мінних полів. Метою цього дослідження є розробка алгоритму та моделі, яка точно прогнозує тактичний та оперативний вплив морських мінних полів на судна в різних ігрових сценаріях. Моделювання розроблено з урахуванням багатьох змінних, таких як різні типи мін та кораблів, різні стратегії висадки, різні параметри навколишнього середовища та погоди. Першою метою цього дослідження є вдосконалення алгоритмів прогнозування пошкоджень, що дозволить моделюванню точніше оцінювати наслідки проходження кораблів через мінне поле. Другою метою є вдосконалення логіки розподілу мін, розробка алгоритмів, які розраховують оптимальну кількість, тип та розподіл мін, необхідних для зупинки або затримки просування противника.

Ключові слова: підводні міни; комп'ютерна гра; структурне моделювання; ігрові двигуни; тактичні стратегічні ігри.

ISSN 2411-4049

Editor-in-Chief
Yevhen Pistun

Energy Engineering and Control Systems

Енергетика та системи керування

Volume 11 • Number 1

Founder and Publisher
Lviv Polytechnic
National University

2025

Volume 11, Number 1, 2025 1

Modeling of Wastewater Sludge Dewatering Kinetics Using the Method of Linear Proportionalities

Orest Verbovskyi*, Vadym Orel, Volodymyr Femiak

Lviv Polytechnic National University, 12 Stepana Bandery St., Lviv, 79013, Ukraine

Received: April 10, 2025. Revised: May 05, 2025. Accepted: May 12, 2025.

Abstract

Sewage sludge accumulating at treatment facilities is aqueous suspensions separated from wastewater during treatment processes. Untreated sludge has been discharged for decades into overloaded sludge beds, dumps, or quarries, leading to environmental safety violations and deteriorating people living conditions. Due to a high content of colloidal substances, sludge poorly releases water. An important step in sludge disposal is dewatering, which significantly reduces sludge volume. Factors such as moisture content, the ratio of free to bound water, the degree of dispersion of solid phase particles, chemical composition, structure, and viscosity significantly influence sludge dewatering. The compressibility of sewage sludge under external pressure is one of its characteristic properties. Modeling was carried out using the method of linear proportions, which allowed the derivation of a uniform functional dependence under different combinations of similarity numbers.

Keywords: dewater ability; water content; sewage sludge; dimensional analysis; linear proportionalities method; similarity numbers.

1. Definition of the problem to be solved

Today, many cities, towns and industrial enterprises face a very acute problem of treatment and disposal of sludge generated during wastewater treatment. Often, untreated sludge has been dumped into overloaded sludge sites, dumps, tailings ponds, and quarries, which has led to a violation of environmental safety and living conditions.

Wastewater sludge that accumulates at wastewater treatment plants is an aqueous suspension released from wastewater in the process of its mechanical, biological or physicochemical treatment, with a volume concentration of polydisperse solid phase from 0.5 to 10%. Sludge is classified as a hard-to-dewater polydisperse suspension. As in all suspensions, moisture in wastewater sludge is in chemical, physical-chemical and physical-mechanical connection with solid particles, as well as in a free state.

The main objective of sludge treatment is to produce a sanitary and transportable product that can be used in agriculture. Due to the large amount of colloidal substances, sludge does not release water well. The water release of sludge is greatly influenced by humidity, the ratio of free to bound water, the degree of dispersion of solid phase particles, chemical composition, structure, viscosity of the sludge, etc.

Sludge produced in wastewater treatment plants represents a small part (about 1%) of the wastewater volume treated, while sludge handling and disposal processes account for 20% to 60% of operating costs, including labor, energy and sludge disposal [1].

* Corresponding author. Email address: orest.v.verbovskyi@lpnu.ua

This paper should be cited as: O. Verbovskyi, V. Orel, V. Femiak. (2025) Modeling of wastewater sludge dewatering kinetics using the method of linear proportionalities. *Energy Engineering and Control Systems*, Vol. 11, No. 1, pp. 1 – 7. https://doi.org/10.23939/jeecs2025.01.001

2. Analysis of the recent publications and research works on the problem

Wastewater sludge disposal is a complex and expensive process; however, sludge is a source of carbon, nutrients and trace elements and can be disposed of effectively [2], [3].

The following sewage sludge treatment processes are used in wastewater treatment plants: compaction, stabilization, conditioning, dewatering, drying, thermal treatment, disposal of valuable products, or sludge disposal.

Densification and dewatering reduce the moisture content, volume, and weight of sludge and are usually an integral part of any sludge treatment process.

Although sludge densification provides the lowest percentage of moisture reduction, it leads to the greatest effect of water removal and maximum decrease of the primary volume of sludge.

Dewatering is carried out by natural drying of stabilized sludge at sludge drying beds to a moisture content of 80...85% or by mechanical dehydration of previously conditioned stabilized or raw sludge using vacuum filters, filter presses or centrifuges to a moisture content of 65...75%.

An important step in the disposal of sludge is its dewatering, which allows for a significant reduction in sludge volume [4], [5]. Depending on the sensitivity of sludge to mechanical dewatering, the water content in sludge can range from 95-99 to 65-85% [6], [7]. Difficulties in sludge dewatering are associated with the high content of organic and colloidal substances in the sludge. Sludge dewatering from wastewater treatment plants is a serious problem due to the large amount of sludge produced annually. In recent years, research and development has focused on improving the dewatering process to reduce the subsequent costs of sludge management and transportation [8].

The disposal and transportation of sludge is expensive due to its high-water content. Reducing the water content of sludge is the most effective strategy to reduce treatment costs. However, sludge contains a large amount of hydrophilic organic substance, which causes poor dewatering. Therefore, research on preconditioning and mechanical dewatering is of great importance for sludge dewatering [9].

To improve dewatering, sewage sludge is chemically conditioned. Chemicals such as aluminum sulfate, iron (III) chloride, iron (II) sulfate [10], [12] and polyelectrolytes are added [11]. Currently, polyelectrolytes are used for the initial treatment of sludge before dewatering processes. However, the use of polyelectrolytes increases the cost of sludge processing and can cause secondary environmental pollution. Therefore, various alternative methods of sewage sludge conditioning, including ultrasonic treatment [13], microwave treatment [14], thermal treatment [15]. Sludge conditioning process was modified to reduce the consumption of chemicals, and new methods of sludge pretreatment were proposed and investigated, such as various combined methods [16].

3. Formulation of the goal of the paper

In order to model the processes occurring during the dewatering of sludge, it is necessary to derive functional dependencies that describe these processes. The aim of this article is to derive functional dependencies that describe the kinetics of mechanical dewatering of sewage sludge and to validate these dependencies through experimental investigation.

4. Presentation and discussion of the research results

The ability of sewage sludge to compress under external pressure is one of its characteristic properties [17]. Velocity, m/s, of sewage sludge filtration [18]:

$$q = f(G,\ e,\ W,\ \mu,\ t,\ p,\ h), \tag{1}$$

where G is sludge compression modulus, Pa; e is sludge porosity coefficient; W is moisture content of the sludge; μ is dynamic viscosity of the filtrate, Pa·s; t is duration of filtration, s; p is liquid pressure in the pores of the sludge, Pa; h is thickness of the sludge layer, m.

Moisture content of the sludge W depends on the sediment porosity coefficient e [18]. The functional relationship (1) was rewritten in the form:

$$\varphi(q,\ G,\ e,\ \mu,\ t,\ p,\ h) = 0. \tag{2}$$

The modeling was performed using the method of linear proportions. Without taking into account the dimensionless quantities, we will compose from dependence (2) linear proportions with linear dimensions, i.e., with the dimensions of length (L, m). The total number of linear proportions will be as follows [19]:

$$K = 0.5 \cdot (n - l - 2) \cdot (n - l - 1) + l, \tag{3}$$

where n is total number of variables included in dependence (2), $n = 6$; l is number of variables with linear differences in dependence (2), $l = 1$.

$$K = 0.5 \cdot (6 - 1 - 2) \cdot (6 - 1 - 1) + 1 = 7.$$

So,

$$\psi\left(\frac{q \cdot \mu}{G}, \frac{q \cdot \mu}{p}, \frac{G \cdot q \cdot t^2}{\mu}, \frac{p \cdot q \cdot t^2}{\mu}, \frac{G \cdot h \cdot t}{\mu}, \frac{p \cdot h \cdot t}{\mu}, q \cdot t, h, e\right) = 0. \tag{4}$$

Let's rewrite function (4) and use similarity numbers:

$$\psi\left(\frac{q \cdot \mu}{G \cdot h}, \frac{q \cdot \mu}{p \cdot h}, \frac{G \cdot q \cdot t^2}{\mu \cdot h}, \frac{p \cdot q \cdot t^2}{\mu \cdot h}, \frac{G \cdot t}{\mu}, \frac{p \cdot t}{\mu}, \frac{q \cdot t}{h}, e\right) = 0. \tag{5}$$

This equation contains redundant information. To get rid of the extra terms, we combine the similarity numbers:

1) The first and second numbers, the third and fourth numbers, and the fifth and sixth numbers differ only in the values of G and p. Therefore, we will keep the first $\frac{q \cdot \mu}{G \cdot h}$, third $\frac{G \cdot q \cdot t^2}{\mu \cdot h}$ and fifth $\frac{G \cdot t}{\mu}$ numbers, and write the relationship between G and p as a simplex $\frac{G}{p}$.

2) Divide $\frac{G \cdot q \cdot t^2}{\mu \cdot h}$ by $\frac{q \cdot t}{h}$, we get $\frac{G \cdot t}{\mu}$. But this number already exists, so you can remove $\frac{G \cdot q \cdot t^2}{\mu \cdot h}$ and not consider it further.

3) Multiply the numbers $\frac{G \cdot t}{\mu}$ and $\frac{q \cdot \mu}{G \cdot h}$ to get the number $\frac{q \cdot t}{h}$. Therefore, we remove the number $\frac{q \cdot \mu}{G \cdot h}$, but if necessary, it can be obtained by combining the numbers $\frac{q \cdot t}{h}$ and $\frac{G \cdot t}{\mu}$.

After the transformation,

$$\theta\left(\frac{G \cdot t}{\mu}, \frac{G}{p}, \frac{q \cdot t}{h}, e\right) = 0. \tag{6}$$

The similarity number $\frac{q \cdot \mu}{G \cdot h}$, which has been removed, is rewritten as $\frac{G \cdot h}{q \cdot \mu}$. Then it can be viewed as the ratio of the elastic force $[F_c] = E \cdot L^2$ and the viscosity force $[F_V] = \mu \cdot V \cdot L$ [20]:

$$\frac{[F_c]}{[F_V]} = \frac{E \cdot L}{\mu \cdot V}, \tag{7}$$

where L is characteristic length; V is velocity; E is compressive modulus.

The simplex G/p can be considered as the ratio of the elastic force $[F_c]$ and the pressure force $[F_p] = p \cdot L^2$ [20]:

$$\frac{[F_c]}{[F_p]} = \frac{E}{p}, \tag{8}$$

The similarity number $\frac{q \cdot t}{h}$ is similar to the homochrony criterion [21]

$$H_0 = \frac{V \cdot t}{L}, \tag{9}$$

which has a physical meaning as a characteristic of unsteady fluid flow [22]. This criterion can be viewed as the ratio of the additional (local) force caused by the unsteady nature of the flow to the force of inertia [21].

Let's rewrite (6) as

$$\frac{q \cdot t}{h} = \phi\left(\frac{G \cdot t}{\mu}, \frac{G}{p}, e\right). \tag{10}$$

The similarity numbers in (5) were combined in different way. The second $\frac{q \cdot \mu}{p \cdot h}$, fourth $\frac{p \cdot q \cdot t^2}{\mu \cdot h}$, and sixth $\frac{p \cdot t}{\mu}$ numbers leave and the relationship between *G* and *p* in the form of a simplex *G/p*. After the transformations:

$$\delta\left(\frac{p \cdot t}{\mu}, \frac{G}{p}, \frac{q \cdot t}{h}, e\right) = 0, \tag{11}$$

The removed similarity number $\frac{q \cdot \mu}{p \cdot h}$, is written as $\frac{p \cdot h}{q \cdot \mu} = \frac{p \cdot h^2}{q \cdot \mu \cdot h}$. The resulting expression is the ratio of the pressure force $[F_p]$ and the viscosity force $[F_V]$ [20]:

$$\frac{[F_p]}{[F_V]} = \frac{p \cdot L}{\mu \cdot V}. \tag{12}$$

This corresponds to the Lagrange's criterion La, which is a criterion for the similarity of pressure and velocity fields in the flow of fluid in straight channels [21]. For a given channel, it characterizes the relationship between the dimensionless pressure and velocity fields.

Let's multiply and divide expression (12) by the force of inertia $[F_i] = \rho \cdot V^2 \cdot L^2$, where ρ is specific mass [20]:

$$\frac{[F_p]}{[F_V]} \cdot \frac{[F_i]}{[F_i]} = \frac{[F_p]}{[F_i]} \cdot \frac{[F_i]}{[F_V]} = \mathrm{Eu} \cdot \mathrm{Re},$$

where Eu is Euler's criterion; Re is Reynolds criterion.

$$\mathrm{Eu} = \frac{[F_p]}{[F_i]} = \frac{p}{\rho \cdot V^2}. \tag{13}$$

$$\mathrm{Re} = \frac{[F_i]}{[F_V]} = \frac{p \cdot V \cdot L}{\mu}, \tag{14}$$

Therefore, the number $\frac{p \cdot h}{q \cdot \mu}$ is similar to the criterion La = Eu·Re. Accordingly, the combination of numbers $\frac{p \cdot t}{\mu}$ and $\frac{q \cdot t}{h}$ is similar to the combination of criteria Eu, Re, La.

We can rewrite (11) as follows

$$\frac{q \cdot t}{h} = \eta\left(\frac{p \cdot t}{\mu}, \frac{G}{p}, e\right). \tag{15}$$

Dependencies (10) and (15) differ in their first similarity numbers. However, taking into account the second number that connects them, we can consider these dependencies to be the same.

5. Comparison of the modeling results with experimental data

The experimental setup scheme and the methodology for studying the kinetics of sludge dewatering from the Lviv wastewater treatment facilities were presented in [18].

The simplex *G/p* in dependencies (10) and (15) is presented (Fig.1) as the dependence $G = f_1(p)$ for a mixture of wastewater sludge on primary and secondary sedimentation tanks in a 1:2 ratio. This relationship can be described by the equation ($R^2 = 0.729$):

$$G = 115.1 \cdot p + 0.76 \cdot 10^7. \tag{16}$$

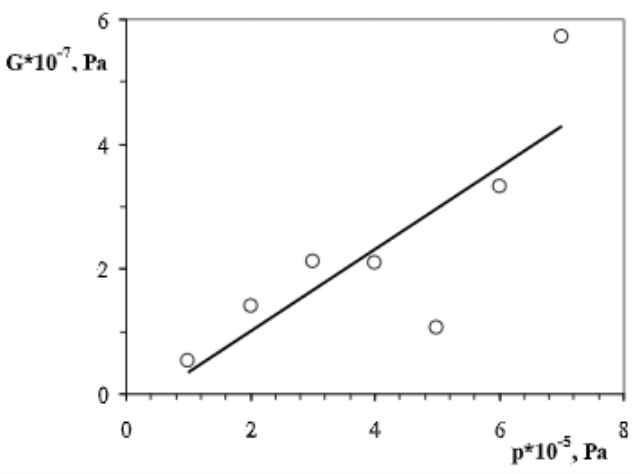

Fig.1. The dependence of the sludge compression modulus G on pressure p.

To evaluate the filtration properties of wastewater sludge, the specific filtration resistance r_o is used. The similarity number $\frac{p \cdot t}{\mu}$, used as the argument in equation (15), can be transformed into the following form:

$$\frac{p \cdot t}{\mu} = \frac{p \cdot t}{\mu \cdot r_o \cdot h^2}. \tag{17}$$

Therefore, dependence (15) can be represented as $\frac{q \cdot t}{h} = f_2\left(\frac{p \cdot t}{\mu \cdot r_o \cdot h^2}\right)$ that is an analogue of the Darcy equation for laminar filtration [18] (Fig. 2). This relationship is described by the equation ($R^2 = 0.9395$):

$$\frac{q \cdot t}{h} = 0.9954 \cdot \frac{p \cdot t}{\mu \cdot r_o \cdot h^2}. \tag{18}$$

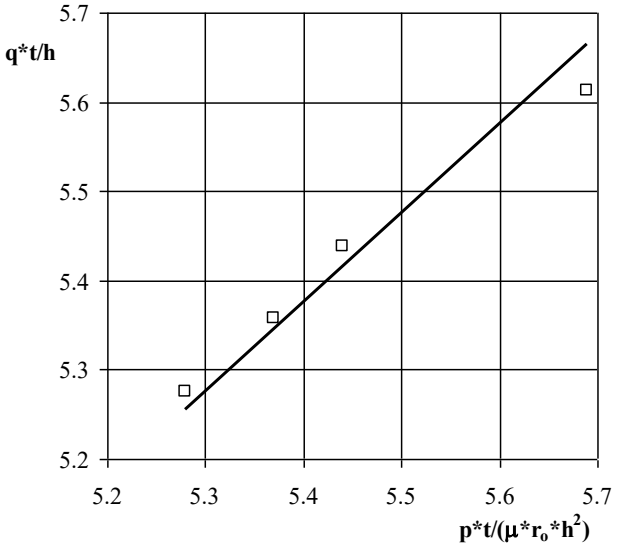

Fig.2. An analogue of the Darcy equation for laminar filtration.

6. Conclusion

Modeling by the method of linear proportions allowed us to obtain the same functional dependence for different combinations of similarity numbers. The similarity numbers have physical meaning as ratios of forces and serve as analogs to similarity criteria.

The physical modeling of the dewatering process of sewage sludge mixture from the Lviv municipal wastewater treatment facilities confirmed the validity of dependencies (10) and (15) derived using the method of linear proportions. An analog of Darcy's equation for laminar filtration was obtained.

References

[1] Foladori, P., Andreottola, G. & Ziglio, G. (2010) Sludge reduction technologies in wastewater treatment plants. IWA publishing.

[2] Gahlot, P., Balasundaram, G., Tyagi, V. K., Atabani, A. E., Suthar, S., Kazmi, A. A., Štěpanec, L., Juchelková, D. & Kumar, A. (2022) Principles and potential of thermal hydrolysis of sewage sludge to enhance anaerobic digestion. Environmental Research, 214, 113856. 10.1016/j.envres.2022.113856

[3] Hušek, M., Moško, J., & Pohořelý, M. (2022) Sewage sludge treatment methods and P-recovery possibilities: Current state-of-the-art. Journal of Environmental Management, 315, 115090. https://doi.org/10.1016/j.jenvman.2022.115090

[4] Zhang, X., Ye, P. & Wu, Y. (2022) Enhanced technology for sewage sludge advanced dewatering from an engineering practice perspective: A review. Journal of Environmental Management, 321, 115938. https://doi.org/10.1016/j.jenvman.2022.115938

[5] Jiang, Y., Gao, F., Zhang, N., Li, J., Xu, M. & Jiang, Y. (2023) Dehydration performance of municipal sludge and its dewatering conditioning methods: a review. Industrial & Engineering Chemistry Research, 62(29), 11337–11357.

[6] Skinner, S. J., Studer, L. J., Dixon, D. R., Hillis, P., Rees, C. A., Wall, R. C., Cavalida, R. G., Usher, S. P., Stickland, A. D. & Scales, P. J. (2015) Quantification of wastewater sludge dewatering. Water Research 82, 2–13. https://doi.org/10.1016/j.watres.2015.04.045.

[7] Wójcik, M. & Stachowicz, F. (2019) Influence of physical, chemical and dual sewage sludge conditioning methods on the dewatering efficiency. Powder Technology 344, 96102.

[8] To, V. H. P., Nguyen, T. V., Vigneswaran, S. & Ngo, H. H. (2016) A review on sludge dewatering indices. Water science and technology, 74(1), 1–16. doi:10.2166/wst.2016.102

[9] Wu, B., Dai, X. & Chai, X. (2020) Critical review on dewatering of sewage sludge: influential mechanism, conditioning technologies and implications to sludge re-utilizations. Water Research 180, 115912. https://doi.org/10.1016/j.watres.2020.115912.

[10] Wei, H., Gao, B., Ren, J., Li, A. & Yang, H. (2018) Coagulation/flocculation in dewatering of sludge: a review. Water research, 143, 608-631. https://doi.org/10.1016/j.watres.2018.07.029

[11] Lau, S. W., Sen, T. K., Chua, H. B. & Ang, H. M. (2017) Conditioning of synthetic sludge and anaerobically digested sludge using chitosan, organic polyelectrolytes and inorganic metal cations to enhance sludge dewaterability. Water, Air, & Soil Pollution, 228, 1–13. DOI 10.1007/s11270-017-3545-8

[12] Fu, Q., Liu, X., Wu, Y., Wang, D., Xu, Q. & Yang, J. (2021) The fate and impact of coagulants/flocculants in sludge treatment systems. Environmental Science: Water Research & Technology, 7(8), 1387–1401. https://doi.org/10.1039/D1EW00165E

[13] Liu, H., Wang, X., Qin, S., Lai, W., Yang, X., Xu, S. & Lichtfouse, E. (2021) Comprehensive role of thermal combined ultrasonic pre-treatment in sewage sludge disposal. Science of the Total Environment, 789, 147862. https://doi.org/10.1016/j.scitotenv.2021.147862

[14] Lo, K. V., Srinivasan, A., Liao, P. H. & Bailey, S. (2015) Microwave oxidation treatment of sewage sludge. Journal of Environmental Science and Health, Part A, 50(8), 882–889. https://doi.org/10.1080/10934529.2015.1019811

[15] Verbovskyi, O., Zhuk, V., Orel, V. & Popadiuk, I. (2023) Optimization of the process of decreasing the filtration resistance of sewage sludge by thermal pretreatment: a case study for the Lviv WWTP. Water Science & Technology, 88(7), 1688–1698. doi: 10.2166/wst.2023.317

[16] Bień, B. (2018) The impact of coagulant PIX 113 modified by ultrasonic field on sewage sludge dewatering. Desalination and Water Treatment, 117, 175–180. https://doi.org/10.5004/dwt.2018.22192

[17] Verbovskyi, O. V. & Davydchak, O. R. (2009) Filtration and compression characteristics of sewage sludge // Environmental protection. Energy saving. Balanced nature management: collection of materials of the I international congress, Lviv, June 28–29 / Lviv: Publishing House of the Lviv Polytechnic National University, 117–118. (in Ukrainian).

[18] Verbovskyi O. V., Sibirny A. V. & Regush A. Ya (2008) Kinetics of sewage sludge dehydration // Bulletin of the Lviv State University of Life Safety. No. 2. 135–139. (in Ukrainian).

[19] Mikhalev, M. A. (2010) Physical modeling of hydraulic phenomena: a textbook. – St. Petersburg: Polytechnic University Publishing House. (in Russian).

[20] Kepych, T. Yu., Kutsenko, O. G. (2004) Fundamentals of similarity theory and dimensional analysis and their application in problems of mechanics: Textbook. – Kyiv: Taras Shevchenko National University. (in Ukrainian).

[21] Minakovskyi, V. M. (1978) Generalized variables of transport theory (fundamentals of theory and reference tables). – Kyiv: Higher School. (in Russian).

[22] Naumenko, I. I. (2005) Hydraulics. Textbook. – Rivne: National University of Water and Environmental Engineering. (in Ukrainian).

Моделювання кінетики зневоднення осадів стічних вод методом лінійних пропорційностей

Орест Вербовський, Вадим Орел, Володимир Фем’як

Національний університет «Львівська політехніка», вул. Ст. Бандери 12, м. Львів, 79013, Україна

Анотація

Осади стічних вод, які скупчуються на очисних спорудах, є водними суспензіями, що виділяють із стічних вод в процесі їх механічного, біологічного або фізико-хімічного очищення. Часто осади в необробленому вигляді протягом десятків років зливалися на переобтяжені мулові площадки, у відвали, кар'єри, що привело до порушення екологічної безпеки й умов життя населення. Через велику кількість колоїдних речовин осади погано віддають воду. На водовіддачу осадів мають великий вплив вологість, співвідношення вільної і зв’язаної води, ступінь дисперсності частинок твердої фази, хімічний склад, структура, в’язкість осаду тощо. На очисних спорудах застосовують наступні процеси обробки осадів стічних вод: ущільнення, стабілізацію, кондиціонування, зневоднення, сушіння, термічну обробку, утилізацію цінних цінних продуктів або ліквідацію осадів. Важливим етапом в утилізації осадів є їх зневоднення, який дає змогу значного зменшення обсягів осадів. Здатність осадів стічних вод стискуватися під дією зовнішнього тиску є однією з характерних його властивостей. Проведено моделювання методом лінійних пропорційностей, що дозволило отримати однакову функціональну залежність за різних комбінацій чисел подібності.

Ключові слова: зневоднення; вміст води; осади стічних вод; метод аналізу розмірностей; метод лінійних пропорційностей; числа подібності.

Volume 11, Number 1, 2025 8

Improvement of Energy Efficiency of Air Distribution in a Room Using Swirled Air Jets

Orest Voznyak, Valentyn Bokhan*

Lviv Polytechnic National University, 12 Stepana Bandery St., Lviv, 79013, Ukraine

Received: April 21, 2025. Revised: May 18, 2025. Accepted: May 23, 2025.

Abstract

This article investigates the aerodynamic behavior and efficiency of swirled air jets used in modern ventilation systems. The influence of rotational motion on turbulence intensity, mixing efficiency, and air distribution uniformity is assessed. Results confirm that swirled jets enhance air mixing and reduce axial velocity and temperature gradients more effectively than traditional non-swirled jets. Key dimensionless parameters, such as velocity and temperature attenuation coefficients, are introduced to simplify calculations. Velocity and temperature profiles across the jet cross-section are examined in detail. The findings demonstrate that swirled jets provide improved control of indoor air distribution, minimize drafts, and help maintain stable thermal comfort. These insights support the implementation of swirl-based air supply solutions in confined and energy-sensitive environments.

Keywords: air distribution; swirled air jet; air velocity; jet border; air flow turbulence; aerodynamics.

1. Introduction

Contemporary standards regulating indoor environmental quality impose stringent criteria regarding airflow organization, thermal consistency, and the maintenance of a stable and comfortable indoor atmosphere [1]. In scenarios involving frequent occupancy — particularly in administrative, public, or industrial buildings — precise management of air circulation is of critical significance [2]. A pivotal factor in this context is the balanced distribution of air across the space, which helps to eliminate stagnant air pockets and mitigate abrupt thermal variations [3].

Conventional ventilation configurations employing standard air outlets often fail to deliver sufficient airflow uniformity [4], struggle to prevent zones of thermal overload or excessive cooling, and are generally inadequate in minimizing localized draughts [5]. Such deficiencies result in compromised thermal comfort, suboptimal working conditions, and can lead to adverse health implications, including respiratory ailments and reduced occupational performance [6]. Moreover, the ineffective operation of air delivery systems contributes to unnecessary energy expenditure, leading to elevated operational costs for climate control [7].

One of the effective strategies for enhancing indoor air mixing and thermal comfort involves the application of rotational (swirled) airflow patterns [8]. These vortex-type air jets, generated through specially designed inlet geometries, contribute to more intensive and uniform distribution of air throughout the occupied zone. By inducing turbulence and directional variability, swirled flows help to eliminate stratification and reduce the presence of thermally stagnant regions, thereby improving the overall microclimatic balance [9].

Numerical modeling and experimental investigations have demonstrated that swirl-inducing ventilation approaches offer superior control over air momentum and temperature gradients. This method allows for a more

* Corresponding author. Email address: valentyn.s.bokhan@lpnu.ua

This paper should be cited as: O. Voznyak, V. Bokhan. (2025) Improvement of energy efficiency of air distribution in a room using swirled air jets. *Energy Engineering and Control Systems*, Vol. 11, No. 1, pp. 8 – 13. https://doi.org/10.23939/jeecs2025.01.008

dynamic interaction between supply air and room air, facilitating enhanced thermal comfort and energy efficiency. The generation of rotational air streams also minimizes localized discomfort by dampening draft effects and promoting even temperature dispersion across diverse indoor environments [10].

2. Analysis of the recent publications and research works on the problem

Modern air distribution strategies increasingly incorporate vortex-forming devices that produce rotational airflows characterized by angular momentum and enhanced turbulence intensity [11]. These swirled jets are highly effective in improving air mixing, reducing temperature gradients, and minimizing zones of thermal stagnation. Depending on the boundary conditions and temperature differentials, such jets can exhibit varied flow regimes, including:

- free swirled jets, developing in open space without interference from nearby surfaces;
- confined swirled jets, influenced by walls, ceilings, or other room boundaries;
- isothermal jets, where inlet and ambient air temperatures are equivalent;
- non-isothermal jets, involving heated or cooled air relative to room temperature;
- laminar vortex flows, observed at low Reynolds numbers (Re < 2,300);
- turbulent vortex flows, dominant at higher Reynolds numbers (Re > 10,000) [12].

Swirled jets typically consist of a vortex core, where rotational velocity remains stable, surrounded by an outer area with increasing mixing and entrainment. A distinct feature of such flows is their ability to generate strong axial and tangential velocity components, which significantly enhance the distribution of thermal energy and reduce stratification effects [13]. This makes them especially suitable for use in spaces with complex air distribution requirements or high occupancy densities.

In the course of experimental investigations of individual swirled jets and their mutual interactions, it was observed that within the main development zone, the jets exhibit a gradual and relatively uniform attenuation in axial velocity v_x and excess temperature $\Delta\ t_x$, defined as the difference between the jet air temperature and the ambient room temperature t_{in}: $\Delta\ t_x = t_x - t_{in}$ [14]. This raises an important question: how does the interaction of multiple swirled jets, generated by a vortex diffuser, influence their aerodynamic behavior and thermal performance?

It is reasonable to hypothesize that the formation of multiple interacting swirled air jets at the outlet of a vortex diffuser significantly increases flow turbulence, promotes more rapid attenuation of axial velocity in the supply stream, and as a result, reduces the velocity attenuation coefficient (Fig.1.) [15].

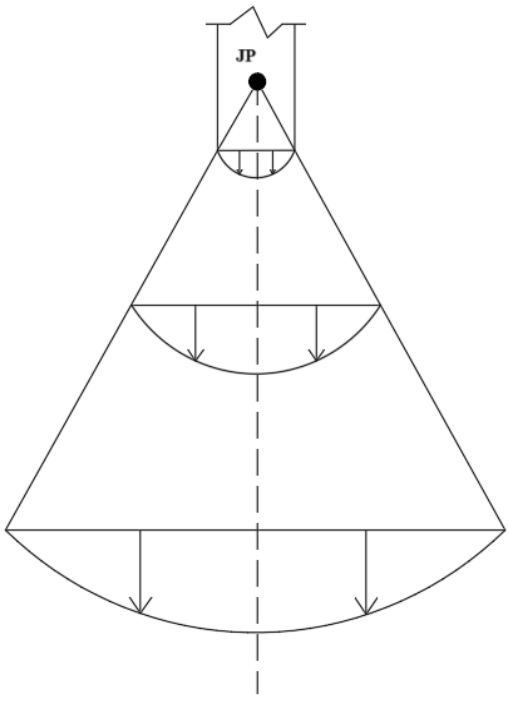

Fig.1. Scheme of a free jet development. Jet pole (JP) is the vertex through which the outer boundaries of the air jet pass.

3. Formulation of the goal of the paper

The aim of this study is to examine the efficiency of using swirled airflow configurations in mechanical ventilation systems, to determine optimal flow parameters, and to evaluate their impact on the uniformity of air distribution and overall microclimate quality within enclosed environments. Special attention is given to the analysis of the aerodynamic behavior of swirled air jets. The methodology combines numerical simulations with experimental investigations, which provides a solid foundation for developing design recommendations for ventilation systems incorporating swirl-inducing air supply components to enhance energy efficiency and indoor comfort.

4. Presentation of research results

In the study of air distribution in indoor environments, swirled jets have gained attention due to their enhanced mixing capabilities and ability to ensure uniform temperature and velocity fields. Unlike plane or compact free jets, swirled flows exhibit complex velocity profiles and increased turbulence, which significantly influence the attenuation of axial velocity and temperature excess in the supply stream.

The axial velocity v_x of an isothermal swirled jet was described by the inverse proportionality law:

$$v_x = \frac{SC}{x}, \tag{1}$$

where x is the axial distance from the outlet, m; SC is the swirl coefficient (a dynamic parameter incorporating both geometric and thermal physical properties of the jet), m^2/s.

The swirl coefficient is determined as follows:

$$SC = \frac{0.66}{\text{tg}\beta}\sqrt{\frac{T_v}{T_0}}\cdot\sqrt[4]{\zeta}\cdot v_o\cdot\sqrt{A_o}, \tag{2}$$

where β is the effective swirl dispersion angle, typically determined by the geometry of the swirl generator (for example, β=45°, so tg$\beta \approx 1$); ζ is the local resistance coefficient associated with the swirl-inducing element; T_o and T_v are the absolute temperatures of the supply air and the room air, respectively, K; v_o is the initial velocity of the flow at the outlet, m/s; A_o is the effective area of the outlet cross-section through which the swirled jet is introduced into the space, m^2.

To simplify practical calculations, a velocity attenuation coefficient s specific to swirled jets is introduced as:

$$s = \frac{0.66}{\text{tg}\beta}\sqrt{\frac{T_v}{T_0}}\cdot\sqrt[4]{\zeta}. \tag{3}$$

Accordingly, the axial velocity at any distance x from the outlet was expressed in a generalized form:

$$v_x = k\cdot v_o\cdot\sqrt{A_o}/x, \tag{4}$$

where k is an empirical constant that may vary depending on the swirl intensity and outlet geometry.

These equations enable a practical estimation of the behavior of swirled air jets, providing a basis for optimizing air distribution strategies in ventilation and air-conditioning systems to improve indoor environmental quality.

The velocity profile of air flow in swirled jets, particularly in the cross-sectional plane, plays a key role in determining the overall distribution efficiency and thermal comfort. The transverse velocity component v_y at any cross-section x and at a radial distance y from the central axis of the jet is defined by Schlichting's empirical formula:

$$v_y = v_x\left[1-\left(\frac{y}{y_b}\right)^{1.5}\right]^2, \tag{5}$$

where v_x and v_y are the axial and lateral velocity components, respectively, m/s; y_b is the jet boundary defined by the extent of significant momentum transfer, m.

For practical analysis, it is beneficial to express the velocity components in dimensionless form: the relative axial velocity $\overline{v}_x = v_x/v_o$ and the relative lateral velocity $\overline{v}_y = v_y/v_x$.In this context, the dimensionless velocity $\overline{v}_x$ was approximated by:

$$\overline{v}_x = \frac{0.48}{a\cdot x/d_e+0.145}, \tag{6}$$

where a = 0.078 is an empirical coefficient; d_e is equivalent diameter of the nozzle or outlet.

In the case of non-isothermal swirled jets, buoyancy effects must be considered due to temperature differences between the supply air and the ambient environment. The ratio of buoyancy to inertial forces at the point of ejection is characterized by the Archimedes number $\mathrm{Ar_o}$:

$$\mathrm{Ar}_o = \frac{g\sqrt{F_o}\cdot\Delta t_o}{V_o^2\cdot T_{in}}, \tag{7}$$

where g = 9.81 m/s^2 is gravitational acceleration; F_o is outlet area, m²; $\Delta t_o = t_o - t_{in}$ is excess initial temperature of the jet over ambient temperature, K; T_{in} is absolute indoor air temperature, K; V_o is initial supply velocity at the outlet, m/s.

Based on the magnitude of the Archimedes number $\mathrm{Ar_o}$, non-isothermal jets are typically classified into two regimes:

- non-isothermal A – where inertial forces dominate and buoyancy effects are negligible;
- non-isothermal B – where buoyancy significantly affects the development and trajectory of the air jet.

Understanding this distinction is essential for accurately modeling the behavior of swirled jets in HVAC systems, especially when maintaining thermal comfort and stratification control in large or thermally sensitive indoor environments.

In the case of horizontally discharged non-isothermal swirled jets classified as **type A** — where buoyancy forces exert a limited influence — the axial excess temperature $\Delta t_x = t_x - t_{in}$ attenuates with distance from the jet origin and was represented as:

$$\Delta t_x = \frac{N}{x}, \tag{8}$$

where x is the axial coordinate, m; N is a thermal parameter describing the initial thermal energy and geometric characteristics of the jet, °C·m.

The thermal parameter is determined as:

$$N = \frac{0.54}{\mathrm{tg}\alpha}\sqrt{\frac{T_{in}}{T_0}}\cdot\frac{1}{\sqrt[4]{\xi}}\cdot\Delta t_o\cdot\sqrt{F_o}, \tag{9}$$

where $\alpha = 12°25'$ is the effective jet spread angle (with $\mathrm{tg}\alpha \approx 0.22$); $\xi = 1$ is local resistance coefficient; T_0 is absolute temperature at the nozzle outlet, K.

For simplified engineering calculations, a temperature attenuation coefficient n is introduced:

$$n = \frac{0.54}{\mathrm{tg}\alpha}\sqrt{\frac{T_{in}}{T_0}}\cdot\frac{1}{\sqrt[4]{\xi}}. \tag{10}$$

Then, the axial excess temperature may be compactly expressed as:

$$\Delta t_x = n\cdot\Delta t_o\cdot\frac{\sqrt{F_o}}{x}. \tag{11}$$

To describe the temperature field across the jet cross-section at any given distance x, the **transverse excess temperature** $\Delta t_y = t_y - t_{in}$ is given by the following expression:

$$\Delta t_y = \Delta t_x\cdot\exp\left(-0.7\sigma_T\bar{y}^2\right), \tag{12}$$

where σ_T is the turbulent Prandtl number (typically 0.65÷0.7 for compact jets); $\bar{y} = y/(cx)$ is the dimensionless transverse coordinate (c=0.28 is an empirical constant).

For the analysis and comparison, dimensionless forms of the excessive temperature are often applied:

- axial, $\Delta\bar{t}_x = \Delta t_x/\Delta t_o$;
- transverse, $\Delta\bar{t}_y = \Delta t_y/\Delta t_x$.

These relationships are essential for understanding the thermal diffusion patterns of swirled jets, which are critical in optimizing ventilation systems for temperature uniformity and thermal comfort in enclosed spaces.

In the range of dimensionless axial coordinates x =0.7÷2.2, calculations were performed to determine the relative axial velocities of swirled jets based on equation (6). The obtained results were used to construct a velocity distribution graph specifically for swirled airflow structures, reflecting the characteristic attenuation of velocity along

the jet axis (see Figure 2). Fig. 2 represents the theoretical curve and the experimental data points. The velocity was measured at a certain coordinate and plotted on the graph.

The calculation of relative axial velocity was based on equation (6), which describes the inverse dependence of velocity on the axial coordinate x. To align the theoretical results with the experimental data shown in Fig. 2, where the dimensionless coordinate $\bar{x} = x / \sqrt{F_0}$ is used, equation (6) was adapted accordingly. Specifically, the axial distance x was expressed in terms of $\bar{x}$, which allowed the relative velocity $\bar{v}_x$ to be represented as a function of the dimensionless coordinate in a normalized form.

Experimental studies were conducted to determine the distribution of the relative axial velocity in a swirling jet at various distances from the jet axis. A specially designed nozzle with a diameter of D=40 mm, equipped with tangential channels to induce rotational motion of the air at the outlet, was used to generate the swirling jet.

The air was supplied to the setup from a compressor through a pressure stabilization system, which maintained a constant volumetric flow rate. The mean velocity profile was measured in the control cross-section of the jet at various distances from the axis using a single-component constant temperature hot-wire anemometer (CTA type), connected to a digital data acquisition system with a sampling frequency of 5 kHz. The velocity measurement error was ±2%.

The experiments were carried out in a laboratory aerodynamic channel under ambient temperature conditions of T=293±1 K and atmospheric pressure. Measurements were performed in a plane perpendicular to the jet axis, at dimensionless axial coordinates x=0.7÷2.2, $\bar{x} = x / \sqrt{F_o}$. At each coordinate, the results were averaged over 10 independent measurements. The obtained velocity values were normalized with respect to the maximum axial velocity. To smooth the experimental data points and construct the theoretical curve, the least squares method was applied using exponential approximation.

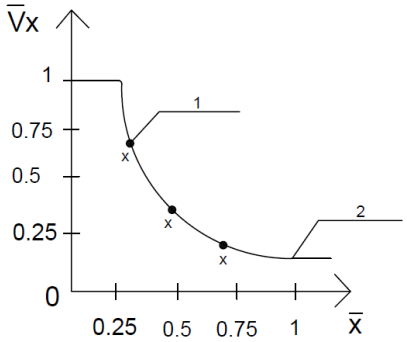

Fig.2. Relationship of relative axial velocity vs dimensionless coordinate x: 1 – experimental data points; 2 – theoretical curve.

5. Conclusion

1) The obtained results confirmed the hypothesis that the introduction of swirl at the jet outlet results in enhanced turbulence and more intensive mixing of air masses.
2) The rotational motion of the air stream significantly accelerates the axial velocity attenuation — by 10–20% depending on the axial position — compared to non-swirled jets.
3) Swirled air jets give a possibility for efficient air supply in confined spaces, distributing airflow more evenly while minimizing the risk of drafts and local discomfort.
4) Due to the vortex structure of the jet, a distinctive velocity profile is formed across its cross-section, characterized by a strong axial core and peripheral rotational zones.
5) The aerodynamic behavior of swirled jets improves air distribution efficiency and provides better control over microclimatic parameters in indoor environments.

References

[1] P. Kapalo, A. Sedláková, D. Košicanová, O. Voznyak, J. Lojkovics, and P. Siroczki (2014) “Effect of ventilation on indoor environmental quality in buildings,” in The 9th International Conference on Environmental Engineering, Selected Papers, Vilnius, Lithuania, May 22-23, CD 265. eISSN 2029-7092/eISBN 978-609-457-640-9

[2] Voznyak, O., Savchenko, O., Spodyniuk, N., Sukholova, I., Kasynets, M., & Dovbush, O. (2022). Air distribution efficiency improving in the premises by rectangular air streams. Pollack Periodica, 17(3), 111-116. https://doi.org/10.1556/606.2021.00518

[3] Myroniuk, K., Voznyak, O., Savchenko, O., Sukholova, I., Dovbush, O. (2024). Attenuation Coefficients of the Air Distributor with the Interaction of Opposing Non-coaxial Air Jets. In: Blikharskyy, Z., Zhelykh, V. (eds) Proceedings of EcoComfort 2024. EcoComfort 2024. Lecture Notes in Civil Engineering, vol 604. Springer, Cham. https://doi.org/10.1007/978-3-031-67576-8_35

[4] Borowski, M., Zwolińska, K., & Halibart, J. (2023). Air Distribution Assessment-Ventilation Systems with Different Types of Linear Diffusers. https://www.aivc.org/sites/default/files/1_C28.pdf

[5] Voznyak O., Spodyniuk N., Yurkevych Yu., Sukholova I., Dovbush O. (2020) Enhancing efficiency of air distribution by swirled-compact air jets in the mine using the heat utilizators. Naukovyi Visnyk Natsionalnoho Hirnychoho Universytetu, No.5(179), p. 89 – 94 doi:10.33271/nvngu/2020-5/089

[6] Jaszczur M., Branny M., Karch M., Borowski M. (2016). Experimental analysis of the velocity field of the air flowing through the swirl diffusers. J. Phys.: Conf. Ser. 745:1-9. DOI: 10.1088/1742-6596/745/3/032049.

[7] Sukholova, I., Voznyak, O., Myroniuk, K. (2011). Indoor air distribution and creation of a dynamic microclimate. Theory and Building Practice. (in Ukrainian). https://ena.lpnu.ua/handle/ntb/19456

[8] Voznyak, O., Myroniuk, K., Spodyniuk, N., Sukholova, I., Dovbush, O., Kasynets, M. (2022). Air distribution in the room by swirl compact air jets at variable mode. Pollack Periodica 17(3), 117–122. http://dx.doi.org/10.1556/606.2022.00515

[9] Voznyak O. (2020) Experiment Planning and Optimization of Solutions in Ventilation Technology. Monograph – Lviv: Lviv Polytechnic National University, 220 p. (in Ukrainian). ISBN: 978-966-553-982-7

[10] Voznyak, O., Sukholova, I., Spodyniuk, N., Kasynets, M., Savchenko, O., Dovbush, O., & Datsko, O. (2023). Enhancing of ventilation efficiency of premise due to linear diffuser. Pollack Periodica, 18(2), 107-112. https://doi.org/10.1556/606.2023.00750

[11] Janbakhsh, S., & Moshfegh B. (2014). Experimental investigation of a ventilation system based on wall confluent jets. Building and Environment, Vol. 80, 18-31. https://doi.org/10.1016/j.buildenv.2014.05.011.

[12] Srebric, J., & Chen, Q. (2002). Simplified Numerical Models for Complex Air Supply Diffusers. HVAC&R Research, 8(3), 277–294. DOI: 10.1080/10789669.2002.10391442.

[13] Allmaras, S.R., Johnson, F.T., & Spalart, P.R. (2012). Modifications and clarifications for the implementation of the spalart-allmaras turbulence model ICCFD7-1902. 7th International Conference on Computational Fluid Dynamics, Hawaii. http://www.iccfd.org/iccfd7/assets/pdf/papers/ICCFD7-1902_paper.pdf

[14] Dovhaliuk, V. et al. (2018). Simplified analysis of turbulence intensity in curvilinear wall jets. FME Transactions, 46, 177–182. doi.org/10.5937/fmet 1802177D.

[15] Gumen, O. et al. (2017). Geometric analysis of turbulent macrostructure in jets laid on flat surfaces for turbulence intensity calculation. FME Transaction, 45, 236-242. doi:10.5937/fmet1702236G.

Підвищення енергоефективності повітророзподілу в приміщенні із використанням закручених повітряних струменів

Орест Возняк, Валентин Бохан

Національний університет «Львівська політехніка», вул. С. Бандери, 12, Львів, 79013, Україна

Анотація

У статті досліджено аеродинамічні характеристики та ефективність закручених повітряних струменів, що застосовуються в сучасних системах вентиляції. У роботі проаналізовано особливості затухання осьової швидкості та надлишкової температури в неізотермічних закручених потоках з урахуванням як теоретичних моделей, так і експериментальних даних. Оцінено вплив обертального руху на інтенсивність турбулентності, ефективність перемішування та рівномірність розподілу повітря. Результати підтверджують, що закручені струмені забезпечують краще перемішування повітря та ефективніше зменшують градієнти швидкості й температури порівняно з традиційними прямолінійними струменями. Запроваджено ключові безрозмірні параметри, такі як коефіцієнти затухання швидкості та температури, що спрощують розрахунки. Детально розглянуто профілі швидкості та температури в поперечному перерізі струменя. Отримані результати свідчать про те, що закручені струмені забезпечують покращене керування повітророзподілом у приміщеннях, мінімізують протяги та сприяють стабільному тепловому комфорту. Отримані висновки підтверджують доцільність використання систем подачі повітря із закрученими струменями у замкнених та енергочутливих просторах.

Ключові слова: розподіл повітря; закручений повітряний струмінь; швидкість повітря; межа струменя; турбулентність повітряного потоку; аеродинаміка.

Volume 11, Number 1, 2025 14

Analytical Study of Operational Efficiency of Industrial Boiler Plants Considering Building Thermophysics and Prospects for Integrating Heat Pumps

Yurii Burda[a,*], Ihor Redko[b], Yurii Pivnenko[a], Artem Cherednik[a], Roman Tkachenko[a]

[a]*O.M. Beketov National University of Urban Economy in Kharkiv, 17 Chornoglazivska St., Kharkiv, 61002, Ukraine*
[b]*Ukrainian State University of Railway Transport, Feuerbach Square 7, Kharkiv, 61050, Ukraine*

Received: April 19, 2025. Revised: May 31, 2025. Accepted: June 06, 2025.

Abstract

This study presents an in-depth analytical investigation into the operational efficiency of boiler plants in industrial enterprises, incorporating the principles of building thermophysics as a fundamental component influencing energy performance. The research focuses on the interaction between the thermophysical properties of building enclosures, architectural design parameters, and the thermal regimes of boiler equipment. It highlights how building structures significantly impact heat losses and overall energy demand within the industrial environment, emphasizing the importance of considering these aspects in the operational analysis of heating systems. The study further explores the potential of modernizing existing boiler plants through the integration of heat pump technologies. Given the increasing demand for energy-efficient and environmentally sustainable solutions, heat pumps are examined as viable alternatives or supplementary components to conventional boiler systems.

Keywords: boiler houses of industrial enterprises; energy efficiency; building thermophysics; heat losses; enclosing structures; heat supply; heat pumps.

1. Introduction

The current stage of industrial development is marked by increasing demands for the energy efficiency of production processes and engineering systems, particularly heating supply. Within the energy consumption structure of industrial enterprises, boiler installations occupy a significant share, and their operational efficiency directly affects overall energy resource expenditures and greenhouse gas emissions. Traditional approaches to the design and operation of boiler plants often neglect the impact of the thermophysical characteristics of the buildings in which these systems operate, resulting in substantial heat losses and excessive fuel consumption. Considering building thermophysics – including the thermal properties of enclosing structures, their capacity to accumulate heat, insulation performance, and the nature of thermal protection – is a necessary condition for forming an objective understanding of the energy processes within the system.

In the context of the global energy transition and the decarbonization of the industrial sector, there is growing interest in the application of innovative technologies, among which heat pumps play a particularly important role. Their integration into the heat supply structure of industrial enterprises offers opportunities for reducing the consumption of conventional energy carriers, optimizing thermal loads, and enhancing the environmental efficiency of systems. At the same time, the use of heat pumps requires careful consideration of the specific characteristics of the facility, the thermal regime of production, the structural features of the building elements, and the climatic conditions of the region.

* Corresponding author. Email address: science.yurii.burda@gmail.com

This paper should be cited as: Y. Burda, I. Redko, Y. Pivnenko, A. Cherednik, R. Tkachenko. (2025) Analytical study of operational efficiency of industrial boiler plants considering building thermophysics and prospects for integrating heat pumps. *Energy Engineering and Control Systems*, Vol. 11, No. 1, pp. 14 – 20. https://doi.org/10.23939/jeecs2025.01.014

Research dedicated to analyzing the operational efficiency of boiler plants while accounting for building thermophysics and the prospects for implementing heat pumps enables the formation of a comprehensive vision for modernizing existing systems. This approach ensures not only increased energy efficiency but also the achievement of high standards in reliability, operational stability, and environmental safety within industrial heat-generating complexes.

2. Analysis of recent research and publications

The issue of improving the energy efficiency of industrial boiler plants is actively addressed in both domestic and international scientific literature. This attention is driven by the increasing demand for energy resource savings, reduced environmental impact, and adaptation to the modern requirements of sustainable development. In recent years, researchers have particularly focused on a systemic approach to evaluating thermal processes, where not only the efficiency of boiler equipment is considered but also a range of external and internal factors, among which the thermophysical characteristics of building structures play a significant role. In the works of domestic scholars, emphasis is placed on the interrelationship between heat losses through enclosing structures, the thermal conductivity coefficients of materials, and the energy consumption level of the heat supply system [1].

In publications by international researchers, the prevailing concepts involve integrated thermal flow management, optimization of heat supply based on digital modeling, and the implementation of adaptive energy systems. A significant number of studies are devoted to the modernization of boiler plants through the integration of alternative energy sources, particularly heat pumps. These studies highlight the effectiveness of heat pumps under variable thermal load conditions and their capacity to reduce overall primary energy consumption [2].

A distinct area of research concerns the dynamics of unsteady thermal processes in industrial facilities, where the thermal inertia of buildings is taken into account. This factor has a direct impact on the selection of boiler equipment parameters and their operational modes. Despite achievements in this field, the scientific community continues to express the need for in-depth investigation of a comprehensive approach that combines building thermophysics, boiler heat engineering, and innovative thermal generation technologies – such as heat pumps – within a unified energy system of an industrial facility.

3. Goal and task setting

The primary goal of this study is to substantiate effective approaches to the operation of boiler plants in industrial enterprises by incorporating the principles of building thermophysics and to determine the prospects for the integration of heat pumps as an energy-efficient alternative or supplement to traditional heat generation systems. A comprehensive combination of the analysis of thermal characteristics of building enclosures, operational modes of thermal generation equipment, and modern heat supply technologies allows for the formation of a holistic vision for system modernization in the context of reducing energy consumption, improving thermal balance, and enhancing the environmental performance of industrial facilities.

The main tasks of the study include identifying the key factors that influence the operational efficiency of boiler plants in relation to the thermophysical properties of buildings; analyzing existing methods for assessing heat losses through building envelopes; evaluating the impact of thermal inertia in industrial buildings on the performance parameters of boiler equipment; investigating the technical and energy characteristics of heat pumps under industrial operating conditions; and developing recommendations for the integration of heat pumps into the heat supply structure, taking into account the specific features of building envelopes and the energy needs of the facility. The fulfillment of these tasks will enable the identification of the most appropriate engineering solutions for improving the energy efficiency of industrial thermal generation systems based on contemporary building science and energy technologies.

4. The main part of the study

The operational efficiency of industrial boiler plants is largely determined by the synergy between the technical parameters of heat-generating equipment, the thermal demands of the facility, and the thermophysical characteristics of the building envelope. Neglecting building thermophysics during the design or modernization of heat supply systems often leads to inefficient heat distribution, excessive loading of boiler units, and increased operational costs.

In this context, a scientific understanding of the thermal behavior of enclosing structures becomes an essential element in assessing the overall energy efficiency of the system.

Key thermophysical parameters that require consideration include thermal conductivity, specific heat capacity, vapor permeability, and the dynamic thermal inertia of enclosing components. For example, buildings with high thermal mass are capable of storing surplus heat during the daytime and releasing it during the nighttime, thus reducing peak demand on boiler systems. In such cases, it is appropriate to implement weather-compensated power regulation or variable operating regimes based on indoor thermal comfort and external climate conditions [3].

Studies indicate that, on average, up to 35% of total heat losses in industrial facilities are attributed to enclosing structures with poor insulation characteristics. Outdated brick buildings with uninsulated facades, for instance, exhibit excessive energy consumption, which – under conditions of rising fuel tariffs – creates a critical burden on the enterprise's energy budget. The application of multilayer insulation systems using materials with low thermal conductivity, such as mineral wool panels or polyurethane foam, combined with airtightness control of enclosures, enables significant reductions in heat loss without requiring the modernization of the main boiler equipment [4].

The integration of heat pumps into the heat generation infrastructure of industrial facilities presents a distinct engineering challenge that requires consideration of both the thermodynamic aspects of pump operation and their interaction with the building structure. Heat pumps operating on the reverse Carnot cycle exhibit a coefficient of performance (COP) that significantly exceeds the efficiency of traditional boilers. When using low-potential heat sources such as soil or wastewater, the COP may reach values of 3 to 5, indicating the potential to obtain 3 to 5 units of thermal energy per unit of consumed electricity.

However, the efficiency of heat pumps is directly dependent on the stability of thermal loads and the temperature regimes within the premises, which are in turn shaped by the building envelope. In cases where the building exhibits low thermal inertia or uneven heat loss distribution, cyclic loading of the heat pump's compressor occurs, reducing both its lifespan and energy efficiency. For this reason, modern engineering solutions often combine heat pumps with buffer tanks, thermal storage systems, or hybrid boilers capable of handling peak loads without compromising energy stability [5].

A notable example is the modernization of a metallurgical facility's boiler system, where, following reconstruction of the enclosing structures to improve thermal protection by approximately 45%, a 250-kW water-to-water heat pump was implemented. As a result, natural gas consumption decreased by 38%, and overall heating costs were reduced by 31%. This case demonstrates the synergistic effect of combining building thermophysics with innovative energy technologies.

The operation of industrial boiler plants is governed by complex thermodynamic processes in which the conversion of chemical energy from fuel into useful thermal energy is central to meeting internal technological and heating demands. The thermodynamic efficiency of the combustion process is primarily evaluated through metrics such as useful heat utilization, enthalpy balances, and flue gas losses. In traditional boiler systems, irreversible losses dominate – particularly in the form of heat dissipation through exhaust channels and suboptimal heat transfer in exchangers – yet these losses often disregard the thermophysical condition of the building shell, which critically influences thermal loads [6].

The incorporation of heat pumps as part of boiler plant modernization shifts the energy transformation paradigm – from direct fuel combustion to the use of low-grade heat sources via the Carnot thermodynamic cycle. Here, the energy conversion coefficient becomes central to evaluating the system's ability to repeatedly return input energy as useful heat. These processes are highly sensitive to the temperature regimes of both the heat source and the end-use environment. Building thermophysics, by shaping the thermal inertia and volumetric storage capacity of indoor spaces, acts as a passive regulator of thermodynamic performance.

For instance, high-thermal-mass buildings provide stable indoor temperatures over daily cycles, enabling heat pumps to operate under consistent load conditions and improving the system's overall COP. Conversely, in structures with low thermal inertia or uneven temperature fields, frequent compressor cycling leads to efficiency loss and accelerated wear of equipment [7].

Thus, boiler plants should not be considered merely as sources of heat, but as integral elements of a unified energy-thermodynamic environment in which heat generation, transfer, and consumption are interdependent with the thermophysical properties of the surrounding medium – including wall resistance, material conductivity, internal

thermal mass, and the nature of thermal flows through building enclosures. Consequently, optimizing a boiler plant without a deep understanding of the thermal behavior of the enclosing structures is inherently limited in effectiveness. Modernization efforts must include synchronized reconstruction of building envelopes and the enhancement or supplementation of thermal generation units.

The integration of heat pumps into the thermal infrastructure of industrial facilities requires an interdisciplinary engineering approach that encompasses thermodynamics, building thermophysics, and control automation. The effectiveness of heat pumps, particularly those operating on the reverse Carnot cycle, is closely linked to the thermal behavior of the building envelope. These systems achieve high coefficients of performance (COP), particularly when utilizing low-grade energy sources such as ground heat, ambient air, or process wastewater. However, their actual efficiency is largely dependent on the stability of internal thermal conditions, which are governed by the thermophysical parameters of the enclosing structures. [8]

Buildings with high thermal inertia and efficient insulation significantly reduce the frequency of compressor cycling, thereby increasing system lifespan and maintaining high COP values. In contrast, structures with low heat accumulation capacity or non-uniform thermal loads cause frequent start-stop operation, leading to reduced energy performance and accelerated equipment wear. This highlights the importance of synchronizing building design and retrofitting strategies with the thermal characteristics of heat pump systems [9].

Modern engineering practice increasingly favors hybrid thermal generation models that combine heat pumps with conventional boiler units, thermal storage tanks, and automated control systems. Such configurations allow for adaptive load balancing, peak shaving, and optimized energy use depending on real-time thermal demand and external temperature fluctuations. For instance, during periods of mild ambient temperatures, heat pumps can handle the entire heating load, while during extreme cold spells, auxiliary boilers can provide supplementary heat to ensure uninterrupted operation and thermal comfort [10].

A representative example can be seen in the case of a metallurgical enterprise where an integrated modernization effort included the reconstruction of building envelopes and the installation of a 250-kW water-source heat pump. Following these measures, natural gas consumption was reduced by 38%, and total heating expenses dropped by over 30%. This result underscores the synergistic potential of combining advanced building thermophysics with progressive thermal technologies.

Thermophysical analysis also plays a critical role in evaluating the exergy efficiency of thermal systems. Traditional boiler plants are characterized by substantial exergy losses, especially when operating with low-temperature return water. Heat pumps, by contrast, are inherently more efficient in low-temperature applications such as underfloor heating or pre-heated ventilation air, as they minimize exergy destruction and align thermal supply more closely with demand.

From a thermodynamic standpoint, the building's ability to store and buffer heat contributes to stabilizing operational modes and optimizing energy recovery. Systems with high volumetric thermal capacity and well-regulated insulation can function as passive energy stabilizers, thereby enhancing the thermodynamic stability and energy responsiveness of the entire thermal network.

Furthermore, the deployment of intelligent control systems is critical for unlocking the full potential of combined boiler–heat pump installations. Automation technologies based on SCADA platforms, IoT sensor networks, and machine learning algorithms allow for real-time monitoring, predictive control, and adaptive optimization. These systems enable not only efficient thermal management but also synchronization with energy tariffs, weather forecasts, and production cycles.

Feedback systems equipped with sensors for humidity, solar radiation, CO_2 levels, and infrared thermography facilitate multidimensional control over the indoor climate. This is especially important in industrial processes where environmental conditions directly impact production quality. In such cases, the integration of thermophysical knowledge with control systems leads to energy harmonization – where both the equipment and the building envelope adapt dynamically to optimize performance.

By adopting such comprehensive strategies, industrial heat supply systems evolve from isolated heat sources into intelligent, thermally adaptive ecosystems. These systems achieve maximum efficiency not by increasing energy input but by dynamically balancing generation, storage, and consumption through thermophysically informed design and smart control.

The prospects for integrating heat pumps into industrial heating systems are highly promising, offering a range of advantages in terms of energy efficiency, cost reduction, and environmental sustainability. As industries face increasing pressure to reduce energy consumption and minimize environmental impacts, heat pumps present a viable solution by utilizing renewable energy sources such as geothermal and ambient air heat. This enables a significant reduction in reliance on conventional fossil fuels, contributing to a greener, more sustainable energy landscape. One of the key advantages of integrating heat pumps is their ability to operate efficiently even at low ambient temperatures, making them ideal for regions with colder climates. By extracting heat from the environment, heat pumps provide a highly effective means of maintaining consistent heating throughout the year, ensuring stable operational conditions for industrial processes.

The thermophysical characteristics of buildings directly impact the efficiency of heating systems, as they determine how well heat is retained or lost through walls, roofs, windows, and other building elements. The integration of heat pumps into industrial heating systems, when combined with a detailed analysis of building thermophysics.

The generalized data and characteristics are presented in Table 1.

Table 1. Dependence of the efficiency.

Temperature (K)	Boiler Efficiency (%)	COP of Heat Pump (Coefficient of Performance)	Energy Consumption (kWh)
278.15	85	3.2	500
283.15	84	3.3	480
288.15	82	3.5	460
293.15	80	3.8	440
298.15	77	4.0	420
303.15	75	4.1	400
308.15	72	4.3	380
313.15	70	4.4	360
318.15	68	4.5	340
323.15	65	4.6	320

Below is the graph showing the dependence of the efficiency of boiler houses and heat pumps on the ambient temperature and energy consumption (Fig. 1).

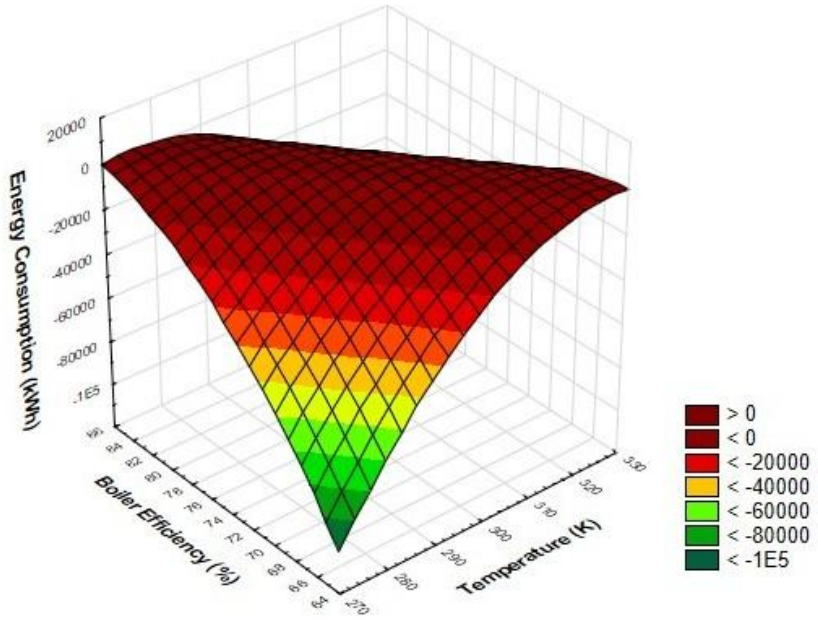

Fig.1. Dependence of efficiency of boiler houses and heat pumps on the ambient temperature and energy consumption.

Further, the role of building thermophysics extends to the optimization of heat exchange processes in industrial heating systems. By understanding how heat moves through different materials and building structures, engineers can design more efficient boiler and heat pump systems, reducing energy consumption while maintaining optimal thermal comfort inside the industrial facility. The continuous monitoring of these thermophysical properties, along with advancements in building materials and insulation technologies, will play a pivotal role in future innovations aimed at boosting the energy efficiency of industrial heating systems.

Thus, a comprehensive approach to the analysis of boiler houses, based on considering the thermophysical characteristics of buildings and the potential for using heat pumps, allows for the formulation of an effective energy strategy for industrial enterprises. Further research should focus on the development of adaptive heating control models using real-time monitoring technologies, artificial intelligence for load forecasting, and digital twins of facilities, which will enable achieving even higher levels of energy efficiency, reliability, and environmental safety in the industrial sector.

5. Conclusion

The analysis of the operational efficiency of boiler houses at industrial enterprises, taking into account building thermophysics and the integration of heat pumps, allows for several key conclusions regarding the improvement of energy efficiency and the reduction of operating costs in industrial heating systems.

In conclusion, the integration of building thermophysics with industrial boiler plant operations and heat pump technologies offers a comprehensive approach to enhancing energy performance. It enables the development of adaptive systems that can dynamically adjust to varying environmental conditions, resulting in reduced energy consumption, extended equipment life, and improved environmental sustainability.

Increasing efficiency through the integration of technologies. The implementation of heat pumps into the heating system of industrial enterprises significantly reduces energy consumption by utilizing renewable energy sources, optimizing heat usage even at low ambient temperatures.

The dependence of efficiency on temperature fluctuations. The study found that as the ambient temperature rises, the efficiency of boiler houses decreases, while the coefficient of performance (COP) of heat pumps increases. This highlights the importance of adaptive control systems that can automatically regulate the operation of boilers and pumps depending on external conditions.

The implementation of combined heat generation systems significantly reduces fuel and energy resource costs, which is a crucial aspect in today's economic realities. With proper design and system configuration, substantial savings can be achieved compared to traditional heating methods.

References

[1] Pyarimohan Dehury, Shahil Chaudhari, Tamal Banerjee, Sarit Kumar Das. Prediction of thermophysical properties of deep eutectic solvent-based organic nanofluids: A machine learning approach. Journal of Molecular Liquids. Volume 411, 1 October 2024, 125809. https://doi.org/10.1016/j.molliq.2024.125809

[2] Yichuan He, Yanhui Feng, Lin Qiu, Dawei Tang. Data-driven approach augmented by attention mechanism in critical and boiling thermophysical properties prediction of fluorine/chlorine-based refrigerants. Energy. Volume 306, 15 October 2024, 132490. https://doi.org/10.1016/j.energy.2024.132490

[3] Bernadeta Jasiok and all. Thermophysical properties of the SPC/E model of water between 250 and 400 K at pressures up to 1000 MPa. Fluid Phase Equilibria. Volume 584, September 2024, 114118. https://doi.org/10.1016/j.fluid.2024.114118

[4] Rui Zhang, Xu, Lin Chen. Asymptotic thermophysical behaviors of near-critical fluid under parameter scaling. International Journal of Heat and Fluid Flow. Volume 108, September 2024, 109442. https://doi.org/10.1016/j.ijheatfluidflow.2024.109442

[5] Sohail A. Khan, T. Hayat, A. Alsaedi. Chemically reactive flow beyond constant thermophysical characteristics. Case Studies in Thermal Engineering. Volume 61, September 2024, 104980. https://doi.org/10.1016/j.csite.2024.104980

[6] M. Abd El-Hamid, Gaosheng Wei. Effect of varying the thermophysical properties of phase change material on the performance of photovoltaic/thermal-PCM hybrid module numerically. Journal of Energy Storage. Volume 86, Part B, 10 May 2024, 111326. https://doi.org/10.1016/j.est.2024.111326

[7] Sujata Kalsi and all. Thermophysical properties of nanofluids and their potential applications in heat transfer enhancement: A review. Arabian Journal of Chemistry. Volume 16, Issue 11, November 2023, 105272. https://doi.org/10.1016/j.arabjc.2023.105272

[8] Rupali Tiwari and all. Investigation of thermophysical properties of Turkey oak particleboard for sustainable building envelopes. Developments in the Built Environment. Volume 16, December 2023, 100228. https://doi.org/10.1016/j.dibe.2023.100228

[9] Fatemeh Zarei-Jelyani, Fatemeh Salahi, Behnaz Rahmatmand, Mohammad Reza Rahimpour. 3 - Thermophysical properties of natural gas hydrates. Advances in Natural Gas: Formation, Processing, and Applications. Volume 3: Natural Gas Hydrates. 2024, Pages 47-63. https://doi.org/10.1016/B978-0-443-19219-7.00006-0

[10] Bo Jin, Shuhong Liu, Kai Xu, Qiang Lu b, Yong Du. Thermophysical properties in the Al-Cu-Ag system: A combined CALPHAD and first-principles study. Journal of Molecular Liquids. Volume 370, 15 January 2023, 121001. https://doi.org/10.1016/j.molliq.2022.121001

Аналітичне дослідження ефективності експлуатації котелень промислових підприємств із урахуванням будівельної теплофізики та перспективи інтеграції теплових насосів

Юрій Бурда[a], Ігор Редько[b], Юрій Півненко[a], Артем Чередник[a], Роман Ткаченко[a]

[a]*Харківський національний університет міського господарства імені О.М. Бекетова, вул. Чорноглазівська, 17, Харків, 61002, Україна*

[b]*Український державний університет залізничного транспорту, майдан Фейєрбаха 7, Харків, 61050, Україна*

Анотація

У статті представлено аналітичне дослідження ефективності експлуатації котелень промислових підприємств з урахуванням будівельної теплофізики та перспектив інтеграції теплових насосів у систему теплопостачання. Важливість такого підходу полягає в можливості зниження енергоспоживання та покращення енергетичної ефективності промислових котелень за рахунок оптимізації використання теплових ресурсів, зокрема через впровадження сучасних технологій, таких як теплові насоси, які забезпечують використання відновлювальних джерел енергії. Будівельна теплофізика є ключовим елементом при проектуванні та аналізі роботи котелень, оскільки вона дозволяє врахувати теплопередавальні характеристики матеріалів та будівельних конструкцій, що суттєво впливають на загальну ефективність системи теплопостачання. Зокрема, правильний підбір матеріалів для утеплення будівель, а також врахування теплових втрат та нагрівальних характеристик дозволяє значно підвищити ефективність роботи котелень та зменшити витрати на енергоресурси. Таким чином, інтеграція теплових насосів у котельні промислових підприємств із урахуванням будівельної теплофізики є важливим кроком на шляху до сталого розвитку та зниження енергетичних витрат, що сприяє підвищенню енергоефективності та екологічної безпеки промислових об'єктів.

Ключові слова: котельні промислових підприємств; енергоефективність; будівельна теплофізика; теплові втрати; огороджувальні конструкції; теплопостачання; теплові насоси; енергоефективність.